IN-34
6335
P-108

NASA Contractor Report 198408
ICOMP–95–17; CMOTT–95–3

Center for Modeling of Turbulence and Transition: Research Briefs—1995

(NASA-CR-198408) CENTER FOR MODELING OF TURBULENCE AND TRANSITION: RESEARCH BRIEFS, 1995 (NASA. Lewis Research Center) 108 p

N96-12237

Unclas

G3/34 0071422

October 1995

Prepared for
Lewis Research Center
Under Cooperative Agreement NCC3–370

National Aeronautics and
Space Administration

INSTITUTE FOR COMPUTATIONAL MECHANICS IN PROPULSION
NASA
ICOMP
Lewis Research Center
Ohio Aerospace Institute

Table of Contents

Page

Turbulence Program for Propulsion Systems
Tsan-Hsing Shih 1

$k - \epsilon$ Eddy Viscosity Turbulence Models: Development and Applications
Zhigang Yang 7

Turbulence Models for CFD Codes
Jiang Zhu 13

Eddy Diffusivity Models for Heat Transfer
Aamir Shabbir 33

Computation of Compressible Turbulent Benchmark Flows
William W. Liou 45

Modeling of Turbulent, Reacting Flows by PDF Methods
Andrew T. Norris 57

Application of PDF to Compressible Turbulent Reactive Flows
Andrew T. Hsu 63

Turbulence Model Development for NPARC
J. Zhu, Z. Yang, and T.-H. Shih 73

Calculations of Turbulent Reacting Flows in Can Combustors
A.T. Norris and W.W. Liou 89

Assessment of Turbulence Models in Turbomachinery Flows 95

Appendix A : Industry-Wide Workshop 97

Appendix B : Organization - 1995 101

Appendix C : List of Member's Publications 103

Turbulence Program for Propulsion Systems

Tsan-Hsing Shih

1. Introduction

1.1 Background

- The center for modeling of turbulence and transition (CMOTT) at NASA Lewis Research Center (LeRC) has been in existence for about four years. In the first three years, its main activities were developing and validating turbulence and combustion models for propulsion systems, in an effort to remove the deficiencies of existing models. Three workshops on computational turbulence modeling were held at LeRC (1991, 1993, 1994).
- A peer review of the turbulence modeling activities at LeRC was held in September, 1993. Seven peers from GE, P&W, RocketDyne, Cornell University, University of California at Berkeley and NASA Ames conducted the review. The objective of the review was to assess the turbulence program at LeRC/CMOTT and to suggest the future direction of turbulence modeling activities for propulsion systems. In September of 1994, a NASA-wide turbulence program peer review was held at NASA Ames Research Center (ARC) by sixteen peers from the aerospace industry, universities and other agencies.

1.2 Recommendations from the 1993 peer review

- "LeRC should spend substantial effort being responsive to industry's current pressing perceived needs; this involves extensive discussion with industry during every phase of model development, analysis of industry's problems, goal oriented model development, evaluation of models relative to industry's intended application ..."
- "LeRC has an obligation not only to respond to industry's requests for help, but to play an autonomous, independent leadership role in providing models of the highest quality, ..., which can be employed not only by the aircraft gas turbine and rocket industries but also by other industries ..."
- "In the present financial climate, industry does not have the resources to undertake model development and evaluation. LeRC's help in this regard via the creation of its turbulence modeling effort, is, therefore, welcome from the industry's standpoint."
- "It is important to work with the industry to evaluate the models and rank-order them by performance and cost in order to identify the most appropriate models for particular situations."
- There are many other useful suggestions and comments including collaboration with industry, joint programs, industry-wide workshops, etc.

1.3 Recommendations from the 1994 NASA-wide turbulence peer review

- NASA needs a right well defined turbulence program in order to help industry meet its needs.
- The turbulence program needs a certain level of support, coordination, linkage to industry needs, technology transfer, management and leadership.
- The current progress is not reflective of real problems.

Based on the peers' comments and the current environment of NASA LeRC, we have planned and carried out a turbulence program for propulsion systems. The program is briefly explained in the following sections.

2. Program goals at CMOTT

- Develop reliable turbulence and bypass transition models and combustion models for complex flows in propulsion systems.
- Integrate developed models into deliverable CFD tools for propulsion systems in collaboration with researchers at NASA LeRC and industry partners.

3. Program approaches

- Develop turbulence and combustion subprograms or modules for CFD users.
- Develop collaboration program with NASA LeRC and industry partners to facilitate technology transfer.
- Conduct turbulence modeling research for propulsion systems:
  - ◇ One-point moment closures for non-reacting flows,
  - ◇ Scalar PDF method for turbulent reacting flows,
  - ◇ Validation of existing and newly developed models.

4. Development of turbulence and combustion subprograms (modules)

4.1 Objective

Build quick and efficient vehicles for turbulence and combustion technology transfer to CFD users in propulsion systems, for example, inlet/nozzle, turbomachinery and combustion, etc.

4.2 The features of the turbulence module

- It contains various turbulence models from which users can choose the model appropriate for the flows of interest.
- It is self-contained, i.e., it contains its own solver for the turbulence model equations.
- It can be easily linked to industry CFD codes.

4.3 The features of the PDF combustion module

- It can be easily coupled with any existing industry flow codes.
- It has a novel averaging scheme to reduce memory requirement.
- It contains a general chemistry package.
- There is a parallelized workstation version.

4.4 NPARC Turbulence module

NPARC is a CFD code widely used by NASA and industry. A turbulence subprogram has been developed for this code.

- The models already built-in at the present time are:
  two mixing length models; the Chien $k-\varepsilon$ model; and the CMOTT $k-\varepsilon$ model.
- The models to be built-in are:
  the CMOTT Reynolds stress algebraic equation model; a Reynolds stress transport equation model; and other models requested by CFD users.
- A robust numerical solver is built-in for the model equations.

4.5 V-STAGE turbomachinery turbulence module

V-STAGE is an advanced turbomachinery code developed at NASA LeRC.

- The built-in turbulence model is the CMOTT $k-\varepsilon$ model.

5. Collaboration program and technology transfer

5.1 Joint programs with NASA LeRC and industry

- Preliminary programs with engine companies and others have been initiated (GE, P&W, RocketDyne, Naval Research Laboratories).
- Joint programs with the offices of Advanced Subsonic Technology (AST), High Speed Research (HSR) and Numerical Propulsion System Simulation (NPSS) have been developed as ongoing programs with which industry partners will also be closely involved.

5.2 Industry-wide workshop

The industry-wide workshop will be a regular program held once every other year to:

- release Lewis turbulence and combustion modules to CFD users; and
- discuss the needs of industry and the state of the art in engineering turbulence modeling.

6. Models developed at CMOTT

Turbulence and combustion model development and validation are ongoing research activities. The following are a part of work done at CMOTT.

- Isotropic eddy viscosity models:
  NASA TM 105633[1], 105768[2], 106263[3], 106721[4].
- Reynolds stress and scalar flux algebraic equation models:
  NASA TM 106116[5], 106513[6], 106644[7], IJNMF[8].
- Second moment transport equation models:
  NASA TM 105351[9], 106469[10], 106681[11], 105954[12].
- Multiple-scale models for compressible turbulent flows:
  NASA TM 106072[13].
- Bypass transition models:

NWTF[14].

- PDF models for turbulent reacting flows:
  NASA TM 106614[15], AIAA[16], AIAA[17].

PROGRAM SUMMARY

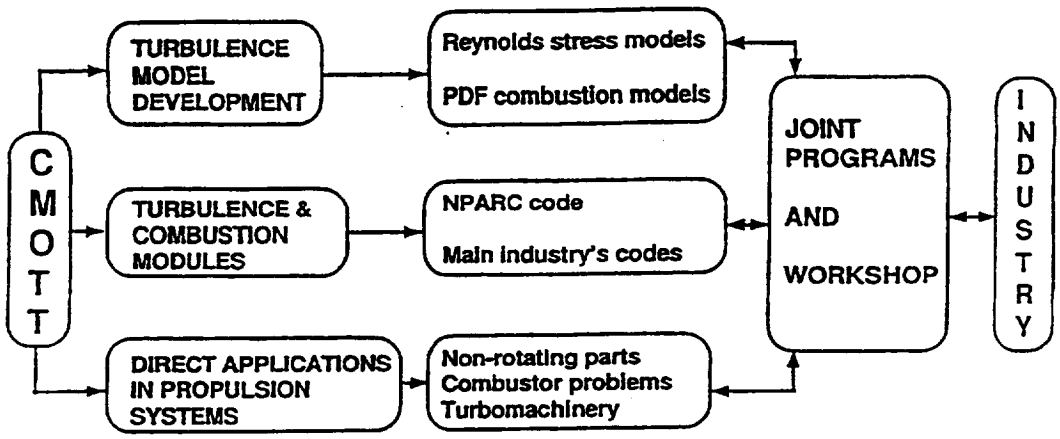

References

[1] Shih, T.-H. and Lumley, J. L., "Kolmogorov behavior of near-wall turbulence and its application in turbulence modeling," NASA TM 105663 (1992), also, *Comp. Fluid Dyn.* 1993, Vol. 1, p.43-56.

[2] Yang, Z. and Shih, T. -H., "A new time scale based $k - \epsilon$ Model for Near Wall Turbulence," NASA TM 105768, also, AIAA J. **31**, 1191-1198 (1993).

[3] Yang, Z. and Shih, T. -H., "A Galliean and tensorial invariant $k - \epsilon$ model for near wall turbulence," NASA TM 106263, also, AIAA 93-3105.

[4] Shih, T.-H., W.W. Liou, A. Shabbir, Z. Yang and J. Zhu, "A new $k - \varepsilon$ eddy viscosity model for high Reynolds number turbulent flows — model development and validation,", NASA TM 106721, August, 1994, also, *Computers Fluids* Vol. 24, No.3 pp.227-238, 1995.

[5] Shih, T.-H. and Lumley, J., "Remarks on turbulent constitutive relations," NASA TM 106116 (1993), also, *Mathl. Comput. Modeling* Vol. 18, No. 2, pp. 9-16, 1993.

[6] Shih, T.-H., J. Zhu and J. Lumley, "Modeling of wall-bounded complex flows and free shear flows," NASA TM 106513 (1994).

[7] Shih, T.-H., J. Zhu and J. Lumley, "A new Reynolds stress algebraic equation model," NASA TM 106644 (1994), also, to appear in *Comput. Methods Appl. Mech. Eng.*

[8] Zhu, J. and T.-H. Shih, "Computation of confined coflow jets with three turbulence models," *Int. Journal for Numerical Methods in Fluids,* Vol. 19, pp. 939-956 (1994).

[9] Shih, T.-H. and Lumley, J.L., "Critical comparison of second order closures with direct numerical simulation of homogeneous turbulence," NASA TM 105351, also, AIAA J., **31**, 663-671 (1993)

[10] Shih, T.-H., Shabbir, A. and Lumley, J.L., "Realizability in Second Moment Turbulence Closures Revisited," NASA TM 106496 (1994).

[11] Shih, T.-H. and Shabbir, A., "Methods of Ensuring Realizability for Non-Realizable Second Order Closures," NASA TM 106681 (1994).

[12] Shabbir, A. and Shih, T.-H., "Critical comparison of second order turbulence models in homogeneous flows," NASA TM 105954 (1994).

[13] Liou, W. W., Shih, T. H. and Duncan, B. S., "A multiple-scale model for compressible turbulent flows," NASA TM 106072 (1993), also, *Phys. Fluids A*, Vol.7 (3), 1995.

[14] Yang, Z. and Shih, T.-H., "A $k - \varepsilon$ model for turbulent and transition boundary layers," Near-Wall Turbulent Flows, R.M.C. So, C.G. Speziale and B.E. Launder (Editors), 1993 Elsevier Science Publishors B.V.

[15] Noris A.T. and Hsu, A., "Comparison of PDF and Moment Closure Methods in the Modeling of Turbulent Reacting Flows," NASA TM 106614 (1994)

[16] Hsu, A. T., "Study of hydrogen diffusion flames using PDF turbulence model," AIAA paper 91-1780 (1991).

[17] Hsu, A., Raju, M.S. and Norris, A.T., "Application of a PDF method to compressible turbulent reacting flows," AIAA-94-0781, 1994.

$k-\epsilon$ Eddy Viscosity Turbulence Models: Development and Applications

Z. Yang

1. Motivation and Objective

The purpose of this research is to develop $k-\epsilon$ eddy viscosity models for the complex flows of engineering interest and to incorporate the resulting models into general purpose computational fluid dynamics (CFD) codes used to calculate practical flows relevant to aerospace and aero-propulsion systems.

2. Work Accomplished

In the following, work on model development and model applications will be reported briefly.

2.1 Model development

Because of the limitations of computer speed and storage, DNS (direct numerical simulation) is limited to flows of moderate Reynolds numbers and simple geometries. For the present and the foreseeable future, turbulence modeling is the only viable approach for the calculation of complex turbulent flows of engineering interest. In turbulence modeling, the k-ϵ eddy viscosity model is the most widely used model in engineering calculations. Many flows have been calculated by $k-\epsilon$ models. A set of model constants have emerged from these computational experiences, giving rise to what is commonly referred to as the standard $k-\epsilon$ model[1,2]. The standard $k-\epsilon$ model can be directly used for free shear flows. For wall bounded flows, it can be used in conjunction with wall functions which prescribe the flow field at the equilibrium log layer instead of at the wall. However universal wall functions do not exist in complex flows and it is thus necessary to develop a form of $k-\epsilon$ model equations which can be integrated down to the wall. Jones and Launder[3] were the first to propose such a low Reynolds number $k-\epsilon$ model for near wall turbulence, which was then followed by a number of similar $k-\epsilon$ models. A critical evaluation of the pre-1985 models was made by Patel et al.[4]. More recently proposed models are found in Lang and Shih[5].

The existing $k-\epsilon$ eddy viscosity models for near wall turbulence suffer from some well known deficiencies. (Some of the existing models may be free from one or two of these deficiencies.) First, a near wall pseudo-dissipation rate was introduced to remove the singularity in the dissipation rate equation at the wall. However, the definition of the near wall pseudo-dissipation rate was quite arbitrary. Second, the model constants were different from those of the standard $k-\epsilon$ model, making the near wall models less capable of handling flows containing both high Reynolds number turbulence and near wall turbulence, which is often the case for a real flow situation. Patel et al.[4] listed as the first criterion the ability of the near wall models

to be able to predict turbulent free shear flows. Third, the variable y^+ was used in the damping function f_μ of the eddy viscosity formula. Since the definition of y^+ involves u_τ, the friction velocity, any model containing y^+ can not be used in flows with separation and reattachment. In addition, y^+ may not be well defined for flows with complex geometries.

All the $k-\epsilon$ models for near turbulence reviewed in references 4 and 5 were constructed based on the standard $k-\epsilon$ model, i.e., they took the standard $k-\epsilon$ model form as the base form and added on it modifications due to the near wall effect. The standard $k-\epsilon$ model form itself has the following deficiencies: 1) the model is not realizable in that physically unrealistic Reynolds stresses could be obtained from the model in certain flow situations; 2) contrary to the experimental findings, the predicted spreading rate for a round-jet is larger than that for a planar-jet, a phenomenon commonly known as the planar-jet/round-jet anomaly; 3) the inadequate predicted response to pressure gradient of turbulent boundary layer flows with adverse pressure gradients is also attributed to the model form of the standard $k-\epsilon$ model, as pointed out by Wilcox[6].

The purpose of our research in the area of eddy viscosity modeling is to propose a $k-\epsilon$ eddy viscosity model which is free from the deficiencies mentioned above. In addition, we require the proposed model to be free from coordinate parameters in the model formulation. While coordinate information, distance to the wall for example, provides a convenient parameter to calibrate the model's damping functions, its use makes the model not tensorially invariant and thus unable to be incorporated into computational fluid dynamics (CFD) codes with unstructured grids. The final product of the present research is aimed at a realizable, tensorially invariant, and Galilean invariant $k-\epsilon$ eddy viscosity model which has the capability for both free shear flows and wall bounded flows.

The components for such a model have been developed in the past few years. A variable C_μ formulation has been proposed, in which C_μ depends on the solutions of the mean flow field and the turbulence field. The C_μ formulation was derived based on the realizability constrains, rapid distortion theory (RDT), and the invariants theory. The Reynolds stresses from the $k-\epsilon$ eddy viscosity model using the proposed C_μ formulation are always realizable in that no physically un-admissible Reynolds stresses will ever be produced. The variations of C_μ with flow situations are in the right direction as well, i.e., the value of C_μ is smaller than 0.09 in regions where it should be. Such a variation of C_μ with flow situations make the model calculation numerically more robust, particularly when the model is used to calculate flows with large strain rate variations, for example, the flow of shock-wave/turbulent boundary layer interactions. The detail of the proposed C_μ formulation and the corresponding model performance for benchmark free shear flows and wall bounded flows can be found in Shih et al.[7]

The dissipation rate equation in the standard $k-\epsilon$ model has a singularity at the wall, where the turbulent kinetic energy is equal to zero. To remove this singularity, and yet without introducing an arbitrary pseudo-disspation rate, the $k-\epsilon$ model was reformulated using velocity-scale and time-scale instead of the traditionally

used velocity-scale and length-scale. It was further argued that the turbulent time scale should be bounded from below by the Kolmogorov time scale which is always non-zero. With such a turbulence time scale, the resulting dissipation rate equation remains singularity-free everywhere in the flow field. The resulting dissipation rate equation is computationally very robust. The details of using Kolmogorov behaviors to aid the $k-\epsilon$ eddy viscosity models for near wall turbulence can be found in Yang and Shih[8] and Shih and Lumley[9].

It is a challenging task to propose a $k-\epsilon$ eddy viscosity model for near wall turbulence which does not contain coordinate information. The difficulty lies in the lack of proper parameter(s) to calibrate the near wall effect. In their paper on the first $k-\epsilon$ eddy viscosity model for near wall turbulence, Jones and Launder[3] used R_t, the turbulence Reynolds number, to calibrate the near wall effect. R_t is a field quantity, and does not depend on the coordinate system. Thus, a $k-\epsilon$ model with R_t is tensorially invariant. However, the performance of the resulting model is not very satisfactory, partly due to the fact that the near wall region for R_t is confined to y^+ about 20 while the near region for the damping function f_μ extends to the lower end of the equilibrium log layer, which normally has a y^+ value of about 60. Other researchers have later used y, the distance to the wall, as a parameter to calibrate the near wall effect. Models using y in the damping functions are found to give a better performance due to the fact that y grows more gradually in the near wall region compared with R_t. However, any model with coordinate information will not be tensorially invariant. In addition, the definition of wall distance will be ambiguous in complex flows with complex geometries.

Recently, Yang and Shih[10] have introduced a new parameter R to calibrate the near wall effect. R is defined as $R = \frac{k}{S\nu} = \frac{k^2}{\epsilon\nu} / \frac{Sk}{\epsilon}$, and is related to the following two important physical parameters: the turbulent Reynolds number and the time scale ratio of the turbulence to the mean flow. R defined above is expressed in terms of the local field variables and is thus coordinate independent. In the near wall region, R is found to increase with y^+ in a gradual and monotonic manner. This property makes R an ideal candidate for constructing the damping function. In Yang and Shih[10], such a damping function f_μ was constructed to model the near wall effect. The proposed $k-\epsilon$ model for near wall turbulence uses the standard $k-\epsilon$ model as the corresponding high Reynolds number model and the resulting model was validated for turbulent channel flows and turbulent boundary layer flows with different pressure gradients.

To adequately capture the effect of pressure gradient on turbulent boundary layers, inhomogeneity effect was introduced in the dissipation rate equation. Since the dissipation rate represents the energy transfer from the large eddies to the small eddies in a turbulent flow, it is expected that the inhomogeneity in the large eddies would have an effect on the energy transfer rate. The previously used dissipation rate model is a homogeneous model in the sense that other than the diffusion term, the source terms remain the same for both homogeneous flows and inhomogeneous flows. In the present study, the effect of flow inhomogeneity is modeled directly as an extra production/destruction source term in the dissipation rate equation.

This extra source term is required to vanish when the flow is homogeneous. In the framework of $k-\epsilon$ eddy viscosity model, and for the case of weak inhomogeneity, we characterize the inhomogeneity by ∇k and ∇S, which represent the inhomogeneity of the turbulent field and the inhomogeneity of the mean field, respectively. Invariants theory was used to deduce the possible forms of the source term. The resulting model constants in the source term were further calibrated against a turbulent boundary layer flow with favorable pressure gradients (the Herring and Norbury flow[11]) and a turbulent boundary layer flow with adverse pressure gradients (the Bradshaw flow[12].) The resulting model was found to work well for other boundary layer flows with different pressure gradients. The model description and flow calculations can be found in Yang and Shih[13].

The round-jet/planar-jet spreading rate anomaly is a long standing issue for turbulence modeling community. This anomaly is not only observed for two equation eddy viscosity models, it is also observed for second order closure models. This suggests that the dissipation rate equation needs to be modified in order to resolve this anomaly, as pointed out by other researchers. The present research confirms this conjecture and finds that either the extra source term in the dissipation rate equation due to the inhomogeneity effect reported in reference 13 or the new dissipation rate equation based on the dynamic equation for the fluctuating vorticity reported in reference 7 can resolve this round-jet/planar-jet spreading rate anomaly. The computational results are found in the corresponding references.

Now, we have in place all the essential components to construct a realizable, tensorially invariant, and Galilean invariant $k-\epsilon$ eddy viscosity model which works well for both free shear flows and wall bounded flows. The variable C_μ formulation will ensure the realizability of the proposed model; the analysis of the Kolmogorov behaviors of turbulence will make the model singularity-free without introducing any arbitrary pseudo-dissipation rate; a new parameter R has been found which possess the needed properties to calibrate the damping functions for near wall flows; the effects of pressure gradients on turbulent boundary layers are captured via an extra source term in the dissipation rate equation representing the contribution from flow inhomogeneity; the round-jet/planar-jet spreading rate anomaly can be resolved via the changes in the model dissipation rate equation, either by the contribution of the inhomogeneity effect or by the new dissipation rate equation based on the dynamic equation for the fluctuating vorticity. Now, what needs to be done is to put all the components together and test the resulting model against a large variety of flows of practical interest. This is a topic of our current research.

2.2 Model applications

The purpose of engineering turbulence modeling research is to use the proposed turbulence models to calculate flows of engineering interest. Thus, the ultimate test for our research on turbulence models lies in the ability of the proposed models to calculate flows in aerospace and aero-propulsion systems. To this end, it is necessary to install the proposed models into a CFD code which serves as a numerical test-bed. In order to isolate the effect of turbulence model, the numerical test-bed should be a well established code with a well developed numerical scheme. The code should

be able to handle a wide range of flow situations and should be widely used in the aerospace and aero-propulsion community.

In the present study, NPARC is chosen as the numerical test-bed for model applications. NPARC is a general purpose computational fluid dynamics (CFD) code. It has a large user group in aerospace and aero-propulsion community. The code solves the Navier-Stokes equations in a conservation form in a general coordinate system. It can handle complex geometries and different types of boundary conditions. A description of the code and its numerical scheme is given by Cooper and Sirbaugh[14]. Updates of code capabilities and a listing of bibliographies of using the NPARC code to calculate flows of practical interests can be found in the current version of the NPARC User Guide[15]. The NPARC code is actively supported by NASA Lewis Research Center via the NPARC Alliance, a partnership formed between NASA Lewis Research Center and Air Force Arnold Engineering Development Center. The NPARC users are represented by the NPARC Association currently headed by Boeing Company and McDonnell Douglas Company.

Two-equation $k - \epsilon$ eddy viscosity turbulence models are incorporated into the NPARC code via a separate turbulence subprogram written by Dr. Zhu of CMOTT. (For a description of the philosophy and the structure of the subprogram, please see Zhu and Shih[16].) Different turbulence models have been tested against typical flows in propulsion systems, including, for example, the ejector nozzle flows, transonic diffuser flows, and the boat-tail nozzle flows. Details of flow calculations using the NPARC code and the turbulence subprogram are going to be presented by Yang et al.[17] in the upcoming 1995 AIAA Joint Propulsion Conference.

By installing the advanced turbulence models into the NPARC code, NPARC's turbulence modeling capability is enhanced. Turbulence model development for NPARC is CMOTT's long term activity in supporting NASA's High Speed Research (HSR) Program. Research in this area, together with model applications using the NPARC code, is described in more detail in this research brief in the article entitled "Turbulence Model Development for NPARC."

3. Future Plans

1) Turbulence modeling: development and applications

We will first finish the research on a realizable, tensorially invariant, and Galilean invariant $k - \epsilon$ eddy viscosity model. The model is going to be validated for both simple shear flows, such as free shear flows and boundary layer flows, and the complex flows in aero-propulsion systems. Then, we will proceed with the development of Reynolds stress models for wall bounded turbulent flows. The final product in the latter area of research is a realizable, tensorially invariant, and Galilean invariant second order closure model.

2) Transition modeling

We will be working on the modeling and calculation of transitional flows over a low-pressure (LP) turbine blade. This research will be part of NASA's Low Pressure Turbine Flow Physics Program. For such flows, the transition is induced by the high turbulence level associated with the free-stream and the incoming wake, giving rise

to what is referred to as the bypass transition. The final product of this research will be a two equation model for transitional flow of bypass transition type.

4. References

[1] Launder, B.E. and Spalding, D.B., "The numerical computation of turbulent flow," Computer Methods in Applied Mechanics and Engineering **3**, 269 (1974).

[2] Rodi, W., *Turbulence Models and Their Application in Hydraulics*, Book Pub. of International Association for Hydraulic Research, Delft, the Netherlands, 1980.

[3] Jones, W.P., and Launder, B.E., "The calculation of low-Reynolds number phenomena with a two-equation model of turbulence," Intl. J. of Heat and Mass Transfer **16**, 1119 (1973).

[4] Patel, V.C., Rodi, W., and Scheuerer, G., "Turbulence models for near-wall and low-Reynolds number flows: a review," AIAA J. **23**, 1308 (1985).

[5] Lang, N.J. and Shih, T.H., "A critical comparison of two equation turbulence models," NASA TM 105237 (1991).

[6] Wilcox, D.C., "Application of low Reynolds number two-equation turbulence models to high Reynolds number flows," in *Near Wall Turb. Flows*, Elsevier, 1993.

[7] Shih, T.-H., Liou, W.W., Shabbir, A., Yang, Z. and Zhu, J., "A new k-ϵ eddy viscosity model for high Reynolds number turbulent flows - Model development and validation," J. of Computers and Fluids, **24**, no. 3, 1995.

[8] Yang, Z. and Shih, T.H., "A new time scale based $k-\epsilon$ model for near wall turbulence," AIAA J. **31**, 1191 (1993).

[9] Shih, T.-H., and Lumley, J.L., "Kolmogorov behavior of near-wall turbulence and its application in turbulence modeling," Comp. Fluid Dyn. **1**, pp.43-56 (1993).

[10] Yang, Z. and Shih, T.H., "A Galilean and tensorial invariant $k-\epsilon$ model for near wall turbulence," AIAA Paper 93-3105 (1993).

[11] Herring, H.J., and Norbury, J.F., "Some experiments on equilibrium turbulent boundary layers in favorable pressure gradients," J. Fluid Mech. **27**, 541 (1967).

[12] Bradshaw, P., "Equilibrium boundary layer in moderate positive pressure gradient," *Computation of Turbulent Boundary Layers-1968 AFSOR-IFP Stanford University*, Coles, D. E. and Hirst, E. A. edt., Vol.2, pp.241-248.

[13] Yang, Z. and Shih, T.H., "Flow inhomogeneity and the dissipation rate equation," Accepted for presentation at the 5th Euro. Turb. Conf., July 1994, Siena, Italy.

[14] Cooper, G.K. and Sirbaugh, J.R., *PARC code: theory and usage*, AEDC-TR-89-15, Arnold Engineering Development Center, 1989.

[15] NPARC Alliance Technical Team, *A User's Guide to NPARC*, Version 2.0, 1994.

[16] Zhu, J. and Shih, T.H., "A turbulence module for the NPARC code," to be presented at the AIAA Joint Propulsion Conference, San Diego, July (1995).

[17] Yang, Z., Georgiadis, N., Zhu, J. and Shih, T.H., "Calculations of inlet/nozzle flows using a new k-ϵ model," to be presented at the AIAA Joint Propulsion Conference, San Diego, July (1995).

Turbulence Modules for CFD Codes

Jiang Zhu

1. Motivation and Objectives

It has been long recognized that there is a gap between turbulence model developers and CFD users. The former mainly use simple flows to verify new modeling concepts and evaluate the resulting models, while the latter are usually reluctant to implement and test new, more advanced turbulence models unless and until they see such models showing good performance for a wide range of complex flow situations. Turbulence model equations also require special treatment to ensure numerical realizability such as the positiveness of the turbulent kinetic energy and its dissipation rate.

In order to bridge this gap, we develop turbulence modules for industry's CFD codes. The modules are written in a self-contained manner so that the user can use any turbulence model in the modules without worrying about how it is implemented and solved. The input to a module is mean flow variables, boundary and geometric information which are to be provided by a mean flow solver, and the output of the module is the turbulent diffusivity and relevant turbulent source terms which are needed for the mean flow calculation. The interaction between the mean flow solver and the turbulence module will give the final turbulent flow solution. With the aid of the modules, we can also take the advantage of the well-established and sophisticated CFD codes to test turbulence models for a variety of complex flows which are intractable with the simple research codes.

2. Work Accomplished

2.1 The NPARC Code

The NPARC code has been used extensively by the U.S. aerospace community to analyze propulsion flows. However until recently, only algebraic models such as the Thomas and Baldwin-Lomax have been available in NPARC for turbulent flow simulations. The Chien low Reynolds number k-ϵ model with modifications for compressibility has been available in the 2D version but was not successfully installed in the 3D version. Another k-ϵ model (the NPARC 1.0 k-ϵ model) was installed in both the 2D and 3D versons but has not provided desirable accuracy and stability.

In order to improve the NPARC's capability to calculate turbulent flows, the two-equation turbulence model in the NAPRC code (both the 2D and 3D versions) was modified[1] so that the model is based on the low Reynolds number k-ϵ model of Chien and no longer on the NPARC 1.0 k-ϵ model. Stability enhancements and a new inflow boundary condition for the turbulent quantities were also added to the k-ϵ model. Comparisons of the NPARC solutions obtained using the previous and new models with experimental data indicated that the Chien k-ϵ model installed in this work improves the capability of the NPARC to calculate propulsion flows.

2.2 A Turbulence Module for the FAST2D Code

FAST2D is a computer program developed at the CFD group of Prof. Rodi[2] for calculating two-dimensional, incompressible, elliptic flows with complex boundaries. Here "two-dimensional" stands for plane or axisymmetric flows with or without swirling. FAST2D is a finite-volume procedure and uses non-staggered grids and the cell-center arrangement, i.e., the flow variables are stored at the geometric centers of control volumes, with grid lines forming the faces of the control volumes. FAST2D is being used at CMOTT as a research code. The turbulence module, termed as FAST2DTS-1, is similar in structure to FAST2D. To reduce numerical diffusion while maintaining necessary stability, the second-orde accurate HLPA scheme[3] is used for the convective terms of the turbulent transport equations. This scheme is implemented such as to blend two schemes by a parameter λ, with limiting values λ=0 for the (first-order) upwind and λ=1 for the second-order and bounded solution. Seven turbulence models have been built into the module: the standard k-ϵ, CMOTT k-ϵ, k-ω, CMOTT Reynolds stress algebraic equation model, Launder-Sharma, Chien and Shih-Lumley, with the first four being high- and the last three being low-Reynolds number models. The module includes the four most commonly used boundary conditions - inflow plane, outflow plane, symmetry plane and solid wall. The solid wall boundary condition is formulated either by the standard wall-function approach or by a low-Reynolds-number procedure, depending on the turbulence models used. The program also allows the user to introduce boundary conditions other than these four types. Care has been taken to make the module user-friendly. This is achieved by providing a few parameters defining the types and locations of boundaries, which allows the user to choose the boundary conditions given in the module by simply specifying these parameters. The system of algebraic difference equations is solved using the alternating direction TDMA of Thomas.

2.3 A Turbulence Module for the NPARC 2D Code

NPARC is a compressible flow code. Its 2D version is currently restricted to plane or axisymmetric flows without swirling. The turbulence module (NP2DTS-1)[4] written for NPARC 2D has much in common with the above FAST2DTS-1. Only the following points are worthy of mention: (a) the cell-corner arrangement is used, i.e., the flow variables are stored at grid nodes rather than at the centers of control volumes; (b) contrary to NPARC and most other compressible codes, the non-delta form of equations is used which leads to simple linearization and is more effective to ensure the positiveness of the turbulent kinetic energy and its dissipation rate than the delta form; and (c) four turbulence models have been built into the module: Baldwin-Lomax, Chien, Shih-Lumley and CMOTT realizable models, the first being the algebraic eddy-viscosity model and the last three the low Reynolds number k-ϵ models. The NPARC 2D code coupled with the module NP2DTS-1 have been applied[5] to a series of flows including the flow over a flat plate, in an ejector nozzle, in a transonic diffuser, and a boat-tail nozzle flow. Both NP2DTS-1 and FAST2DTS-1 were released at the 1994 Industry-Wide Workshop on Computational Turbulence Modeling, held at the Ohio Aerospace Institute.

2.4 A Turbulence Module for the VSTAGE Code

NASA LeRC currently has a very extensive research program on turbomachinery flow physics that is both experimental and computational. World class experimental facilities exist to provide a multitude of experimental data for both component design needs and CFD comparisons. CFD turbomachinery tools are also well developed after many years of testing and validation. The VSTAGE code, developed at Dr. Adamczyk's group of the Lewis Research Academy, is one such tool. At present it is a proven CFD code which is being used by major U.S. engine companies in their design analysis. In a recent blind testing for a rotor compressor (designated Rotor 37) organized by the ASME/International Gas Turbine Conference held at the Hague, 1994, the VSTAGE prediction turned out to be among the best of predictions submitted by a total of 12 groups. However, the best predictions for Rotor 37 were still less than satisfactory for the purpose of design, and this was mainly attributed to turbulence modeling. The VSTAGE is equipped only with the commonly used Baldwin-Lomax mixing length model. The limitations of such model are quite apparent from the predictions for Rotor 37 case. It is questionable whether improvements in predicting transonic rotor flows can be made using this model. Thus a turbulence module is developed for VSTAGE. The reasons of developing this module are twofold: 1) to provide VSTAGE with more general and advanced turbulence models beyond the algebraic level; and 2) using VSTAGE as a common numerical platform to assess the performance of different existing and newly developed turbulence models for turbomachinery flows. The module has the same numerical framework as that of the NPARC module but is written exclusively for VSTAGE. As a result, it has the following unique features: (a) the cylindrical coordinate system (x, r, θ) is used as the absolute (fixed) reference frame, and correspondingly the cylindrical coordinate components of the flow velocity are used in the curvilinear transformation of equations; (b) the rotational effect is taken into account by transforming the absolute reference frame to the relative (rotating) frame; (c) instead of the commonly used metrics such as $J, \xi_x, \xi_\theta, ...$, the module uses volumes and areas of control volumes as the major geometric quantities, which is in line with the definition of variables in VSTAGE; and (d) the data transfer between VSATGE and the module is via the Fortran common blocks. Three high Reynolds number k-ϵ models have been implemented, one standard and two CMOTT realizable models. The CMOTT models differ from each other in the dissipation rate equation, one using the standard equation and the other the newly developed equation[6]. The wall function approaches are used to formulate the solid wall boundary conditions. The code validation is being under way, and the preliminary results for Rotor 37 test case look promising.

2.5 Calculation of Wall-Bounded Complex Flows

This study[7] concentrates on complex turbulent shear flows which are of great interest in propulsion systems. These flows are backward-facing step flows, confined coflowing jets, confined swirling coaxial jets, U-duct flows and diffuser flows. Most of these flows have complex structures. For example, the confined coflowing

jet combines several types of flow structures, such as the shear layer, jet, recirculation, separation and reattachment. Accurate prediction of these flows is of great importance for engine design in all its key elements.

The turbulence model used in this study is a recently developed realizable Reynolds stress algebraic equation model[8,9] which is fundamentally different from the traditional algebraic Reynolds stress models. The present model is developed using the invariance theory in continuum mechanics. This theory leads to a general constitutive relation for the Reynolds stress tensor in terms of the mean deformation rate tensor and the turbulent velocity and length scales characterized by the turbulent kinetic energy and its dissipation rate. Realizability is imposed directly on the constitutive relation for the Reynolds stresses to determine the coefficients in the relation. As a result, a realizable explicit expression for the Reynolds stresses is obtained for general three-dimensional turbulent flows. Some model constants were fine-tuned against a backward-facing step flow and then tested in other flows.

The calculations were performed using the FAST2D code. Grid independent and low numerical diffusion solutions were obtained by using differencing schemes of second-order accuracy on sufficiently fine grids. The standard wall function approach was used for wall boundary conditions. Calculations using the standard k-ϵ (SKE) model were also carried out for the purpose of comparison.

Diffuser Flows. Two conical diffuser flows were calculated, one with a 8° total angle (Trupp et al.'s case) and the other 10° (Fraser'case). In both cases, the flows undergo strong adverse pressure gradients but remain attached. Although the flow configuration looks simple, it is not easy to calculate this type of flow accurately, especially for the boundary layer quantities. Fig.1 shows the variation of calculated and measured wall friction coefficient C_f with the axial distance x/R_o (R_o is the inlet duct radius). It is seen that the result of the present model is in good agreement with the experimental data, while the SKE model overpredicts C_f along almost the entire length of the diffuser. The calculated and measured displacement thickness δ^* are compared in Fig.2. The comparison shows that the SKE model gives a good prediction in the upstream region, but deviates significantly from the experiment downstream; the present model prediction is good in the whole region. Fig.3 shows the comparison of calculated and measured shape factor H. This is the case in which the worst agreement with the measurement has been found for both models. Nevertheless, the present model still performs considerably better than does the SKE model.

U-Duct Flow. This case is the experiment of Monson et al. (1990) conducted in a 180° planar turnaround duct. It features flow with large streamline curvature. Calculations were compared to the experiment taken at a flow Reynolds number of 10^6. Fig.4 shows the streamlines computed with the present model. A small separation region is found at the bend exit. However, the SKE model did not predict the flow separation. Fig.5 shows the comparison of calculated and measured C_f along the inner wall. The bend is located between $21.7 \leq s/H \leq 24.8$. Both models are seen to behave in the same manner and produce large discrepancies in the bend region. The reason for this may partially due to the use of the wall function which

does not respond to the severe pressure gradient.

Backward-Facing Step Flows. Two backward facing step flows, measured by Driver and Seegmiller (1985) and Kim et al. (1978), were calculated. The former (DS case) has a smaller and the latter (KKJ case) a larger step expansion. The computed and measured reattachment points are compared in Table 1. The calculated reattachment point from the present model agrees well with the experiments. Fig.6 shows the comparison of the computed and the measured static pressure coefficient C_p along the bottom wall. The SKE model is seen to predict a premature pressure rise, which is consistent with its underprediction of the reattachment length, while the present model captures the pressure rise quite well. Fig.7 shows the comparisons of predicted and measured turbulent stresses $\overline{uu}$, $\overline{vv}$ and $\overline{uv}$ at the location x=2 which is in the recirculation region. In the KKJ-case, no reliable experimental data exist for the turbulent stresses due to the unsteadiness of the flow. However, the experimental data of the DS-case is considered more reliable because of the smaller unsteadiness of the flow. As compared with the results of the SKE model in Fig.7, it is seen that the anisotropic terms in the present model increase $\overline{uu}$ and decrease $\overline{vv}$, leading to significant improvements in both $\overline{uu}$ and $\overline{vv}$ except in the near-wall region. On the other hand, the anisotropic terms have little impact on $\overline{uv}$. The improvement obtained by the present model for $\overline{uv}$ is mainly due to the reduction in C_μ by strain rate.

Table 1. Comparison of the reattachment points

Case	measurement	SKE	PRESENT
DS	6.26	4.99	5.82
KKJ	7± 0.5	6.35	7.35

Confined Jets. The general features of confined jets are sketched in Fig.8. At the entrance, two uniform flows, a jet of larger velocity and an ambient stream of smaller velocity, are discharged into a cylindrical duct of diameter D_o. The inlet flow conditions can be characterized by the Craya-Curtet number C_t. The experiment shows that recirculation occurs when C_t <0.96. For a given geometry, recirculation as well as adverse pressure gradients can be intensified by reducing the value of C_t at the entrance. The separation and reattachment points of the predicted recirculation bubbles are compared with the experimental data in Fig.9. The experiment indicated that as C_t decreases, the separation point moves upstream while the reattachment point remains practically unchanged. The present model captures this feature well and predicts both the separation and reattachment points much better than does the SKE model. The variation of the pressure coefficient C_p along the duct wall is shown in Fig.10. The pressure distribution is governed by the jet entrainment as well as the contraction and expansion of the flow caused by the recirculation bubble. The decrease in the ambient velocity induced by the entrainment gives rise to an adverse pressure gradient, while the contraction of streamlines produces the opposite effect. These two mechanisms interact more intensely with

each other as C_t decreases and cause the pressure to vary little in the region upstream of the center of the recirculation bubble. However, in the downstream part of the recirculation bubble, the deceleration of the flow sets up an adverse pressure gradient, the slope of which becomes steeper as C_t decreases. Therefore, the ability to capture the location of the recirculation center will have a direct impact on the prediction of the pressure. Regarding the comparison between predictions and experiments, it is seen that although both models predict practically the same total pressure rises which are in excellent agreement with the measurements, the present model captures the steep pressure gradients better than does the SKE model for all of the C_t values.

Confined Swirling Coaxial Jets. This is the case experimentally studied by Roback and Johnson (1983). Fig.11 shows the general features of the flow. At the inlet, an inner jet and an annular jet are ejected into an enlarged duct. Besides an annular recirculation bubble due to sudden expansion of the duct, a centerline recirculation bubble is created by flow swirling. Fig.12 compares the calculation of the centerline velocity with the experiment. The negative velocity indicates the central recirculation. It is seen that both models predict the strength of central recirculation and the front stagnation point quite well, but the present model predicts the rear stagnation point much better than does the SKE model. Fig.13 shows the comparison of calculated and measured mean velocity profiles at x=5.1cm. Both models give reasonably good profiles which are within experimental scatter, except for the peak values of the axial and radial velocities. Both models have been found to give nearly the same results in the downstream region, which can also be seen from Fig.12.

These comparisons show that the present realizable Reynolds stress algebraic equation model significantly improves the predictive capability of k-ϵ equation based models, expecially for flows involving massive separations or strong shear layers. In these situations, the standard eddy viscosity model overpredicts the eddy viscosity and, hence, fails to accurately predict wall shear stress, separation, recirculation, etc. We find that the success of the present model in modeling the above mentioned complex flows is largely due to its effective eddy viscosity formulation which accounts for the effect of mean shear rates. According to the present model, the effective eddy viscosity will be significantly reduced by the mean strain rate and maintained at a correct level to mimic the complex flow structures.

2.6 A New k-ϵ Eddy Viscosity Model

The model[6] has a new dissipation rate equation and a new realizable eddy viscosity formulation. The former is based on the dynamic equation for fluctuating vorticity and the latter is derived from the realizability analysis. The model contains the effect of mean rotation on turbulent stresses, and its dissipation rate equation has an always positive production term, which is expected to enhance the numerical stability in turbulent flow calculations, especially when using more advanced closure schemes such as second-order closures.

Comparisons with experimental data show that the model performs better than the standard k-ϵ model for almost all the flows tested[6]. The performance of the

model for complicated recirculating flows is demonstrated through calculations for two backward-facing step flows, one (DS-case) with smaller and the other (KKJ-case) with larger step height, both of which have been extensively used in the literature to benchmark calculations of separated flows. Sufficiently fine grids, with 201×109 points in the DS-case and 199×91 points in the KKJ-case, were used to establish numerical credibility of the solutions. The computational domain had a length of 50 step heights, one fifth of which was placed upstream of the step. The experimental data were used to specify the inflow conditions, the fully-developed flow conditions were imposed at the outflow boundary, and the standard wall function approach was used to bridge the viscous sublayer near the wall. The comparison with the standard k-ϵ model and the experiments is shown in Table 2 for the reattachment length.

Table 2. Comparison of the reattachment point locations

Case	measurement	standard model	present model
DS	6.26	4.99	6.02
KKJ	7± 0.5	6.35	7.5

The comparison of the size of the separation bubble, the skin friction pressure coefficients shows that the overall performance of the present model is better than that of the standard model.

2.7 A New Reynolds Stress Algebraic Equation Model

A new Reynolds stress algebraic equation model has been developed using a truncated constitutive relation[10]. This model differs from the previous one[8] mainly in: (a) it has a simpler quadratic form; (b) it shows the proper lack of a rotation effect on the isotropic turbulence, satisfying the rapid distortion theory; and (c) it is fully realizable, i.e., it ensures both the positivity of the normal Reynolds stresses and the Schwarz' inequality between turbulent velocity correlations. The model were first calibrated using well-studied basic flows such as homogenous shear flow and the surface flow in the inertial sublayer and then applied to complex flows including the separated flow over a backward-facing step and the flow in a confined jet.

Basic flows. Two basic cases were considered; they are Tavoularis and Corrsin's (1981) homogeneous shear flow and the direct numerical simulation of channel flow (Kim, 1990). The model gives $b_{12} = -0.156$, $b_{11} = -b_{22} = 0.123$ for the homogeneous shear flow at $U_{1,2}k/\epsilon = 6.08$ and gives $b_{12} = -0.122$, $b_{11} = -b_{22} = 0.14$ for the channel flow in the inertial sublayer at $U_{1,2}k/\epsilon = 3.3$. These results show that the present model gives reasonable anisotropy of Reynolds stresses for both the homogeneous shear flow and the boundary layer flow compared to the standard k-ϵ eddy viscosity model which gives $b_{11} = b_{22} = 0$ for both the flows and gives $b_{12} = -0.273$ for the homogeneous shear flow and $b_{12} = -0.149$ for the boundary layer flow. Detailed comparisons with the experimental and DNS data are shown in Table 3 for the homogeneous shear flow and in Table 4 and Fig.14 for the channel

flow.

Table 3. Anisotropy in the homogeneous shear flow

	experiment	standard	present
b_{12}	-0.142	-0.273	-0.156
b_{11}	0.202	0.	0.123
b_{22}	-0.145	0.	-0.123

Table 4. Anisotropy in the channel flow

	DNS data	standard	present
b_{12}	-0.145	-0.149	-0.122
b_{11}	0.175	0.	0.14
b_{22}	-0.145	0.	-0.14

Backward-facing step flows. Figs.15(a) and (b) show the friction coefficient C_f at the bottom wall calculated with the SKE model and the present model; also included in fig.15(a) are the experimental data for the DS-case, but no such data are available for the KKJ-case. It can be seen that the grid refinement does produce some differences for the results of the present model, more noticeable in the KKJ-case, and this is also the case for the SKE results. This indicates that the solutions obtained on the coarse grids are not sufficiently close to the grid-independent stage. Recently, Thangam and Hur (1991) have conducted a highly-resolved calculation for the KKJ-case. They have found that quadrupling a 166×73 grid leads to only a minimal improvement. Therefore, the present results on the fine grids can be considered as grid-independent. For the DS-case, the fine grid computations with the SKE model and present model required 703 and 691 iterations, and took approximately 7.1 and 9 minutes of CPU time on the Cray YMP computer. In the following, only the fine grid results are presented.

The wall friction coefficient C_f is a parameter that is very sensitive to the near-wall turbulence modeling. It is C_f that the various low Reynolds number k-ϵ models tested predict much worse than those using wall functions. However, the influence of the near-wall turbulence modeling is mainly restricted to the near-wall regions. It is seen from fig.15(a) that both the SKE model and the present model largely underpredict the negative peak of C_f, pointing to limited accuracy of the wall function approach in the recirculation region.

The computed and measured reattachment points are compared in Table 5. They are determined in the calculation from the point where C_f goes to zero. The reattachment point is a critical parameter which has often been used to assess the overall performance of turbulence models as well as numerical procedures. Table 5 clearly demonstrates the significant improvement obtained with the present model. It is important to mention that this improvement is mainly due to the behavior of C_μ in the present model, and that the anisotropic behavior of the turbulent stresses only makes a marginal contribution to it.

Table 5. Comparison of the reattachment points

Case	measurement	SKE	PRESENT
DS	6.26	4.99	5.80
KKJ	7± 0.5	6.35	7.27

Figs.16(a) and (b) show the comparison of computed and measured static pressure coefficients C_p along the bottom wall. In both cases, the SKE model is seen to predict premature pressure rises which is consistent with its underprediction of the reattachment lengths.

Finally, the comparisons of predicted and measured turbulent stresses $\overline{uu}$, $\overline{vv}$ and $\overline{uv}$ are shown in figs.17 and 18 at various x-locations. In the KKJ-case, no experimental data for the turbulent stresses are available in the recirculation region, and the reattachment point was found in the experiment to move forward and backward continuously around seven step heights downstream of the step, leaving an uncertainty of ± 0.5 step height for the reattachment length. This also points to some uncertainty in the measured turbulent quantities in the recovery region. On the other hand, the experimental data in the DS-case should be considered more reliable because of the smaller uncertainty of the reattachment location, indicating a smaller unsteadiness of the flow. The SKE model gives unrealistic results about normal Reynolds stresses: $\overline{vv} > \overline{uu}$ at all the locations. In contrast, the present model gives at least qualitatively correct results due to the non-linear terms which increase $\overline{uu}$ while decreasing $\overline{vv}$, leading to an overall improvement in both $\overline{uu}$ and $\overline{vv}$ results.

Confined Jets. The predicted axial mean velocity profiles at two C_t numbers are shown and compared with the experimental data in fig.19, where R and Um are the radius of the cylinder and the sectional mean velocity, respectively. Both models are seen to predict very well the upstream evolution of the flow. As for the downstream development, the results of the present model remain in good agreement with experiments while the SKE model underpredicts the centerline velocity decay at all C_t numbers. The variation of the pressure coefficient C_p along the duct wall is shown in fig.20. The pressure distribution is governed by the jet entrainment as well as the contraction and expansion of the flow caused by the recirculation bubble. The decrease in the ambient velocity induced by the entrainment gives rise to an adverse pressure gradient, while the contraction of streamlines produces the opposite effect. These two mechanisms interact more intensely with each other as C_t decreases and cause the pressure to vary little in the region upstream of the center of the recirculation bubble. However, in the downstream part of the recirculation bubble, the deceleration of the flow sets up an adverse pressure gradient, the slope of which becomes steeper as C_t decreases. Therefore, the ability to capture the location of the recirculation center will have a direct impact on the prediction of the pressure. Regarding the comparison between predictions and experiments, it is seen that although both models predict the same total pressure rises which are in excellent agreement with the measurements, the present model captures the pressure distribution much better than does the SKE model for all the C_t values.

3. Future Plans

1) To develop a 3D version of the turbulence module for the NPARC code;
2) To develop and validate the turbulence module for the VSTAGE code;
3) To test turbulence models developed at the CMOTT and elsewhere.

4. References

[1] Georgiadis, N.J., Chitsomboon, T. and Zhu, J., "Modification of the two-equation turbulence model in NPARC to a Chien low Reynolds number k-ϵ formulation," NASA TM 106710 (1994).

[2] Zhu, J., "FAST-2D: A computer program for numerical simulation of two-dimensional incompressible flows with complex boundaries," Report 690, Institute for Hydromechanics, University of Karlsruhe (1991).

[3] Zhu, J., "On the higher-order bounded discretization schemes for finite-volume computations of incompressible flows," *Comput. Meths. Appl. Mech. Eng.* 98, pp.345-360 (1992).

[4] Zhu, J. and Shih, T.H., "A turbulence module for the NPARC code," to be presented at the AIAA Joint Propulsion Conference, San Diego, July (1995).

[5] Yang, Z., Zhu, J. and Shih, T.H., "Calculations of inlet/nozzle flows using a new k-ϵ model," to be presented at the AIAA Joint Propulsion Conference, San Diego, July (1995).

[6] Shih, T.-H., Liou, W.W., Shabbir, A., Yang, Z. and Zhu, J., "A new k-ϵ eddy viscosity model for high Reynolds number turbulent flows - Model development and validation," NASA TM 106721 (1994), also to appear in *Computers and Fluids.*

[7] Shih, T.H., Zhu, J. and Lumley, J.L., "Modeling of wall-bounded complex flows and free shear flows," NASA TM 106513, also presented at the ASME Fluids Engineering Conference, Symposium on Boundary Layer and Free Shear Flows, Nevada, June (1994).

[8] Shih, T.H., Zhu, J. and Lumley, J.L.,"A realizable Reynolds stress algebraic equation model," NASA TM 105993 (1993).

[9] Zhu, J. and Shih, T.H., "A numerical study of confined turbulent jets," *J. Fluids Eng.* 116, pp.702-706 (1994).

[10] Shih, T.-H., Zhu, J. and Lumley, J.L., "A new Reynolds stress algebraic equation model," NASA TM 106644 (1994), also to appear in *Computer Methods in Applied Mechanics and Engineering.*

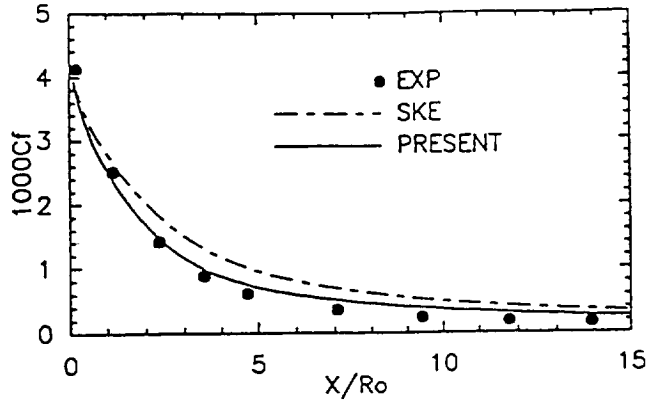

Fig.1 Wall friction coefficient (Case of Trupp et al.)

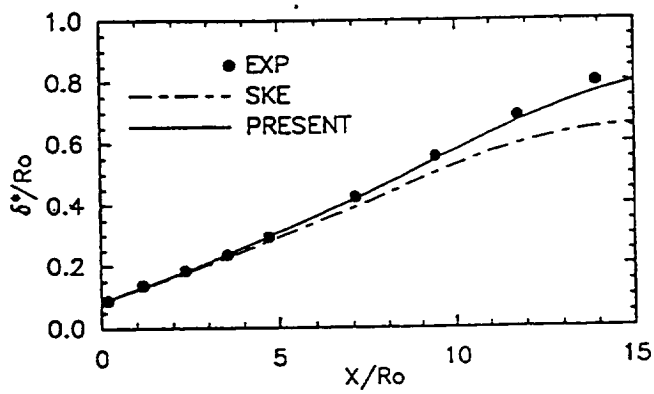

Fig.2 Displacement thickness (Case of Trupp et al.)

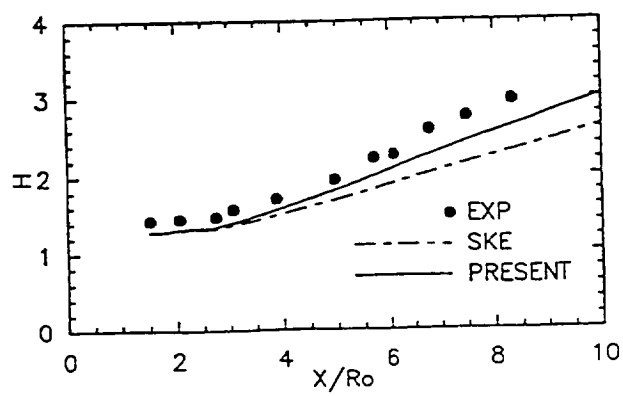

Fig.3 Shape factor (Case of Fraser)

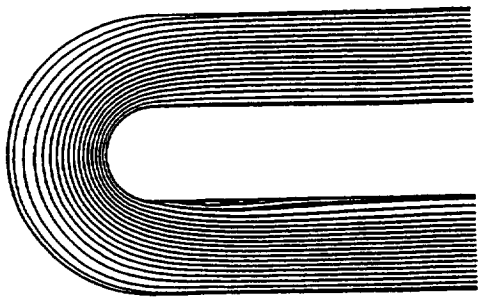

Fig.4 Streamlines

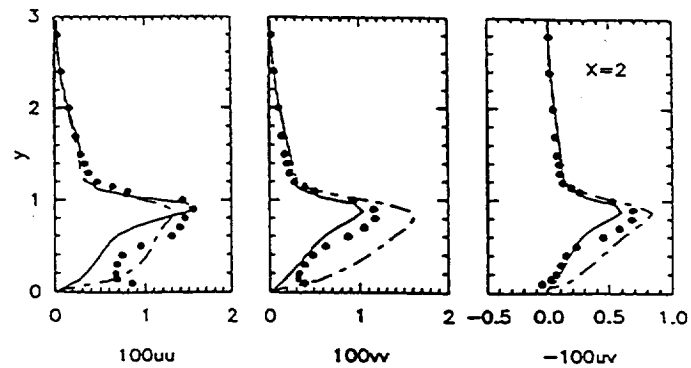

Fig.7 Turbulent stress profiles
(legend as in Fig.5)

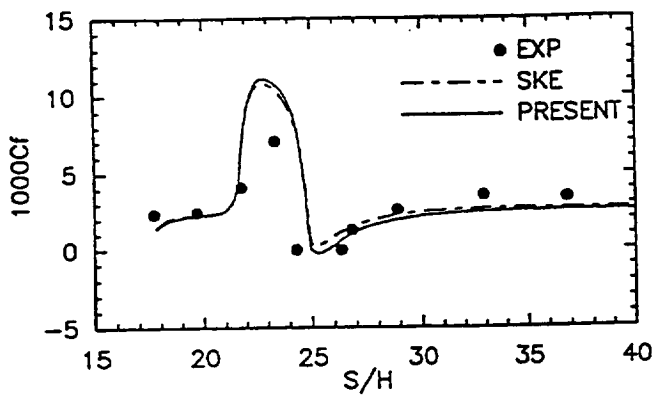

Fig.5 Friction coefficient along the inner wall

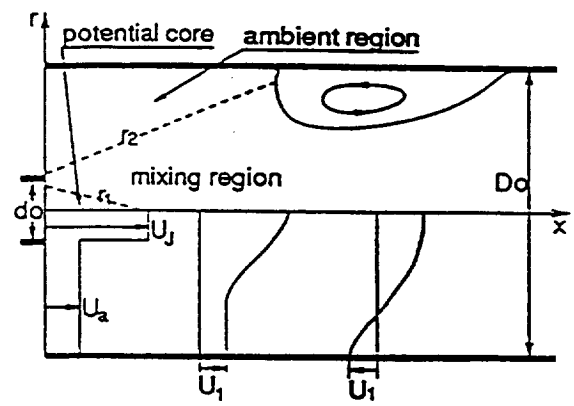

Fig.8 Flow configuration and notations

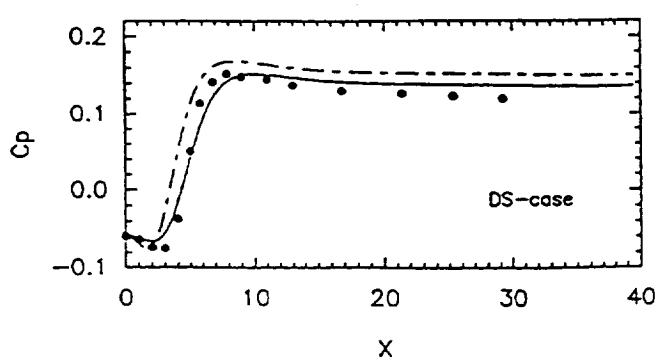

Fig.6 Pressure coefficient along the bottom wall
(legend as in Fig.5)

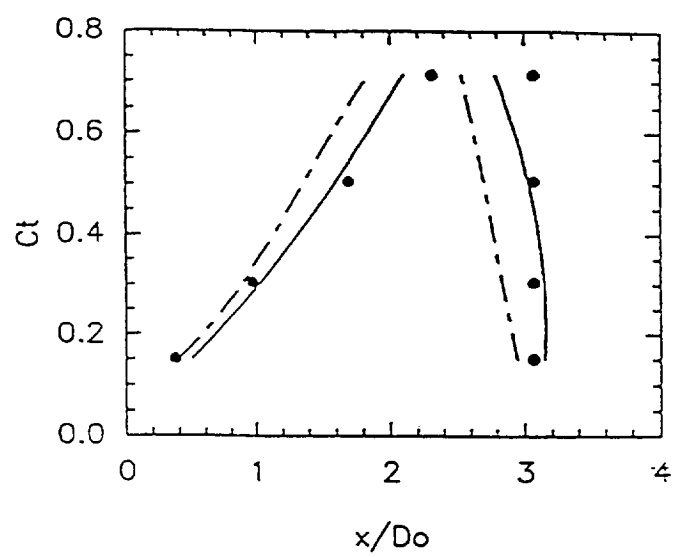

Fig.9 Separation and reattachment points
(legend as in Fig.5)

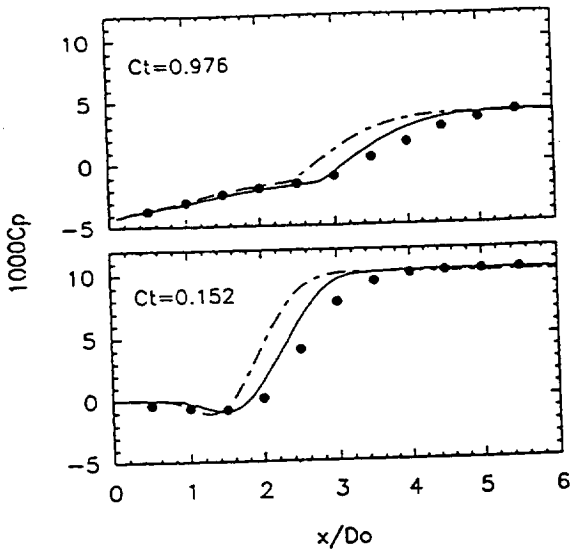

Fig.10 Pressure coefficient along the duct wall (legend as in Fig.5)

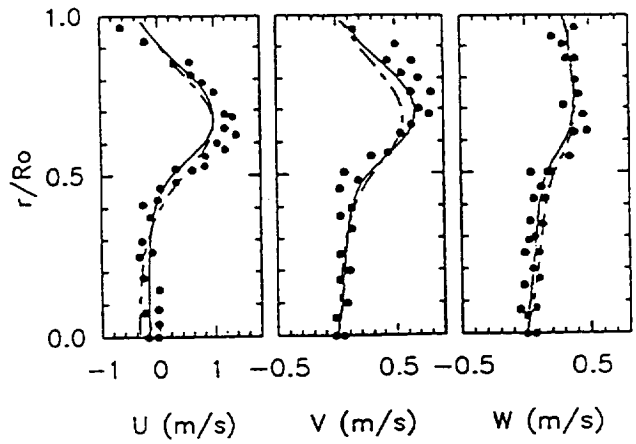

Fig.13 Mean velocity profiles at x=5.1cm (legend as in Fig.12)

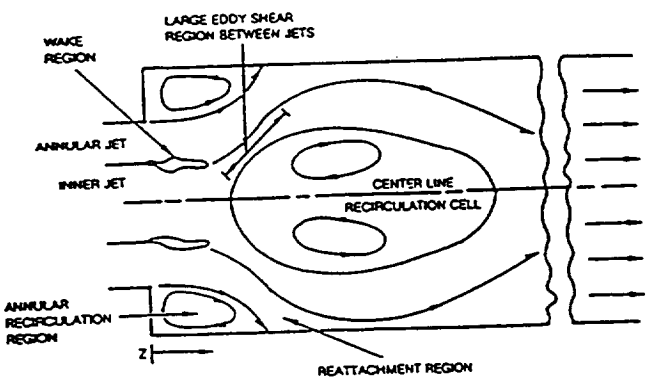

Fig.11 Flow configuration

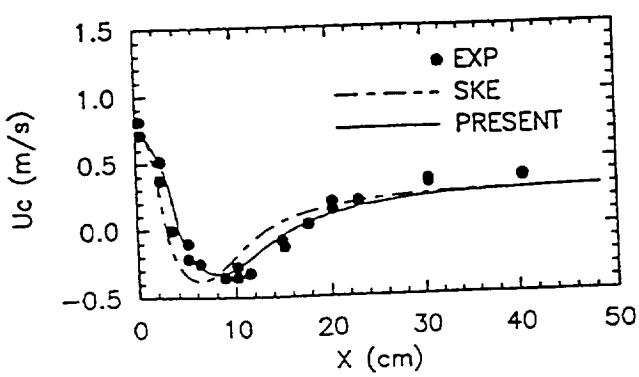

Fig.12 Centerline velocity

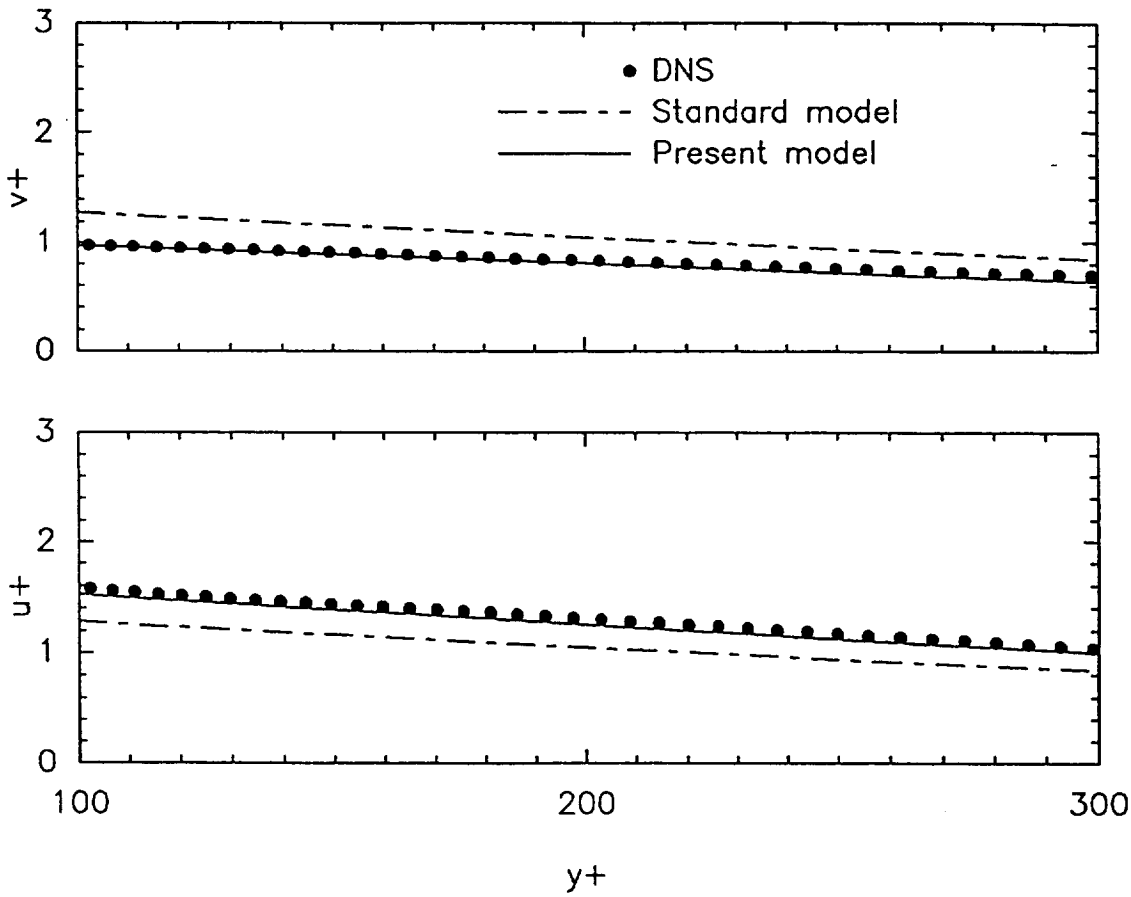

Fig.14 Direct comparison with DNS data of channel flow

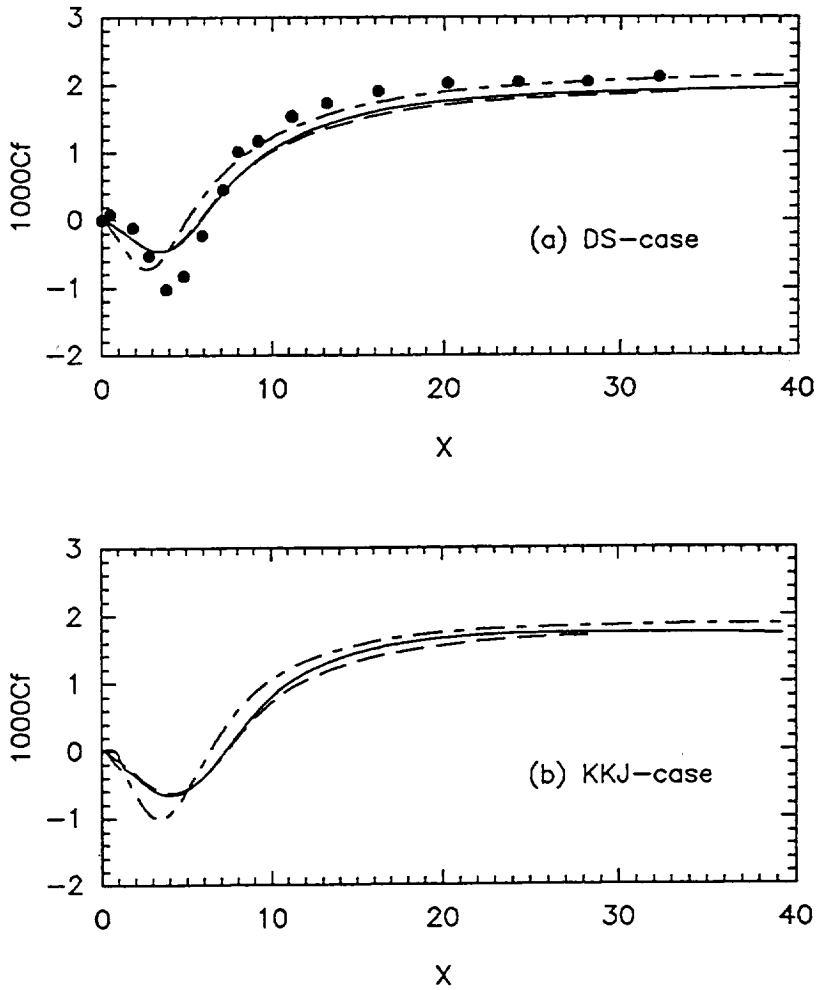

Fig.15 Friction coefficient along the bottom wall.
——: present model, fine grid; — —: present model, coarse grid;
— - —: SKE, fine grid; •: experiment

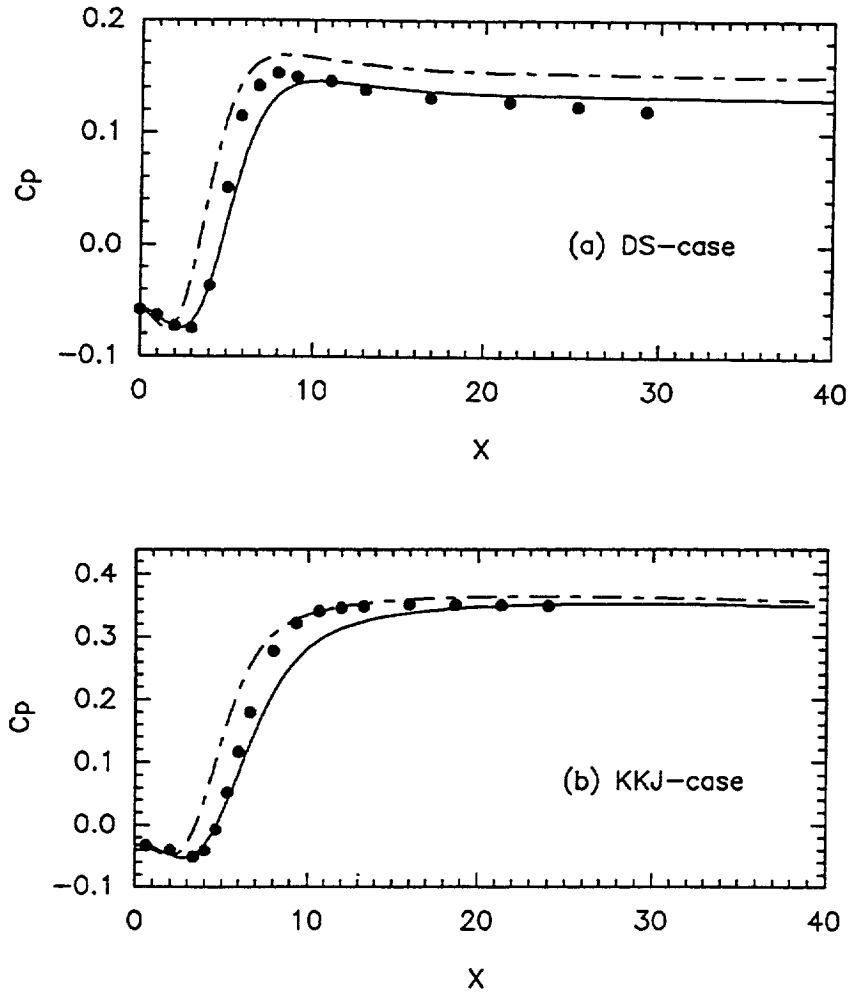

Fig.16 Pressure coefficient along the bottom wall.
——: present model; — - —: SKE; •: experiment

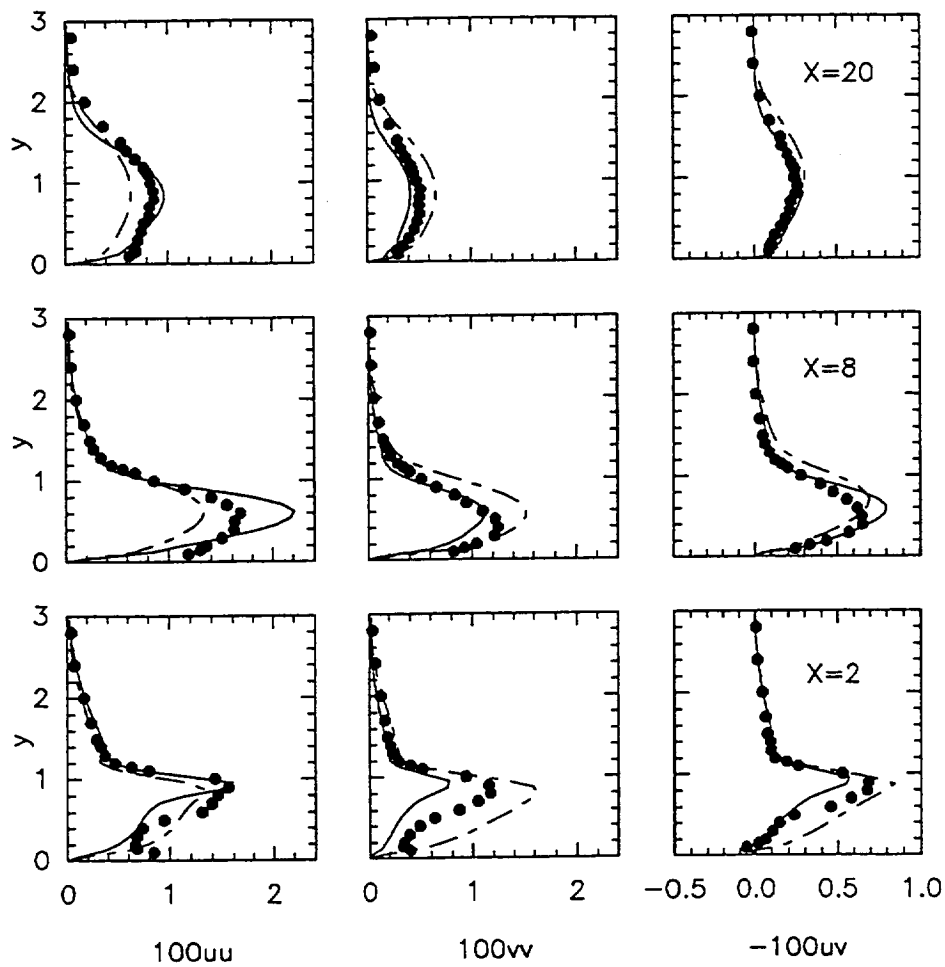

Fig.17 Turbulent stress profiles in DS-case.
——: present model; — - —: SKE; •: experiment

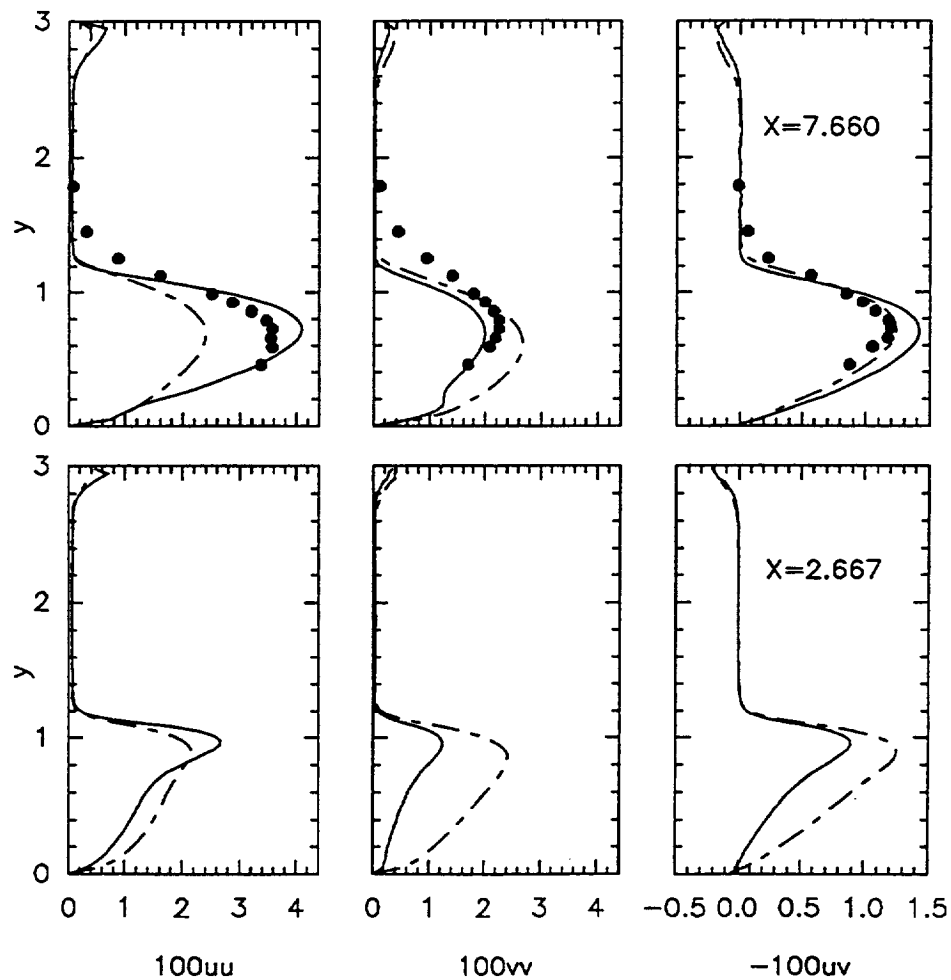

Fig.18 Turbulent stress profiles in KKJ-case.
——: present model; — - —: SKE; •: experiment

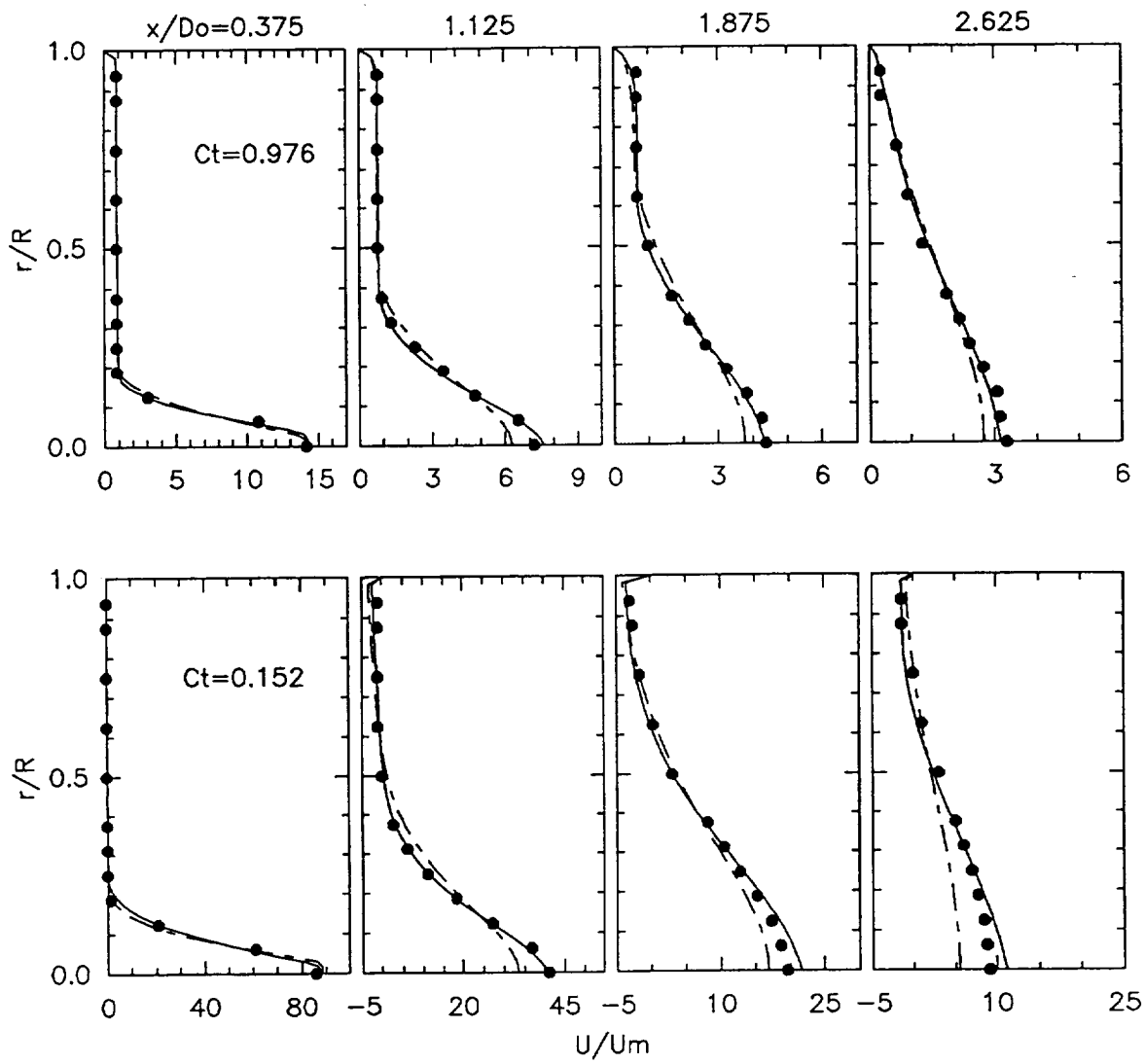

Fig.19 Axial mean velocity profiles.
——: present model; — - —: SKE; •: experiment

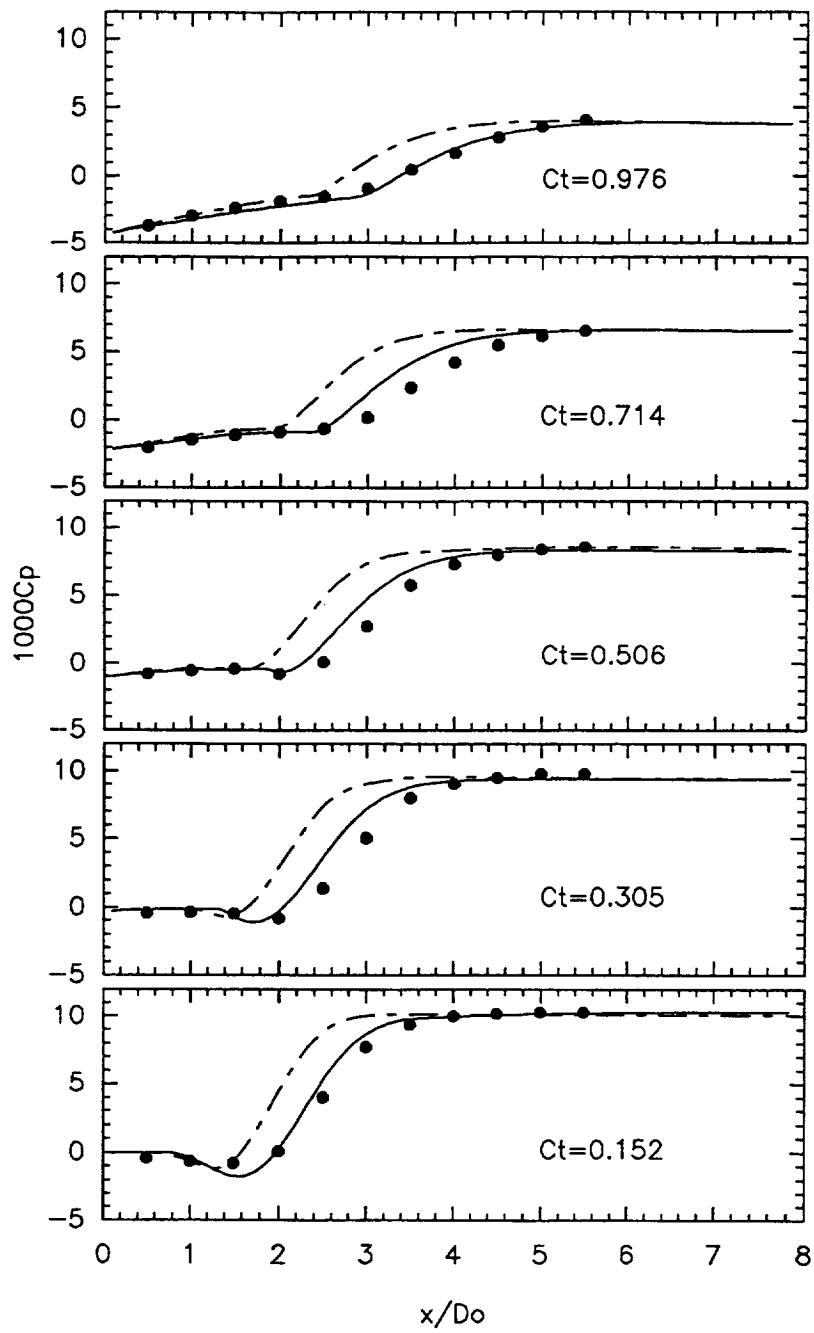

Fig.20 Pressure coefficient along the duct wall.
——: present model; — - —: SKE; •: experiment

Eddy Diffusivity Model for Turbulent Heat Transfer

Aamir Shabbir

1. Motivation and Objectives

Commonly, the turbulent heat transfer is calculated by assuming a constant value of the turbulent Prandtl number. A mixing length turbulence model or a two equation $k - \epsilon$ model is usually used in such calculations to calculate the turbulent eddy viscosity. Obviously this approach has limitations in situations where the turbulent Prandtl number is not constant. Realizing this, some recent studies have proposed new eddy diffusivity models in which the transport equations for the scalar variance and its dissipation rate are solved to calculate the thermal diffusivity. These include, for instance the work of Nagano and Kim[1] and Youssef, Nagano and Tagawa[2], Hattouri, Nagano, and Tagawa[3]. The last study presents an updated and refined version of Nagano and Kim model. There are several other studies reported in the literature where the near wall modeling issues are discussed. In this report only the high Reynolds number version of the models is discussed, and therefore, reader should consult other papers which deal with this issue (for instance the review paper by So[4]). Recently Schwab and Lakshminarayana[5] also propsed a two equation model for scalar field in which a scalar time scale equation is used instead of the scalar dissipation rate. They sucessfully applied their model to a host of homogeneous flows.

In last year's research briefs I descirbed my project aimed at developing a new two equation eddy diffusivity model for calculating turbulent heat transfer. In this model transport equations for the scalar variance and its dissipation rate are used to calculate the turbulent eddy diffusivity. As was pointed out then, the present effort differs from the other work in the following two respects. (1) In the above cited works, the extension of the scalar dissipation rate equation is based upon the work of Newman *et al.*[6] who developed its production/destruction mechanisms analogous to those of the mechanical dissipation rate equation. The model equation proposed in the present study is based on the exact transport equation for scalar dissipation and, its production/destruction mechanisms differ from those proposed in the other studies. (2) The model coefficient in the the scalar flux constitutive relation used in the present study is not a constant but is a function of the local invariants.

2. Work Accomplished

2.1 A New eddy viscostiy $k - \epsilon$ model for High Reynolds Number Flows

Some of the effort was directed in developing and assessing the performance of a new two equation k-epsilon model in a joint effort with the other CMOTT researchers. The details of the model development and application can be found in

the paper by Shih et al.[7] The model performs reasonably for a host of benchmark flows which includes: rotating homogeneous shear flow; various flat plate boundary layers; mixing layers; and jets. We, in this section, only show the application of the model to the rotating homogeneous shear flow, for which a large eddy simulation was carried out by Bardina *et al.*[8]. We will compare the results from the present $k-\epsilon$ model as well as the standard $k-\epsilon$ model with the LES data for four different cases of Ω/S (which are Ω/S=0.0, Ω/S=-0.50, Ω/S=0.25, and Ω/S=0.50). The initial conditions in all these cases correspond to isotropic turbulence and $\epsilon_0/Sk_0 = 0.296$. Figure 1 (a) compares the evolution of turbulence kinetic energy, normalized by its initial value k_0, with the non-dimensional time St for the case of $\Omega/S = 0.0$. For this case both the present and the standard $k-\epsilon$ (denoted by ske hereafter) models show the trends exhibited by LES, with the present model closer to the LES data. Figure 1 (b) shows the comparisons for the case $\Omega/S = 0.25$. The LES shows that the growth rate of the turbulence kinetic energy is increased over the no rotation rate case. The present model is able to pick up this trend while the ske model does not. Figures 1 (c) and 1 (d) compare the evolution of turbulence kinetic energy for two more cases of $\Omega/S = 0.5$ and $\Omega/S = -0.5$. For the first of these cases the LES shows that the growth rate of the turbulence kinetic energy decreases over the no rotation rate case. The present model is able to pick up this trend and although the agreement between the present model and the LES is not as good as it is for the other cases, it still is a lot better than the ske model. For the case of $\Omega/S = -0.5$ the ske model does not show the effect of rotation on turbulence as it gives the same growth rate of turbulence kinetic energy as it did for the no rotation case, a result which is already known. On the other hand the present model is in reasonable agreement with the LES data as it shows the decay of the turbulence kinetic energy with time.

2.2 A New eddy diffusivity $\overline{\theta^2}-\epsilon_\theta$ model for High Reynolds Number Flows

The details of the development of the scalar (or thermal) dissipation rate equation and the scalar flux can be found in the last year's research briefs. Since then the model has been extended to inhomogeneous flows by modeling the diffusion term in the disspiation rate equation. A simple gradient diffusion type model is used for the diffusion term $(\overline{u_j\epsilon_\theta})_{,j}$. With this the scalar dissipation rate equation is given by

$$\epsilon_{\theta,t} + U_j\epsilon_{\theta,j} = (\frac{\alpha_T}{\sigma_\phi}\epsilon_{\theta,j})_{,j} + C_{\theta 1}\epsilon_\theta S + C_{\theta 2}\frac{\sqrt{\epsilon_\theta\epsilon}}{\sqrt{Pr}}\Phi - C_{\theta 3}\frac{\epsilon_\theta\epsilon}{(k+\sqrt{\nu\epsilon})} \tag{1}$$

where the model constant σ_ϕ is to be determined. To do so we consider the log-law region of a wall, where the turbulent scalar (or heat) flux is constant. In this region the advection term can be ignored and equation (1) reduces to

$$\frac{\partial}{\partial y}(\frac{\alpha_T}{\sigma_\phi}\frac{\partial\epsilon_\theta}{\partial y}) + C_{\theta 1}\epsilon_\theta S + C_{\theta 2}\frac{\sqrt{\epsilon_\theta\epsilon}}{\sqrt{Pr}}\Phi - C_{\theta 3}\frac{\epsilon_\theta\epsilon}{(k+\sqrt{\nu\epsilon})} = 0 \tag{2}$$

Using the log-law relations, and the fact that in the log-layer production equals the dissipation rate, the above equation gives the following relation for the model constat σ_ϕ

$$\sigma_\phi = \frac{(C_\lambda/C_\mu)k^2}{C_\mu^{1/2}C_{\theta 3} - C_{\theta 1} - C_{\theta 2}(\frac{K}{K_\theta}\frac{1}{Pr})^{1/2}} \tag{3}$$

where the Von Karman constant K is 0.41 and K_θ is 0.482[9]. We know that in the log-layer $C_\mu = 0.09$ and $C_\lambda = 0.1$. With these values we obtain $\sigma_\phi = 1.8$ from (3). The expression for the model constant C_λ used previoulsy was somewhat cumbersome. We have now considerably simplified it and is given by equation (7). The model for the scalar (or thermal) field can now be summarized by the following equations.

$$U_j\frac{\partial\overline{\theta^2}}{\partial x_j} = (\frac{\alpha_T}{\sigma_t}\overline{\theta^2}_{,j})_{,j} - 2\overline{u_i\theta}\frac{\partial\Theta}{\partial x_i} - 2\epsilon_\theta \tag{4}$$

$$U_j\frac{\partial\epsilon_\theta}{\partial x_j} = (\frac{\alpha_T}{\sigma_\phi}\epsilon_{\theta,j})_{,j} + C_{\theta 1}\epsilon_\theta S + C_{\theta 2}\sqrt{\frac{\epsilon_\theta\epsilon}{Pr}}S_T - C_{\theta 3}\frac{\epsilon_\theta\epsilon}{k} \tag{5}$$

$$\overline{u_i\theta} = -C_\lambda\frac{k^2}{\epsilon}(\frac{2}{r})^{1/2}\Theta_{,i} + \frac{k^3}{\epsilon^2}(\frac{2}{r})^{1/2}(a_2U_{i,j} + a_3U_{j,i})\Theta_{,j} \tag{6}$$

$$C_\lambda = \frac{(2 + 2r + 0.5r^2)}{26 + 3.2\eta^2 + 2\xi^2} \tag{7}$$

$$S_T = \sqrt{\Theta_{,i}\Theta_{,i}}, \quad S = \sqrt{2S_{ij}S_{ij}}, \quad \eta = Sk/\epsilon, \quad \xi = \frac{k}{\epsilon}(\frac{k}{\overline{\theta^2}})^{1/2}S_T, \quad r = \frac{2k}{\epsilon}\frac{\epsilon_\theta}{\overline{\theta^2}}$$

$$C_{\theta 1} = C_1 - 0.33, \quad C_{\theta 2} = 0.63, \quad C_{\theta 3} = C_2 - 1 + r, \quad \sigma_t = 1.0, \quad \sigma_\phi = 1.8$$

2.3 Application of Model

Since the expression for C_λ has been simplified than what was reported previously, it is instructive to re-calculate the flows which were calculated previously. Figures 1-7 show the evolution of the temperature variance and its dissipation rate for the seven different cases of Sirivat and Warhaft[10] experiment. We note that the present model is in reasonable agreement with the experiment, and performs better than the Hattouri, Nagano and Tagawa model (HNT). The results on the overall are same as what was reported previously. Same is true for the homogeneous shear flow with a constant temperature gradient, for which the results are shown in figure 8.

The model was also applied to the flat plate boundary layer whose surface is heated to a constant temperature. The experiment of Gibson *et al.*[9] provides one test case for such a flow. This flow constitutes an initial value problem in the stream-wise direction and a boundary value in the cross-stream direction. It was calcualted using a quasi-implicit finite difference scheme. Since only the high Reynolds number form of the present model is developed so far, it is used here in conjunction with the

wall functions. For the k and ϵ quantities the standard wall functions were used. The wall functions used for the thermal field are summarized in Appendix B. (It is found that with these wall functions the log-layer temperature profile agrees well with the data but the Stanton number is underestimated by about 7%. Work is underway to address this aspect of the wall functions.) The equations set consisted of: mean momentum and mean energy equations; turbulence kinetic energy and its dissipation equation; temperature variance and its dissipation equation.

The results for the mean temperature are shown in figure 9. We note that the agreement with the experiment is reasonable. For comparisons purposes results are also shown for the HNT model which agrees with the experiment very well. Note that the HNT model was not used with the wall functions but was instead integrated to the wall.

3. Future Plans

The present model will be extended for integration to the wall. This will necessitate the formulation of damping functions for the model. However, due to the changing research environment at NASA, most of the next year will be spent on application of two-equation models to the turbomachinery flows.

Acknowledgements

The help of Dr. Z. Yang in the numerical aspects of the boundary layer calculations is gratefully acknowledged. Helpful discussions with J. Schwab of NASA Lewis are also acknowledged.

4. References

[1] Nagano,Y. and C. Kim. "A two equation model for heat transport in wall turbulent shear flows", J. Heat Transfer, 110, 583-589, (1988).

[2] Youssef, M.S., Y. Nagano and M. Tagawa. "A two-equation heat transfer model for predicting turbulent thermal fields under arbitrary wall thermal conditions", Int. J. Heat Mass Transfer, 35, 11, 3095-3104, (1992).

[3] Hattori, H., Ngano, Y., and Tagawa, M. "Analysis of Turbulent Heat Transfer under Various Thermal Conditions with Two-Equation Models", Department of Mech. Engg., Nagoya Institute of Technology, Gokiso-cho, Showa-ku, Nagoya 466, Japan.

[4] So, R.M.C., S.P.Yuan, and T.P. Sommer. "A hierarchy of near wall closures for turbulent heat transfer", Trends in Heat, Mass, and Momentum Transfer, Vol. 2, pp. 203-221.

[5] Schwab, J.R. and Lakshminarayana. "Dynamic and Thermal turbulent time scale modeling for homogeneous shear flows", NASA TM 106635, 1994.

[6] Newman, G.R., B.E. Launder and J.L. Lumley. "Modeling the behaviour of homogeneous scalar turbulence", J. Fluid Mech., 111, 217-232, (1981).

[7] Shih, T.-H., W.W. Liou, A. Shabbir, Z. Yang and J. Zhu. "A new high Reynolds number $k - \epsilon$ model", Computers Fluids, 24, 3,227-238, 1995.

[8] Bardina, J., J.H. Ferziger and W.C. Reynolds, "Improved Turbulence Models Based on Large-Eddy Simulation of Homogeneous, Incompressible Turbulent Flows". Stanford Univ. Report TF-19, 1983.

[9] Gibson, M.M., Verriopoulos, C.A. and Nagano, Y., "Measurements in the Heated Turbulent Boundary layer on Mildly Curved Convex Surface", Turbulent Shear Flows 3 (ed. Bradbury, L.J.S., et al.), Springer-Verlag, 80-89, 1982.

[10] Sirivat, A., and Z. Warhaft. "The effect of a passive cross-stream temperature gradient on the evolution of temperature variance and heat flux in grid turbulence", J. Fluid Mech., 128, 326-346, (1983).

[11] Tavoularis, S., and S. Corrsin. "Experiments in nearly homogeneous turbulent shear flow with a uniform mean temperature gradient", Part 1, J. Fluid Mech., 104, 311-347, (1981).

[12] Launder, B.E. "On the computation of convective heat transfer in complex turbulent flows", J. Heat Transfer, 110,1112-1128, (1988).

Appendix A

The $k-\epsilon$ model used in the present study is that of Shih *et al.*[7] and is summarized below.

$$U_j \frac{\partial k}{\partial x_j} = (\frac{\nu_T}{\sigma_k} k_{,j})_{,j} - \overline{u_i u_j} \frac{\partial U_i}{\partial x_j} - \epsilon \tag{A1}$$

$$U_j \frac{\partial \epsilon}{\partial x_j} = (\frac{\nu_T}{\sigma_\epsilon} \epsilon_{,j})_{,j} + C_1 S\epsilon - C_2 \frac{\epsilon^2}{k} \tag{A2}$$

$$\overline{u_i u_j} = \nu_T (U_{i,j} + U_{j,i}) - \frac{2}{3} k \delta_{ij} \tag{A3}$$

$$\nu_T = C_\mu \frac{k^2}{\epsilon}, \qquad C_\mu = \frac{1}{4.0 + A_s U^*(k/\epsilon)} \tag{A4}$$

$$S_{ij} = \frac{1}{2}(\frac{\partial U_i}{\partial x_j} + \frac{\partial U_j}{\partial x_i}), \qquad \Omega_{ij} = \frac{1}{2}(\frac{\partial U_i}{\partial x_j} - \frac{\partial U_j}{\partial x_i}) \tag{A5}$$

$$\tilde{\Omega}_{ij} = \overline{\Omega}_{ij} - 2\epsilon_{ijk}\omega_k, \qquad \overline{\Omega}_{ij} = \Omega_{ij} - \epsilon_{ijk}\omega_k, \qquad S = \sqrt{S_{ij}S_{ij}}, \tag{A6}$$

$$W = S_{ij}S_{jk}S_{ki}/S^3, \qquad \phi = \frac{1}{3} arc\ cos(\sqrt{6}W), \qquad A_s = \sqrt{6} Cos\phi \tag{A7}$$

$$U^* = \sqrt{S_{ij}S_{ij} + \tilde{\Omega}_{ij}\tilde{\Omega}_{ij}} \tag{A8}$$

Note that the $\overline{\Omega}_{ij}$ is the mean rotation rate as viewed in the rotating reference frame and ω_k is the angular velocity at which the reference frame is rotating. The constants in the ϵ equation are: $C_1 = 0.42$ and $C_2 = 1.9$.

Appendix B

This appendix gives the wall functions which were used to obtain the boundary conditions for the thermal field (i.e the values of Θ, $\overline{\theta^2}$, and ϵ_θ at the first grid point off the wall). Note that the standard wall functions were used for the velocity field and, therefore, are not listed here.

For the mean temperature the standard log-law for a flat plate with constant surface temperature was used as a boundary condition (see e.g. Launder[12]) and is given as

$$\Theta^+ = \frac{\Delta\Theta}{\theta_\tau} = \frac{1}{K_\theta} ln y^+ + C_\theta \qquad (B1)$$

where $\Delta\Theta$ is the difference between the wall temperature and the local temperature. From the experiment of Gibson *et al.*[9] $K_\theta = 0.482$ and $C_\theta = 3.8$. For the turbulent part of the temperature field the local equilibrium assumption was invoked (i.e. $P_\theta = \epsilon_\theta$) to obtain the following relation for the boundary conditions on $\overline{\theta^2}$.

$$\frac{\overline{\theta^2}}{\theta_\tau^2} = C_\mu^{1/2} / C_\lambda \qquad (B2)$$

Once $\overline{\theta^2}$ is known the boundary condition on ϵ_θ can be readily obtained by using the definition of the time scale ratio.

$$\epsilon_\theta = r(\frac{\epsilon}{2k})\overline{\theta^2} \qquad (B3)$$

Note that for the log-layer the time scale ratio r is 2.0; $C_\mu = 0.09$; and $C_\lambda = 0.1$.

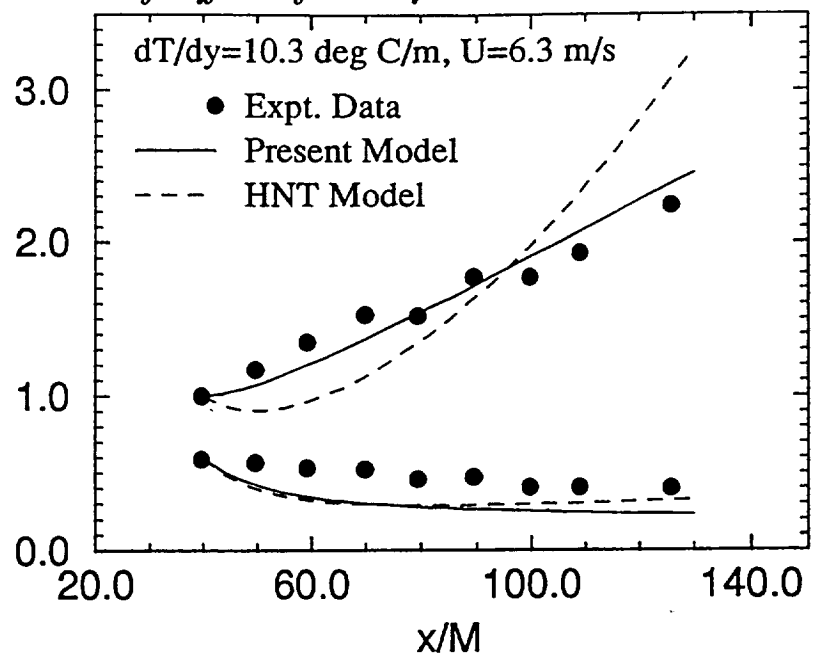

Figure 1. Evolution of the normalized temperature variance and thermal dissipation rate in the experiment of Sirivat and Warhaft (1983). The temperature variance is normalized as $\overline{\theta^2}' = \overline{\theta^2}/\overline{\theta^2}_0$ and the thermal dissipation is normalized as $\epsilon'_\theta = \frac{\epsilon_\theta}{\overline{\theta^2}_0 u_0/l_0}$. For this case $\overline{\theta^2}_0 = 0.0128\ {}^0C^2$, $u_0 = 0.145515 m/s$, and $l_0 = 0.011937 m$.

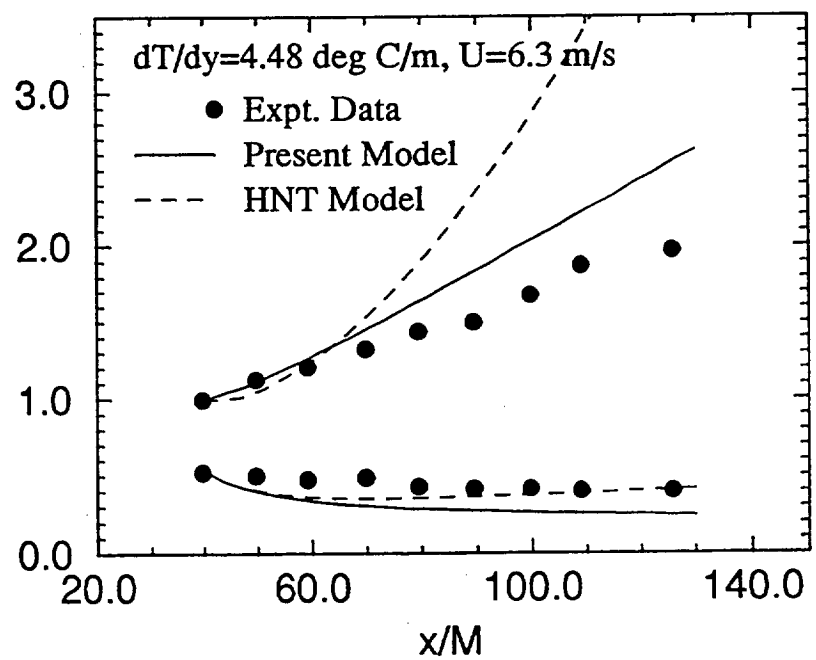

Figure 2. Evolution of the normalized temperature variance and thermal dissipation rate in the experiment of Sirivat and Warhaft (1983). The temperature variance is normalized as $\overline{\theta^2}' = \overline{\theta^2}/\overline{\theta^2}_0$ and the thermal dissipation is normalized as $\epsilon'_\theta = \frac{\epsilon_\theta}{\overline{\theta^2}_0 u_0/l_0}$. For this case $\overline{\theta^2}_0 = 0.002287\ {}^0C^2$, $u_0 = 0.145515 m/s$, and $l_0 = 0.011937 m$.

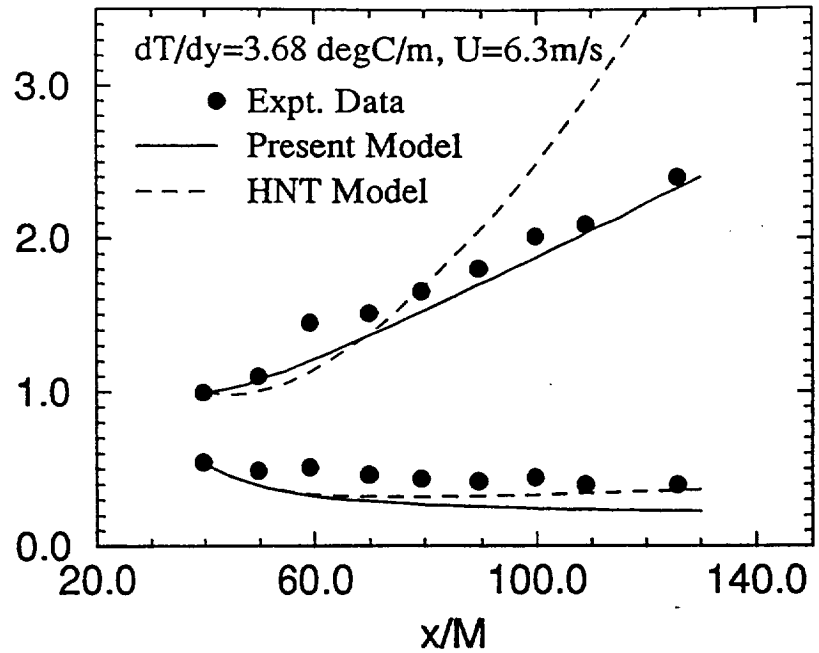

Figure 3. Evolution of the normalized temperature variance and thermal dissipation rate in the experiment of Sirivat and Warhaft (1983). The temperature variance is normalized as $\overline{\theta^2}' = \overline{\theta^2}/\overline{\theta^2}_0$ and the thermal dissipation is normalized as $\epsilon'_\theta = \frac{\epsilon_\theta}{\overline{\theta^2}_0 u_0/l_0}$. For this case $\overline{\theta^2}_0 = 0.001705\ {}^0C^2$, $u_0 = 0.145515m/s$, and $l_0 = 0.011937m$.

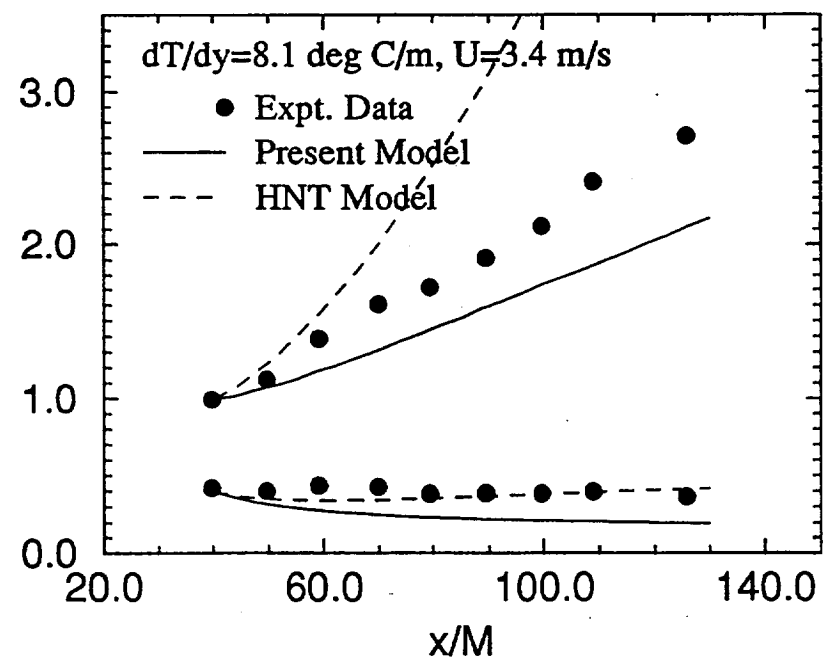

Figure 4. Evolution of the normalized temperature variance and thermal dissipation rate in the experiment of Sirivat and Warhaft (1983). The temperature variance is normalized as $\overline{\theta^2}' = \overline{\theta^2}/\overline{\theta^2}_0$ and the thermal dissipation is normalized as $\epsilon'_\theta = \frac{\epsilon_\theta}{\overline{\theta^2}_0 u_0/l_0}$. For this case $\overline{\theta^2}_0 = 0.009059\ {}^0C^2$, $u_0 = 0.074701m/s$, and $l_0 = 0.011071m$.

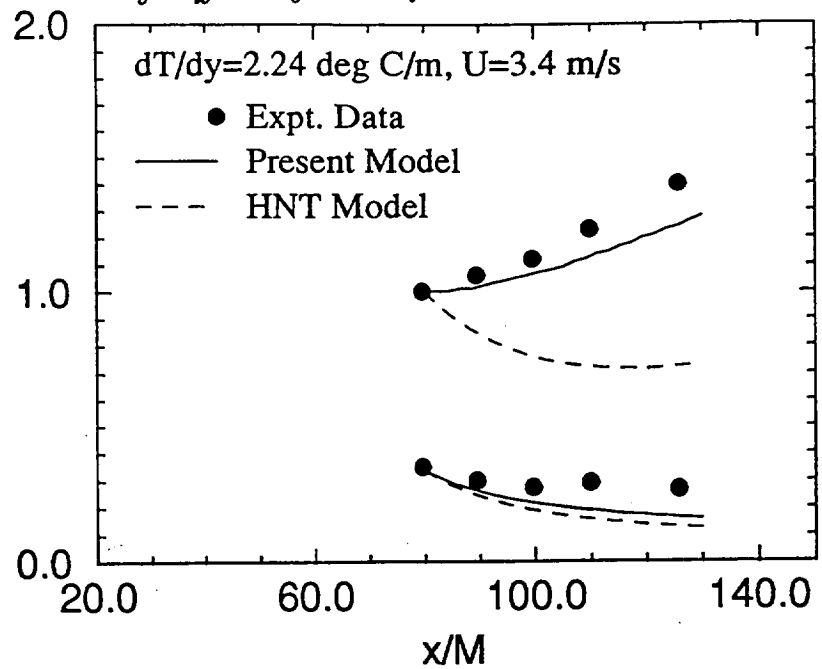

Figure 5. Evolution of the normalized temperature variance and thermal dissipation rate in the experiment of Sirivat and Warhaft (1983). The temperature variance is normalized as $\overline{\theta^2}' = \overline{\theta^2}/\overline{\theta^2}_0$ and the thermal dissipation is normalized as $\epsilon'_\theta = \frac{\epsilon_\theta}{\overline{\theta^2}_0 u_0/l_0}$. For this case $\overline{\theta^2}_0 = 0.000924\ {}^0C^2$, $u_0 = 0.074701 m/s$, and $l_0 = 0.011071 m$.

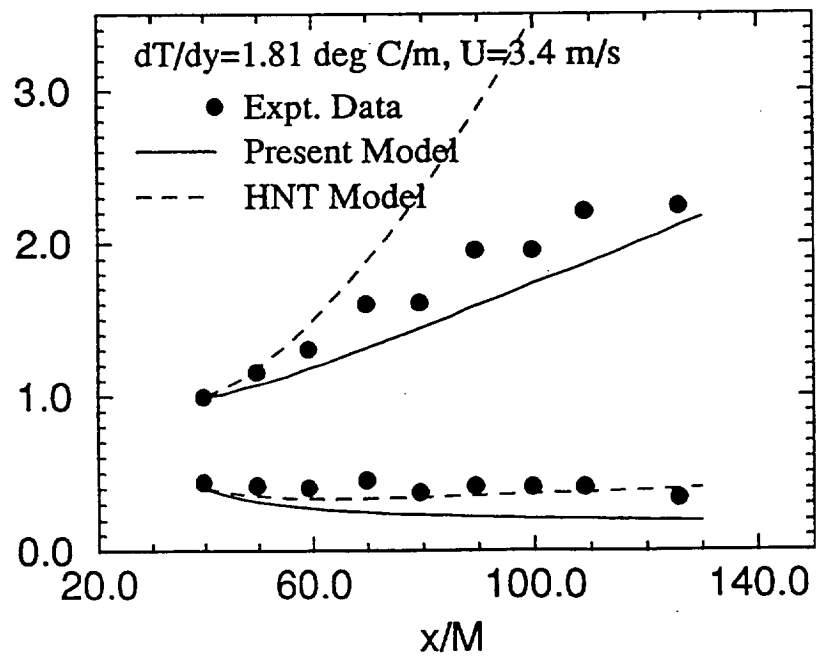

Figure 6. Evolution of the normalized temperature variance and thermal dissipation rate in the experiment of Sirivat and Warhaft (1983). The temperature variance is normalized as $\overline{\theta^2}' = \overline{\theta^2}/\overline{\theta^2}_0$ and the thermal dissipation is normalized as $\epsilon'_\theta = \frac{\epsilon_\theta}{\overline{\theta^2}_0 u_0/l_0}$. For this case $\overline{\theta^2}_0 = 0.0004471\ {}^0C^2$, $u_0 = 0.074701 m/s$, and $l_0 = 0.011071 m$.

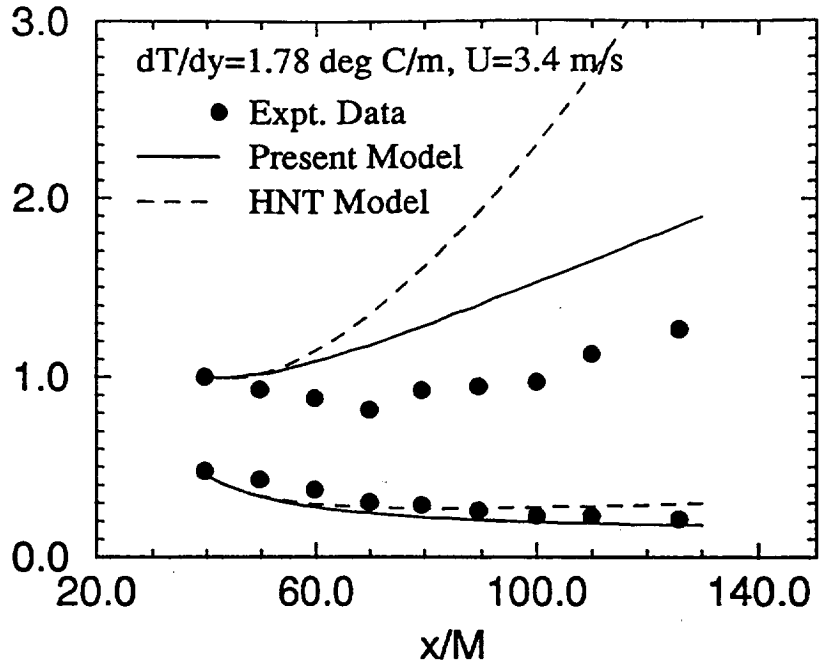

Figure 7. Evolution of the normalized temperature variance and thermal dissipation rate in the experiment of Sirivat and Warhaft (1983). The temperature variance is normalized as $\overline{\theta^2}' = \overline{\theta^2}/\overline{\theta^2}_0$ and the thermal dissipation is normalized as $\epsilon'_\theta = \frac{\epsilon_\theta}{\overline{\theta^2}_0 u_0/l_0}$. For this case $\overline{\theta^2}_0 = 0.0004955\ {}^0C^2$, $u_0 = 0.074701 m/s$, and $l_0 = 0.011071 m$.

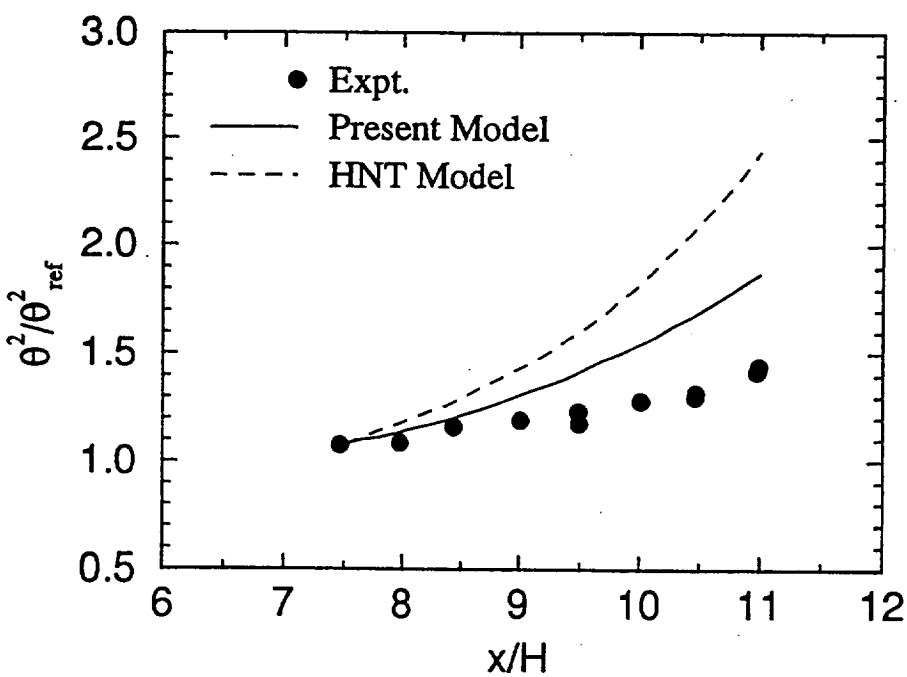

Figure 8a. Evolution of the normalized temperature variance in the experiment of Tavoularis and Corrsin (1981). The temperature variance is normalized with $\overline{\theta^2}_{ref} = 0.01\ {}^0C^2$.

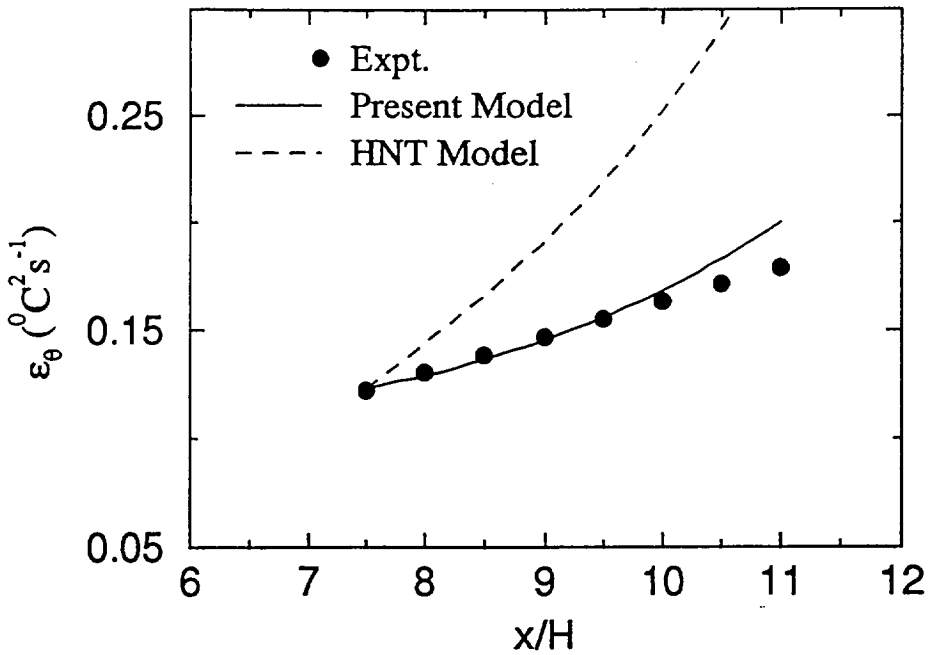

Figure 8b. Evolution of the thermal dissipation rate in the experiment of Tavoularis and Corrsin (1981).

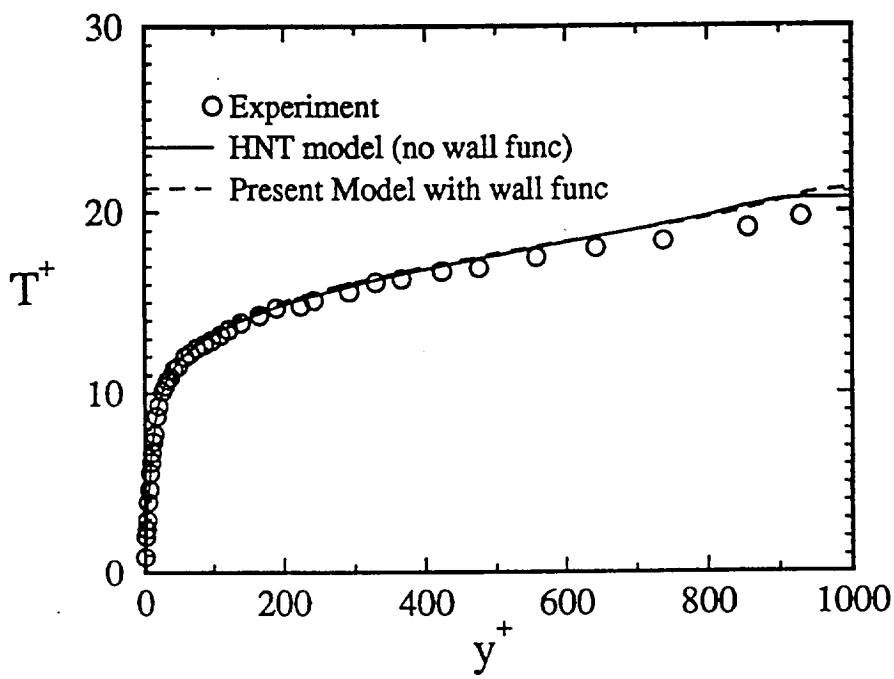

Figure 9. Mean temperature profile in wall units for the constant temperature flat plate boundary layer for the experiment of Gibson *et al.*[9].

Computations of Compressible Turbulent Benchmark Flows

William W. Liou

1. Motivation and Objective

The development of advanced propulsion systems for high speed aerospace vehicles will require accurate computational models of turbulence that can be used in the CFD calculation of individual flow components. Before a new model is used in the calculation of complex flows in propulsion systems, the model has to be assessed in simple benchmark flows that not only contain the essential physical mechanisms at work in engine component flows, but are also well-documented. An immediate objective of the research activity described here is to identify these compressible benchmark flows and performed a preliminary assessment of models developed locally at CMOTT. The long term objective is to develop second–order closure models for compressible flows.

2. Work Accomplished

2.1 Model Validation in Compressible Flows

Six different types of two-dimensional flow fields typically encountered in aero–propulsion systems were selected. They are: (1) compressible free shear layers; (2) compressible boundary layers; (3) transonic bump flows; (4) supersonic ramp flows; (5) oblique shock-wave/turbulent boundary-layer interactions; (6) can combustor. Sketches of the flows are shown in Fig. 1.

(1) The compressible free shear layer is an integral element in engine component flows, such as combustor and nozzle flows. In many instances, the turbulence mixing in the shear layers is a major factor in the operating efficiency of an engine component. Experiments seem to support a state of self-preserving in a fully developed shear flow, which is describable by local characteristic scales. It is also observed in experiments that the spreading rate of a compressible turbulent shear layer is far smaller than an incompressible shear layer with the same velocity and density ratios. The reduced turbulent mixing influences significantly the combustion efficiency and the noise emitted from high speed jet flows. Therefore, it is important that turbulence models can predict correctly the compressible free shear flow; in particular, its spreading rate.

(2) To evaluate model performance in wall bounded compressible flows, models will be assessed in fully developed compressible turbulent boundary layers. It is generally accepted that for free stream Mach numbers less than about 5, the turbulent structure in compressible boundary layers is nearly the same as in the corresponding incompressible (constant density) flows. This is Morkovin's hypothesis. Therefore, with properly scaling, models that gives good results in incompressible flow may

PRECEDING PAGE BLANK NOT FILMED

PAGE 44 INTENTIONALLY BLANK

also perform well in compressible boundary layer with free steam Mach numbers less than 5.

The above two cases provide tests for models in a "clean" environment. The following four cases involve flows with either shock-waves or chemical reactions.

(3) Case 3 resembles the transonic flow over an airfoil, which affects the performance of engine components such as compressors and turbines. The strong viscous/inviscid interactions in the flow, through a change in the effective body-shape, pose a critical test for turbulence closure models. Two flows were chosen. The first one corresponds to the experimental set-up of a flow studied by Delery et. al [1]. The boundary layer developed on the bump mounted on a wind-tunnel wall remains attached throughout the interaction. The flow speed becomes supersonic atop the bump. The wind-tunnel is choked. This flow was also chosen in a recent EUROVAL[2] effort to evaluate the response of a turbulent boundary layer developing on an airfoil to shock–waves. There, the case was designated as ONERA BUMP A. The second configuration corresponds to an experiment by Bachalo and Johnson[3], where a toroidal bump is mounted on a cylinder. The axisymmetric arrangement eliminates the three–dimensional effects due to the boundary layer on the side walls of the wind tunnel. The boundary layer separates downstream of the shock wave. The axisymmetric configuration has made this flow particularly suitable for the study of a flow with separation resulting from strong shock/turbulent boundary–layer interactions.

(4) Cases 4 and 5 involve interactions between shock-wave and boundary layer in supersonic flows. The compression ramp flow is a classical problem that encompasses many complex phenomena and is of great practical importance in the design of engine components, such as inlets and turbomachinery. The four ramp flows selected were investigated in a series of work by Settles and co-workers[4]. The free stream Mach numbers are less than 3 and, depending upon the ramp angle, flow separation may occurs at the corner of the ramp. The flows were proposed for model testing in shock wave/turbulent boundary–layer interactions in the 1980-1981 AFSOR–Stanford Conference on complex turbulent flows.

(5) Case 5 includes another fundamentally important flow that is critical to the performance of inlets and turbomachinery: the impingement of an oblique incident shock–wave on a wall[5]. A reflected shock is formed to turn the downstream flow parallel to the wall. Again, if the shocks were sufficiently strong, the turbulent boundary layer may separate. The challenge for a turbulence model is to predict the incipient separation of the boundary layer and the subsequent separated flow.

(6) The flow in a engine combustor typically involves highly turbulent reacting regions. Therefore, a robust turbulence model is just as important as a quality chemistry model in the design of a high efficiency and low pollutant emission combustor. An axisymmetric can combustor configuration[6] tested in UC Irvine was examined. The experimental set-up includes an air-swirler and gaseous fuel injection of propane. The fuel and air are not premixed before entering the combustor. This configuration is representative of a gas turbine engine combustor.

These test cases are well–documented and should provide good data base for

objective evaluations of turbulence models. For instance, some experiments have reported results obtained using different measurement techniques, i.e. hot wire vs. LDV. In fact, some flows were also selected by previous large–scale model evaluation efforts.

It is more efficiently to calculate the free shear layer and the flat plate boundary layer with a boundary-layer equation solver. When it is necessary to use a Navier–Stokes solver, the model solution of a flat plate boundary layer is compared with the solution obtained from the boundary–layer equation solver to validate the model implementation in the Navier–Stokes solver. The COMTUR code[7] is currently used in the solution of compressible Favre–average Navier–Stokes equations. The FAST2D code[8] is used for solving the variable density form of the Navier–Stokes equations. The chemical reactions were modeled by using a CMOTT scalar probability density function(PDF) code, LPDF2D.

In the following, a few sample results of this model assessment effort are shown. More details can be found in NASA TM reports that are in preparation.

Fig. 2 shows the skin friction and the wall pressure distributions for a supersonic flow over a 24 ramp[4]. The incoming free stream Mach number is 2.8. and the unit Reynolds number is $6.3\times10^7/m$. No compressibility corrections were used. The results show that the standard $k-\epsilon$ model and the multiple–scale model[9] give reasonable predictions for the flow recovery and the flow separation. RNG model[10] and the S&Z[11] model predict a larger separation region than the measurement. Note that only the linear part of the constitutive relation of the S&Z model was used in this calculation.

Fig. 3 shows the variations of the skin friction coefficient and the wall pressure for an oblique shock/turbulent boundary–layer interaction. The incoming free stream Mach number is 2.89 and the unit Reynolds number is $5.73\times10^7/m$. The impinging shock is strong enough to cause the boundary layer to separate. KE1 model[12,13], which is a modified low Reynolds number model of Shih and Lumley[14], performs better than the Chien's model[15]. The high Reynolds number KE2[16] model and the standard $k-\epsilon$ model gives reasonable predictions for both quantities.

The predicted and measured wall pressure distributions for the ONERA BUMP A are shown in Fig. 4. KE2[16] model give a slightly better predication downstream of the shock wave than the other models. All the model predictions asymptote to a value higher than the measurement in the fully developed region. This may be due to three–dimensional effects, such as the boundary layer on the wind–tunnel walls.

The computed and measured wall pressure distribution for the Bachalo and Johnson transonic bump is given in Fig. 5. The incoming free stream is subsonic. A supersonic pocket is formed atop the bump as the flow accelerates through the bump. The combined effect of the shock–wave and the bump geometry results in flow separation near $x/c = 0.7$. KE2 model[16] shows the best overall agreement with the measurement than the three other models tested. KE1 model[12,13], a low Reynolds number model, also gives better results than the Chien's model.

In Fig. 6, the temperature profiles at four measurement stations in the axial direction for the UC Irvine axisymmetric can combustor are shown. Compared with

previous published results[17] obtained by using the KIVA code, the pdf chemistry model give a better agreement with measurement. The standard $k - \epsilon$ model was used in both calculations.

2.2 Low-Reynolds Number Multiple–Scale Model

Damping functions were introduced into the high-Reynolds number multiple–scale model developed earlier[9] so that the model transport equations can be integrated down to the wall. The Kolmogorov behavior of near–wall turbulence proposed by Shih and Lumley[14] were applied to determine the boundary conditions for the turbulent quantities at the wall. The details of the model can be found in a NASA TM in preparation. Fig. 7 shows the skin friction distribution for a flat plate turbulent boundary layer. The free stream Mach number is 2.87. The current model agrees better with the Van Driest II formula than the Launder and Sharma model.

3. Future Plans

(1) Examine the effects of turbulence models on chemically reacting flow calculations. Select a combustor of a different set-up, if necessary.

(2) Broaden the validation cases to include realistic geometries found in gas turbine engine. This will provide means of realistically projecting model performance in engine component flows.

(3) Continue the development of compressible turbulence models.

4. References

[1] J. Delery and J. Reisz, "Analyse experimentale d'une interaction choc-couche limite turbulente a Mach 1.3 (decollment naissant)" ONERA Rapport Technique No. 42/7078 AY 014, Chatillon, December 1980.

[2] *EUROVAL-A European Initiative on Validation of CFD Codes.* Edt. W. Haase, F. Bradsma, E. Elsholz, M. Leschziner and D. Schwanborn, 1992.

[3] W. D. Bachalo and D. A. Johnson, "Transonic, turbulent boundary-layer separation generated on an axisymmetric flow model," AIAA J. **24**, 437–443 (1986).

[4] G. S. Settles, I. E. Vas, and S. M. Bogdonoff, "Details of a shock–separated turbulent boundary layer at a compression corner," AIAA Journal, Vol.12, pp.1709-1715, 1976.

[5] D. C. Reda and J. D. Murphy, "Sidewall boundary-layer influence on shock wave/turbulent boundary-layer interactions," AIAA Journal, Vol.11, pp.1367-1368, 1973.

[6] R. Charles, Detailed Data Set: Velocity (U, W, U_{rms}, W_{rms}) and Temperature (T) Measurement in the Axisymmetric Can Combustor (ASCC) for a Parametric Variation in Inlet Conditions, Technical Report UCI-ARTR-87-6, Univ. of California, Irvine, 1988.

[7] P. G. Huang and T. J. Coakley, "An implicit Navier-Stokes code for turbulent flow modeling," AIAA paper 92-0547.

[8] J. Zhu, FAST-2D: A Computer Program for Numerical Simulation of Two-Dimensional Incompressible Flows with Complex Boundaries, Institut Fur Hydromechanik, Report No. 690, Universitaat Karlsruhe.

[9] W. W. Liou, T.-H. Shih, and B.S. Duncan, "A Multiple–Scale Model for Compressible Turbulent Flows," Phys. Fluids, Vol. 7, pp.658–666 (1995).

[10] V. Yakhot, S. A. Orszag, S. Thangam, T. B. Gatski, and C. G. Speziale, " " Phys. Fluids A, Vol 4, 1992.

[11] T. H. Shih, J. Zhu, and J. L. Lumely, "A realizable Reynolds stress algebraic equation model," NASA TM 105993, 1993.

[12] Z. Yang, N. Georgiadis, J. Zhu, and T.–H. Shih, "Calculations of Inlet/Nozzle Flows Using a New $k-\epsilon$ Model," AIAA paper 95–2761.

[13] W. W. Liou and P. G. Huang, "Calculations of Oblique Shock Wave/Turbulent Boundary–Layer Interactions with New Two–Equation Turbulence Models," Proceedings of the Second Symposium on Transitional and Turbulent Compressible Flows, Hilton Head, South Carolina, 1995.

[14] T.-H. Shih and J. L. Lumley, "Kolmogorov behavior of near-wall turbulence and its application in turbulence modeling," NASA TM 105663, 1992.

[15] K.-Y. Chien, "Predictions of channel and boundary–layer flows with a low Reynolds number turbulence model," AIAA Journal, Vol.20, pp.33-38, 1982.

[16] T. H. Shih, W. W. Liou, A. Shabbir, Z. Yang, and J. Zhu, "A New $k-\epsilon$ eddy viscosity model for high Reynolds number turbulent flows," Computers and Fluids, Vol. 24, pp.227-238, 1995.

[17] G. J. Micklow, M. R. Harper, and J.M. Deur, "The Effects of Turbulence Modelling on the Numerical Simulation of Confined Swirling Flows," AIAA-93-1976 (1993).

Model Evaluation

- Turbulent Shear Flow

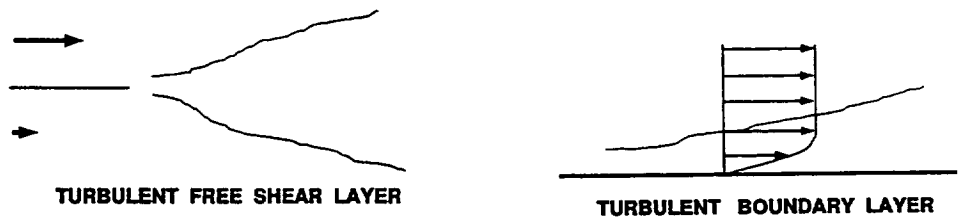

- Shock/Turbulent-Boundary-Layer Interactions
  - ◇ transonic flow

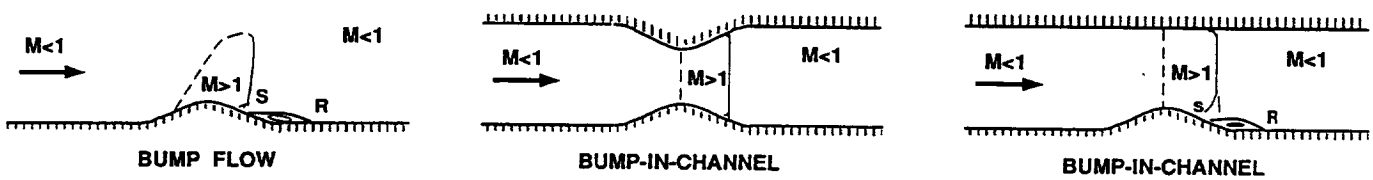

  - ◇ supersonic flow

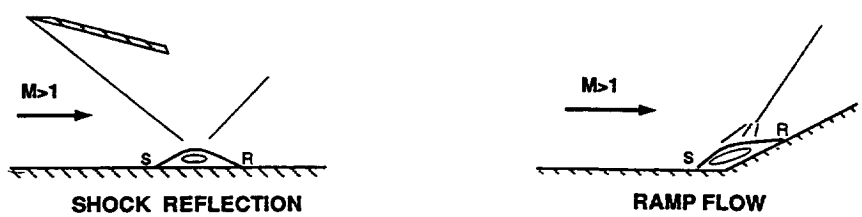

Figure 1. Sketches of validation cases

(a)

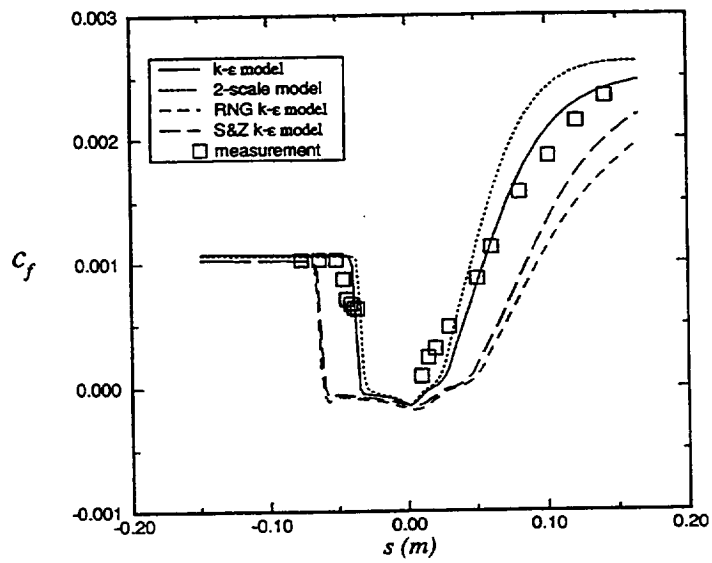

(b)

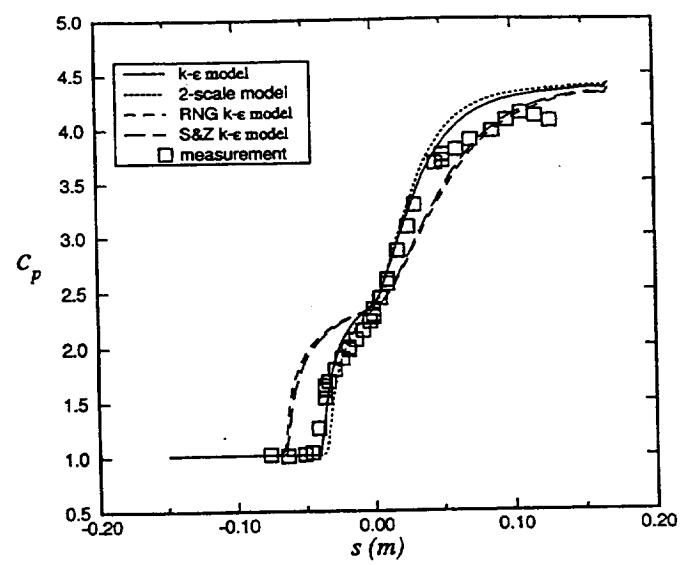

Figure 2. Comparison of surface measurement for supersonic ramp flow. (a) Skin friction coefficient; (b) Wall pressure.

(a)

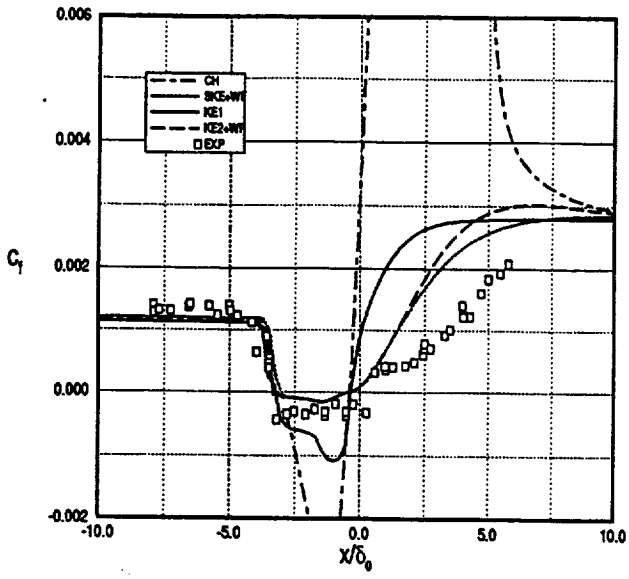

(b)

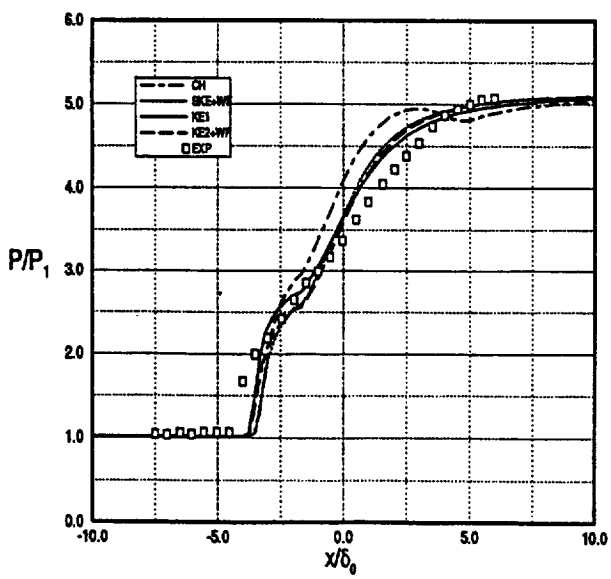

Figure 3. Comparison of surface measurement for oblique shock/turbulent boundary–layer interaction. (a) Skin friction coefficient; (b) Wall pressure.

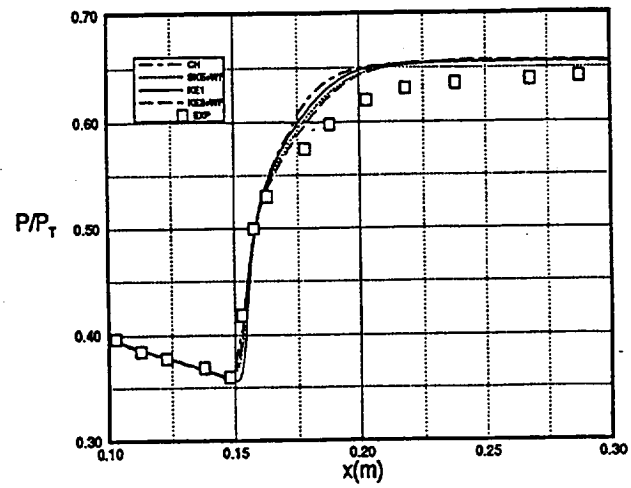

Figure 4. Comparison of wall pressure for ONERA BUMP A.

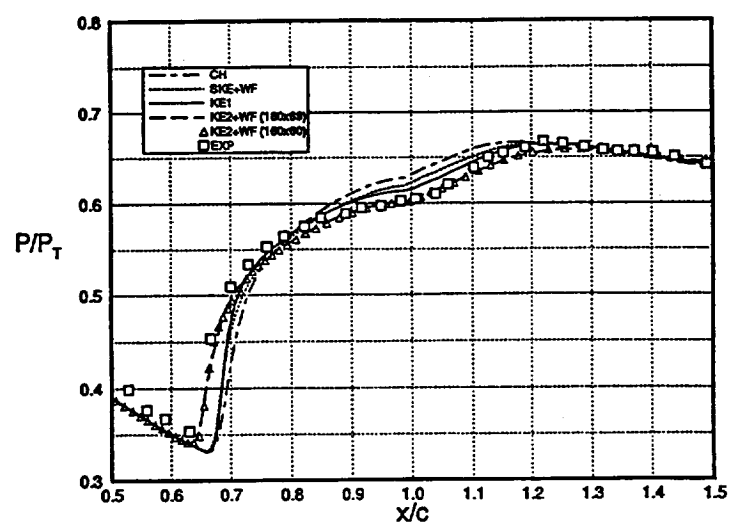

Figure 5. Comparison of wall pressure for the transonic shock/turbulent boundary–layer of Bachalo and Johnson.

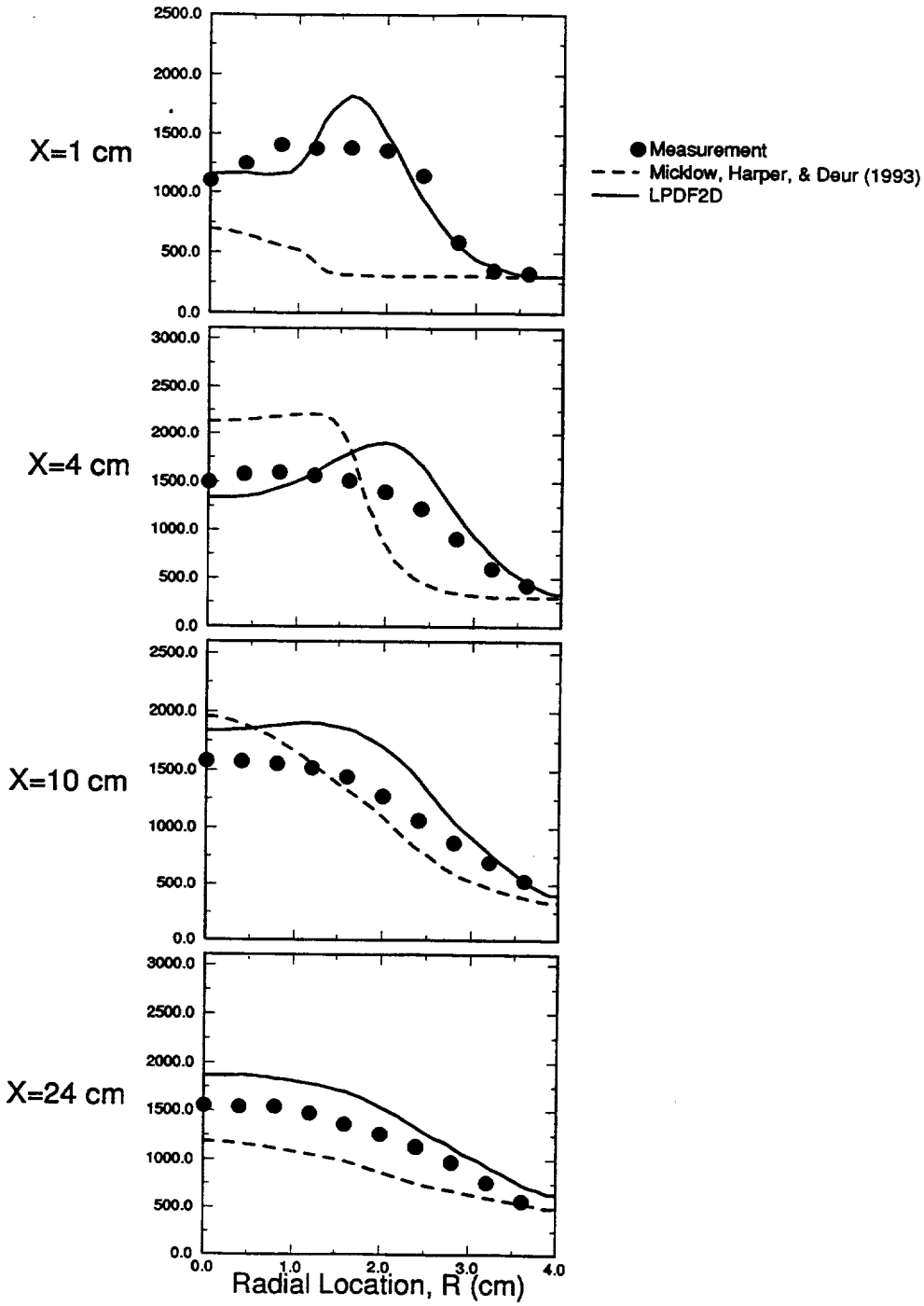

Figure 6. Comparison of temperature (°K) profiles for the UC Irvine axisymmetric can combustor.

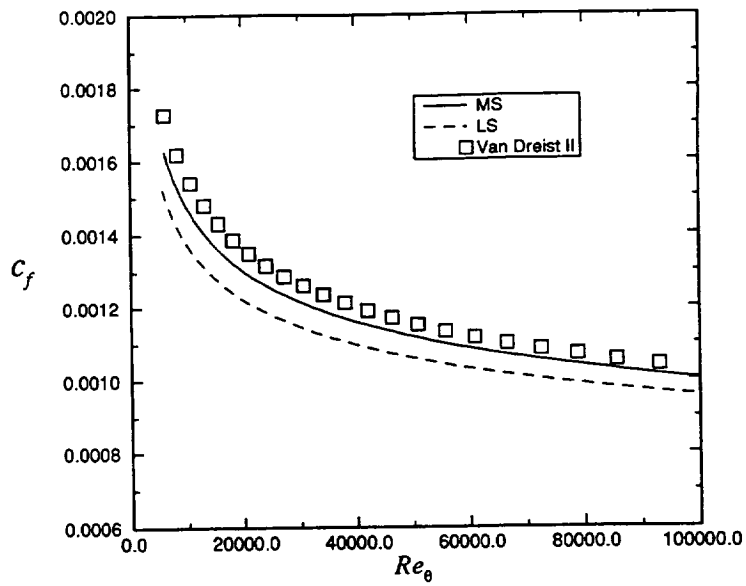

Figure 7. Comparison of skin friction coefficients for a supersonic flat plate turbulent boundary-layer of M_∞=2.87.

Modeling of Turbulent, Reacting Flows by PDF Methods

A. T. Norris

1. Motivation and Objective

The objective of this work is the development, implementation and validation of Probability Density Function (PDF) models for turbulent, reacting flows. In addition, version 1.1 of the LPDF2D code was made available for release, containing many new features and able to be run in a UNIX environment.

2. Work Performed

In this section, the different areas of PDF methods that were worked on this year are described. Some validation tests are also described.

2.1 Introduction.

The basis of Probability Density Function (PDF) methods lies in solving the transport equation for the joint PDF of quantities of interest, such as velocity, dissipation, enthalpy and/or composition. The reason why this approach to modeling turbulent reacting flows is attractive is that the chemical reaction is treated exactly[1].

Consider the transport equation for species ϕ_α:

$$\frac{\partial \phi_\alpha}{\partial t} + U_i \frac{\partial \phi_\alpha}{\partial x_i} = -\frac{\partial J_i^\alpha}{\partial x_i} + S_\alpha; \tag{1}$$

where U_i is the velocity, J_i^α is the scalar flux and S_α is the chemical source term. Now the chemical source term is a unique function of the set of σ species and two state variables;

$$S_\alpha = \hat{S}_\alpha(\phi_1, ..., \phi_\sigma, p, T), \tag{2}$$

where p and T are the state variables pressure and temperature respectively. For all but the simplest of turbulent reactive flows, a solution of Eq.(1) is impossible. However the problem becomes tractable if the solution of the mean scalar field is attempted:

$$\frac{\partial \langle \phi_\alpha \rangle}{\partial t} + \langle U_i \rangle \frac{\partial \langle \phi_\alpha \rangle}{\partial x_i} + \frac{\partial \langle u_i \acute{\phi}_\alpha \rangle}{\partial x_i} = -\frac{\partial \langle J_i^\alpha \rangle}{\partial x_i} + \langle S_\alpha \rangle; \tag{3}$$

where $\langle Q \rangle$ denotes the mean of Q, and $\langle u_i \acute{\phi}_\alpha \rangle$ is the velocity-scalar covariance, an unknown quantity that needs to be modeled. The other term that needs to be modeled is the mean reaction source term, $\langle S_\alpha \rangle$. The reason that this needs to be modeled is because:

$$\hat{S}_\alpha(\phi_1, ..., \phi_\sigma, p, T), \neq \hat{S}_\alpha(\langle \phi_1 \rangle, ..., \langle \phi_\sigma \rangle, \langle p \rangle, \langle T \rangle)\rangle. \tag{4}$$

PRECEDING PAGE BLANK NOT FILMED

It has been shown[1,2] that the two sides in this inequality can differ in both sign and by orders of magnitude. In addition, the modeling of the reaction source term would require different formulations for different fuels and mixtures. This would be clearly impractical.

It is because of the difficulties in modeling the reaction source term that PDF methods hold such attraction for the solving of turbulent reactive flows.

2.2 Hybrid PDF Method.

The PDF code under development is the LPDF2D solver developed by Hsu et al[3]. (1993). This code consists of a particle-based Monte Carlo solver for the solution of the transport equations for the PDF of the species and enthalpy, coupled with a finite-volume flow solver for the velocity, turbulence and pressure fields. Because this method is a combination of PDF and moment closure methods, it is referred to as a Hybrid PDF scheme. The solver can be used to solve steady, 2D turbulent compressible reacting flows and has been extended to 3D. Work this year has focused on the refinement of the numerical algorithms, implementation of several different schemes to calculate reaction rates, porting the code to a UNIX workstation environment, parallel implementation of the code and some validation work.

2.3 Numerical Refinement

One of the drawbacks in implementing a PDF method is the extra computer memory required by the Monte Carlo solver. To help reduce the amount of memory required, important numerical developments were performed on the PDF solver: a new time-averaging was developed and implemented, and a convection algorithm that is accurate even with only a few particles was incorporated in the code.

2.3.1 Time Averaging Scheme.

One of the requirements of the Monte Carlo PDF solver is that it return smooth, or slowly varying values of the mean scalar to the finite-volume part of the code, otherwise the flow solver may not converge or could blow-up. The simple way to achieve this is to increase the number of samples being averaged over. However this will also increase the computer memory requirements.

To achieve a mean scalar value with a small fluctuation, but with only a few particles, the technique of time averaging is used. The requirements of a good time averaging system are that only one set of data need to be stored, that the influence of samples from an earlier time can be minimized and that computation of the average is quick and simple. To fulfill these requirements, the time weighted average scheme was developed. In this method, the weighted time-average of some mean quantity $\langle\phi\rangle$ at the nth time step is given by:

$$\langle\bar{\phi}\rangle_n = \frac{1}{w_n + 1}(\langle\phi\rangle_n + w_n\langle\bar{\phi}\rangle_{n-1}), \tag{5}$$

where the over-bar indicates a time averaged quantity and w_n is a weighting function,

$$w_n = c_n(w_{n-1} + 1). \tag{6}$$

where c_n is a function of n with a value between 0 and 1. For the case of $c_n = 0$, this scheme reduces to the case of no time averaging. With $c_n = 1$, the average is formed over all time steps, each equally weighted.

By trial and error it was found that a value of $c_n = 0.9$ provides a good compromise between quick response time and smoothing for the initial stages of a calculation. When the solution of both the scalar and flow fields has stopped exhibiting transient effects, an increase to $c_n = 0.999$ reduces the scalar fluctuation further, allowing the solution to converge.

It should be noted here, that the concept of convergence in PDF methods is not the same as that in pure moment closure schemes. Due to the statistical error always present, solutions can only converge down to the level fluctuation present in the mean estimates, rather than to machine accuracy.

2.3.2 Convection Scheme.

Convection in the Monte Carlo PDF code consists of the movement of particles from one cell node to another due to the action of the mean velocity and turbulent diffusion. Due to the finite number of particles at each node and the need to move whole numbers of particles, errors occur in this process. For example, if 5.3 particles are to be convected, the existing code would convect 5 particles. By increasing the number of particles at a node, more will be convected and the errors would be decreased, however more particles means more memory required.

To overcome this problem, we make use of the time-averaging used in the code. At each step, the number of particles to be convected is calculated. This number is then rounded to an integer value by a random process, with the probability of rounding up or down dependent on the value of the fractional remainder. ¿From the previous example, 5.3 has a fractional remainder of 0.3. Thus 5.3 would be rounded up to 6 with a 30% probability, and rounded down to 5 with a 70% probability. Because of the time averaging used in the scheme, the mean convection will be 5.3 particles.

Another method would be to save the fractional particles and carry them over to the next time step. This however has two disadvantages. First the fractional value needs to be saved, thus using memory. Secondly, this introduces an occilation into the solution. For example, if 5.1 particles were to be convected, then 5 particles would be convected except for every 10th step when 6 particles would move. This period would be damped out by the time averaging to some extent, but not totally. This small periodic fluctuation could possibly excite some non-physical fluctuations in the solution, such as vortex shedding. For these reasons, this method was not implemented.

2.4 Operating Environments.

In order to make the LPDF2D code accessible to a wider range of users, several changes have been made to the code. The most common computing environment available these days is the UNIX workstation. Because of this, the LPDF2D code has been modified to run on workstations. This has involved the removal of machine

dependent commands, the introduction of a portable random number generator and the ability to perform calculations in a parallel cluster environment.

2.4.1 Random Number Generator.

To aid the portability of the code, a machine independent random number generator was incorporated into the code. This routine provides a "more random" set of numbers than most built-in generators, while making use of the 32 bit wrap-around feature of UNIX machines to speed up the program.

2.5 Chemical Kinetics.

Despite the ability of the PDF method to treat chemical reaction exactly, the implementation of the numerical chemical kinetics in a Monte Carlo scheme is a non-trivial matter. First, the solution of the full system of rate equations for the thermochemistry in turbulent reacting flows requires obtaining solutions for of order 50 chemical species, governed by of order 200 stiff, non-linear rate equations. At present this task is computationally infeasible, and so reduced mechanisms are employed. These reduced mechanisms represent the full composition by a few representative species, typically two to five, and the reaction rates of these species are quasi-global equations derived from the full mechanism. However even the solution of a reduced mechanism is a computationally expensive task. In a typical PDF calculation[5], there are on order 100,000 particles and 1,000 time steps, resulting in the code performing 10^9 solutions of the reduced mechanism.

A computationally efficient way of reducing this task to manageable proportions is to use a look-up table. In this table, the reduced mechanism is integrated for discrete time and composition increments, and stored in a table. Thus integration is replaced by interpolation, at a considerable saving in computer time. By the use of adaptive tabulation techniques[4] the size of the tables can also be minimized.

However, because of the many different combinations of fuel and oxidizer, as well as the differing degrees of complexity of mechanisms, several different options for chemical reaction have been provided apart from look-up tables. These include equilibrium chemistry (where the reaction is assumed to proceed infinitely fast), 1 step global reactions and the option to integrate the full mechanism.

In these options, the CHEMKIN[6] package has been used to provide the species data for the reactions, reducing the amount of input required by the user.

2.6 Parallel Computations.

If the option to use the full mechanism is used, the biggest use of time in the PDF code is the calculation of reaction rates. Because of this, the LPDF2D code has been altered to run on a work-station cluster, with PVM[7] message passing. At present this involves only the calculation of reaction rates in parallel, the rest of the process being performed in serial. Because of the low volume of message passing, and the statistical nature of the PDF code, this has proved to be a very effective method of achieving substantial speedup of the code.

4.0 Validation.

In order to validate the PDF code, and test its performance against that of a

conventional moment closure code with laminar chemistry, a test case was chosen and then modeled by both methods. The flow chosen was the $CO/H_2/N_2$-air flame of Masri et al[8]. This flow was chosen as it has high levels of turbulence in the reactive region of the flame, thus the turbulent/chemical interactions would have a significant effect on the flow.

The conclusion of the study was that the PDF method did provide a superior performance to the moment closure method in predicting turbulent reacting flows. In Figs. 1 and 2, the temperature contour plots for the two numerical methods are shown. It can be seen that the PDF method predicts peak temperatures of about 1400K in a narrow band, in good agreement with the experimental data. However the moment closure results show peak temperatures of 2000K lying in a broad band, contrary to the experimental results.

Details of this comparison are described by Norris and Hsu[9], and were presented at the 30th Joint Propulsion Conference in Indianapolis.

5.0 References

[1] Pope, S.B., "PDF Methods for Turbulent Reactive Flows," Prog. Energy Combust. Sci., **11**, 119-192 (1985).

[2] Pope, S.B., "A Monte Carlo Method for the PDF Equations of Turbulent Reacting Flows.," Combust. Sci. Tech., **25**, 159-174 (1981).

[3] Hsu, A.T., Tsai, Y.L.P. & Raju, M.S., "A PDF Approach for Compressible Turbulent Reacting Flows," Proc. AIAA 31st Aerospace Sciences Meeting and Exhibit, Reno, Nevada, AIAA-93-0087 (1993).

[4] Norris, A.T., *The Application of PDF Methods to Piloted Diffusion Flames,* PhD Thesis, Cornell University, Ithaca, 1993.

[5] Pope, S.B., "Computations of Turbulent Combustion: Progress and Challenges," In 23rd Symposium (International) on Combustion, 591-612 (1990).

[6] Kee, R.J., Rupley, F.M. & Miller, J.A., "CHEMKIN-II: A Fortran Chemical Kinetics Package for the Analysis of Gas-Phase Chemical Kinetics," Report SAND89-8009, Sandia National Laboratories, Livermore, CA 94551

[7] Geist, A., Beguelin, A., Dongarra, J., Jiang, W., Manchek, R. & Sunderam, V., "PVM 3 User's Guide and Reference Manual," Report ORNL TM-12187, Oak Ridge National Laboratory, Oak Ridge TN 37831

[8] Masri, A.R., Dibble, R.W. & Barlow, R.S., "The Structure of Turbulent, Pilot-Stabilised Flames of $CH_4/CO/H_2/N_2$ Fuel Mixtures," Combustion and Flame, in press (1994).

[9] Norris, A.T. & Hsu, A.T., "Comparison of PDF and Moment Closure Methods in The Modeling of Turbulent Reacting Flows" Proc. AIAA 30th Joint Propulsion Conference, Indianapolis, Indiana, AIAA-94-3356 (1994).

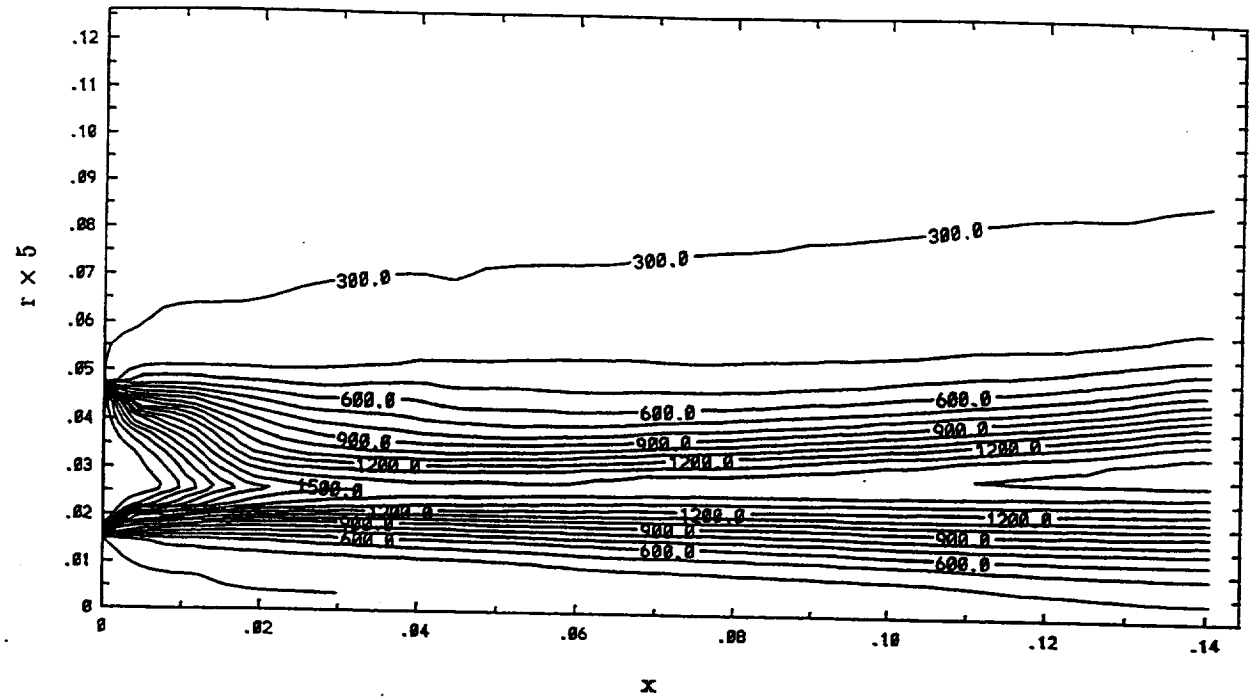

Figure 1: Contour plots of mean flame temperature produced by the PDF method. Note that radial coordinate is stretched by factor of five. Contour levels are in degrees Kelvin.

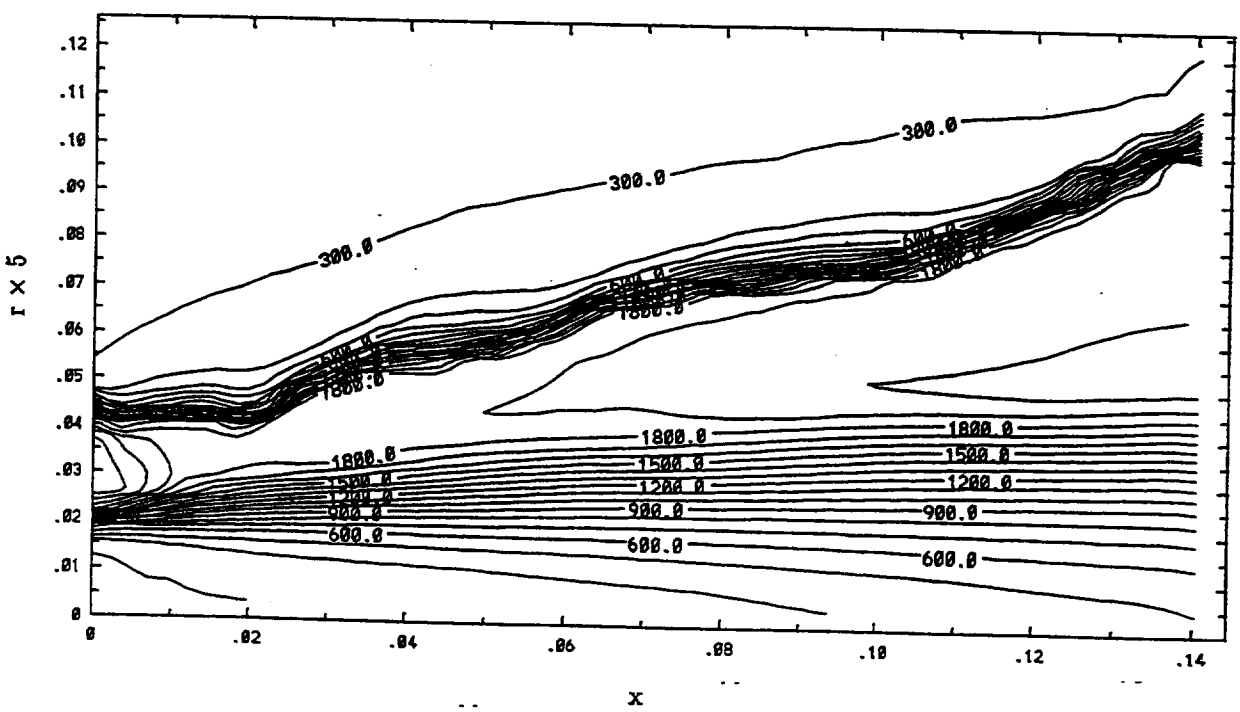

Figure 2: Contour plots of mean flame temperature produced by the moment closure method. Note that radial coordinate is stretched by factor of five. Contour levels are in degrees Kelvin.

Application of PDF to Compressible Turbulent Reactive Flows

Andrew T. Hsu

1. Motivations and Objectives

In an earlier paper[1], we have introduced a probability density function (pdf) approach for high speed reactive flows. The extension of this pdf approach to three-dimensional applications is reported here. The major obstacle to the application of a Monte Carlo pdf solver to complex three-dimensional reactive flows is the limitation imposed by the need of a large number of notational particles in a Monte Carlo simulation to provide a converged, relatively smooth solution free of large statistical errors, which in general requires enormous amount of both computer memory and cpu time. To overcome this obstacle, a novel averaging scheme is introduced. This new averaging scheme allows one to use as few as 50 sample particles per computational cell and yet still provides Monte Carlo solutions that are smooth enough to be applicable in the finite-volume/Monte-Carlo scheme. Further, the averaging scheme automatically eliminates the effect of initial conditions, making it ideal for large-scale applications.

2. Work Accomplished

In turbulent reactive flow computations, the conventional moment closure models have difficulty in treating the nonlinear chemical reaction source terms; this problem is known as the chemical closure problem. One of the methods that can overcome the chemical closure problem is the probability density function (pdf) method. Several key advances were made in the development of pdf methods during the past decade. Most of the earlier advances are primarily in the low-speed combustion area.

In an earlier paper a probability density function turbulence model for compressible reacting flows has been proposed by the present authors [1]. The probability density function of the species mass fraction and enthalpy is obtained by solving a pdf evolution equation using a Monte-Carlo scheme. The pdf solution procedure is coupled with a compressible finite volume flow solver which provides the velocity and pressure fields. A modeled pdf equation for compressible flows, capable of capturing shock waves and suitable to the present coupling scheme, has been proposed and tested. Several 2D supersonic diffusion flames were studied and the results compared favorably with the available experimental data.

In the present paper, the extension of the pdf method to three-dimensional supersonic combustion is reported. The main obstacle to the application of a Monte Carlo pdf solver to complex three-dimensional reactive flows is the limitation of computer memory and cpu time. To overcome this obstacle, a novel averaging

scheme is introduced. This new averaging scheme allows one with the use as few as 50 sample particles per computational cell to obtain Monte Carlo solutions that are smooth enough to be supplied to the finite-volume solver as required during each of the iteration steps of the finite-volume/Monte-Carlo scheme. Furthermore, the averaging scheme automatically eliminates the effect of initial conditions, making it ideal for large-scale steady-state applications.

A three-dimensional jet-in-crossflow hydrogen combustion case has been successfully computed using the present scheme. The results are compared with those from a finite volume reactive flow solver.

2.1 The PDF Method

The modeled pdf equation for the species mass fraction and specific enthalpy used in the present work can be written as follows:

$$(\rho P)_{,t} + (\rho < u_j > P)_{,j} + (\rho w_j P)_{,Y_j} = (D_t P_{,j})_{,j} + M(P) - (S_p P)_{,h}.$$

where the first two terms on the right hand side of the equation are the modeled terms for turbulent diffusion and molecular mixing; the last term is the term representing the compressibility effect.

The turbulent diffusion term is simulated using a simple gradient diffusion model by O'Brien[2] and Pope [3]:

$$- < u'_j | Y_i, h > P = D_t P_{,j}.$$

The use of this gradient diffusion model is consistent with the use of a $k - \epsilon$ model in the flow solver.

The molecular diffusion term is modeled using the continuous mixing model by Hsu and Chen [4]. This model is an extension of Curl's model. In order to achieve continuous mixing, we assume that all the particles within a cell participate in mixing. The extent of the mixing is controlled at the individual particle level. That is to say, the N particles within a given cell are randomly grouped into $N/2$ pairs; the properties of all the particles change according to

$$Y_n(t + \delta t) = AY_m(t) + (1 - A)Y_n(t)$$

$$Y_m(t + \delta t) = AY_n(t) + (1 - A)Y_m(t)$$

The extent of mixing is controlled at the individual particle level through the parameter A, which is defined as

$$A = C' \xi \frac{\delta t}{\tau}$$

where $C' = 2.0$. At the limit $\delta t \to 0$, the above equations becomes

$$\frac{dY_n}{dt} = C' \frac{\xi}{\tau} (Y_m(t) - Y_n(t)).$$

The above equation states that the change of Y_n due to mixing is proportional to the difference between Y_m and Y_n, and inversely proportional to the turbulence time scale, τ.

The compressibility effect is modeled by the following expression:

$$S_p = < p >_{,t} + < u_i >< p >_{,i} + 0.8\rho < k >< u_i >_{,i} - \alpha_2 \rho Pr M_t + \alpha_3 \rho \epsilon M_t^2,$$

which can be regarded as the convection velocity of a sample particle in the h-direction in the space spanned by h and Y_i's. Details of this model are given in Ref. [1]

2.2 Solution Procedure

A fractional-step Monte-Carlo method developed by Pope [3] is used in solving the pdf evolution equation. When coupling a pdf solver with RPLUS, a finite volume flow solver, the species transport equations in the RPLUS code are no longer needed. The information we need, at each marching time step, from the flow solver (RPLUS) includes the mean velocity, pressure, density, and a turbulence time scale or quantities such as the turbulent kinetic energy and dissipation rate. The species transport and chemical reactions are simulated by solving the pdf evolution equation. At every time step, the temperature calculated from the pdf solution is fed back to the mean flow solver for the computation of heat transfer and pressure. The Monte Carlo and finite-volume solvers are run in parallel, and information exchange occurs at every time step until a converged solution is obtained.

2.3 Averaging Scheme

In a Monte Carlo computation, the statistical error is estimated to be of the order of $1/\sqrt{N}$, where N is the number of sample particles per computational cell. If this error is large, it could lead to an erroneous finite-volume solution when information from the pdf solver is transferred to the flow solver. Because of this slow convergence, to obtain a smooth solution from the Monte Carlo solver, one needs thousands or even tens of thousands of sample particles per cell. In our previous paper [1] we proposed a combined ensemble-time averaging scheme. That scheme reduced the required particle per cell, but it requires some more memory for the time averaging process. For any realistic 3D combustion problems, the memory requirement of that scheme exceeds the CRAY-YMP capacity. In what follows we introduce a novel averaging scheme that eliminates the effects of the initial conditions automatically while requiring no additional memory.

Let a_n be the combined time-ensemble average at the nth time step, and let b_n be the ensemble average at the nth time step. A general weighted time average can be written as

$$a_n = \frac{1}{f_n + 1}(b_n + f_n a_{n-1})$$

In terms of ensemble average, the above equation can be written as

$$a_n = \frac{1}{f_n + 1} b_n + \frac{f_n}{(f_n + 1)(f_{n-1} + 1)} b_{n-1} + \frac{f_n f_{n-1}}{(f_n + 1)(f_{n-1} + 1)(f_{n-2} + 1)} b_{n-2} + \cdots$$

Where f_n is a discrete function that can be chosen appropriately to give the desired weighting for solutions from various time levels. For instance, $f_n = n$ would give a equally weighted running average, and the above equation becomes

$$a_n = \frac{1}{n+1}(b_n + b_{n-1} + \cdots + b_1 + b_0)$$

Fig. 1 shows the weighting distribution as a function of the time step when using the following function

$$f_n = nc$$

with $c = 0.6$, 0.8, and 1.0. This weighting procedure gives a fairly smooth Monte Carlo solution, but it eliminates the effect of only the first few time steps. By choosing

$$f_n = c(f_{n-1} + 1)$$

In which case Eq. (9) is equivalent to

$$a_n = \frac{1}{(f_n + 1)}(b_n + cb_{n-1} + c^2 b_{n-2} + \cdots + c^{n-1} b_1 + c^n b_0)$$

The weighting distribution, as shown in Fig. 2, is shifted drastically towards the latest solutions. The weakness of this particular formulation is unevenness of the weight distribution.

Ideally, one would like to eliminate the effect of the initial conditions, yet have a fairly even weight distribution for the later solutions. Such a weighting function can be achieved by replacing the constant c in the equation for f_n by a variable c_n, i.e.,

$$f_n = c_n(f_{n-1} + 1)$$

There are any number of possibilities in choosing c_n. For example, $c_n = 1 - 1/n$, $c_n = 1 - 1/n^x$, $c_n = 1 - 1/e^n$, $c_n = x^{1/n}$, etc. One formulation we have found to be fairly successful is

$$c_n = 1 - \frac{1}{x^n}$$

with $x > 1$. Fig. 3 shows the weight distribution for $x = 1.014$, 1.0088, and 1.007. The advantages of this weighted averaging procedure are that the effect of the initial condition can be effectively eliminated, and that after a certain number of iterations, the solutions are equally weighted. For example, in the case of $x = 1.014$, the effect of the solutions from the first 200 time steps are completely eliminated, and after about 500 time steps, the solutions are equally weighted in the averaging procedures. The pdf results reported in what follows are obtained using this weighting scheme.

2.4 3D Application

In the present work, one of our major objectives is to demonstrate the feasibility of applying the pdf method to realistic 3D supersonic combustion problems. Unfortunately, there is a lack of experimental data in this area. The case we have chosen

to demonstrate the application of the pdf method is a supersonic jet in crossflow. A $300°K$, Mach 1.5 hydrogen jet is vertically injected into a Mach 2 crossflow with $1000°K$ vitiated air. The jet diameter is 6 mm. Figs. 4-8 are the temperature and species mass fraction contours from the pdf solution as compared to the solution from a finite volume code (RPLUS) using laminar chemistry. The grids used in both calculations are $40 \times 15 \times 25$. The computational domain reaches about 30 jet diameters downstream of the jet. The Monte Carlo simulation of the pdf equation used 50 sample particles per computational cell. The coupling between the pdf solver and the finite volume flow solver is done through feeding density, velocity, and turbulent time scale from the finite volume solution to the pdf solver, and feeding temperature distribution from the pdf solver to the finite-volume flow solver.

Fig. 4 shows the central-plane temperature distribution. The results show that the pdf solution gives a much shorter cold jet core than that from the finite volume scheme, which is consistent with our previous 2D results. The maximum temperature from both solutions are the same. Fig. 5 shows the temperature contours at a cross section at about 12 jet diameters downstream of the injection port. The basic structure of the two solutions are similar, with some differences in details: The finite volume solution gives a very high temperature region at the bottom wall away from the centerline while the pdf solution does not show this. This difference could be caused by the different boundary conditions used at the wall.

Figs. 6, 7, and 8 show the mass-fraction contours of hydrogen, oxygen, and water vapor, respectively. The results for the mass fractions are consistent with what we have observed from the temperature distribution. For instance, the hydrogen distribution from the finite volume solution shows a maximum of about 0.8 near the center while the pdf solution there has a lower value of only 0.35 indicating some of the differences observed between the solutions. In Fig. 8, where it corresponds with the high temperature at the wall, there is a higher concentration of water vapor (about 0.35) in the finite-volume solution while the pdf solution shows a maximum of only 0.12.

Because of the lack of experimental data, it is difficult to judge the validity of either solution. However, the contours from the Monte Carlo solution is as smooth as that from the finite volume solution, showing that it is feasible to make large scale computations on practical problems using the Monte Carlo pdf solver.

2.5 Concluding Remarks

A pdf method for high speed turbulent combustion has been successfully extended to 3D applications. A novel averaging scheme has been introduced which made the applications of the present pdf method to realistic large scale computations feasible.

3. Future Work

3.1 PDF

Parallel computing and NOx prediction will be the two major areas for future PDF applications. The goal is to make the PDF method an industrial design tool.

4. References

[1] Hsu, A.T., Tsai, P.Y. and Raju, M.S., " A PDF Approach for Compressible Turbulent Reacting Flows," AIAA 93-0087, January, 1993, Reno, NV.

[2] O'Brien, E.E., "The Probability Density Function Approach to Reacting Turbulent Flows." Turbulent Reacting Flows, Springer-Verlag, Berlin, P. 185, 1980.

[3] Pope, S.B., " A Monte Carlo Method for the PDF Equations of Turbulent Reactive Flow." Combustion Science and Technology, vol 25, p.159, 1981.

[4] Hsu, A.T. and Chen, J.Y., "A Continuous Mixing Model for PDF Simulations and its Applications to Combusting Shear Flows." Proceedings of the 8th Symposium on Turbulent Shear Flows, Munich, September, 1991.

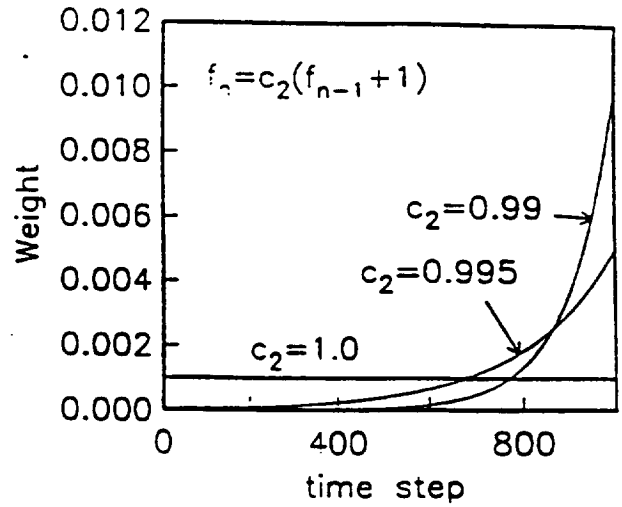

Fig. 2. Weight distribution for the first 1000 time steps using Eq. (12).

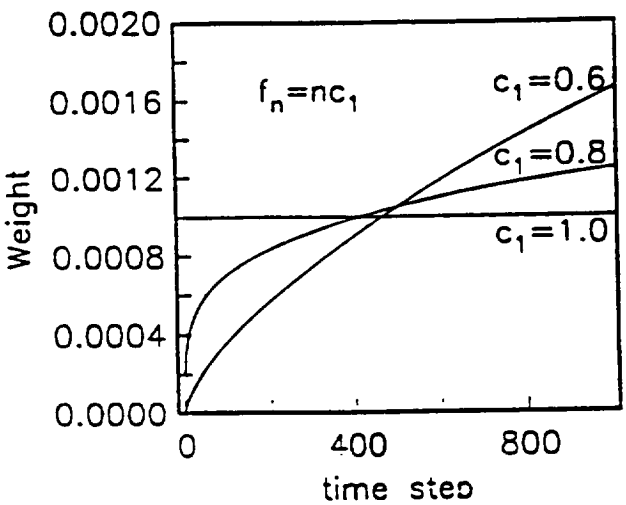

Fig. 1. Weight distribution for the first 1000 time steps using Eq. (11).

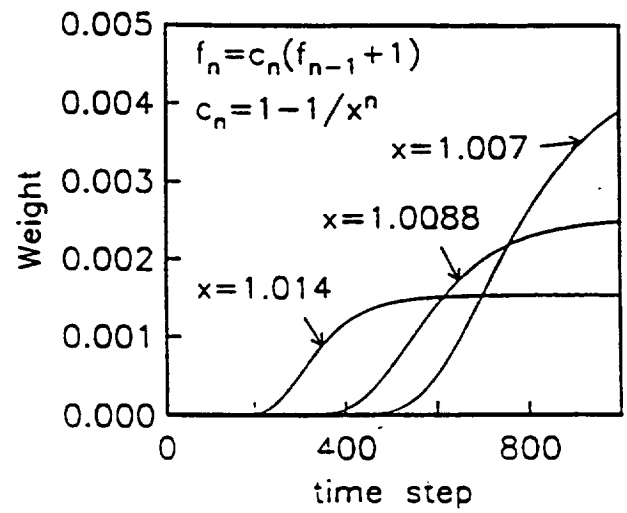

Fig. 3. Weight distribution for the first 1000 time steps using Eqs. (14) and (15).

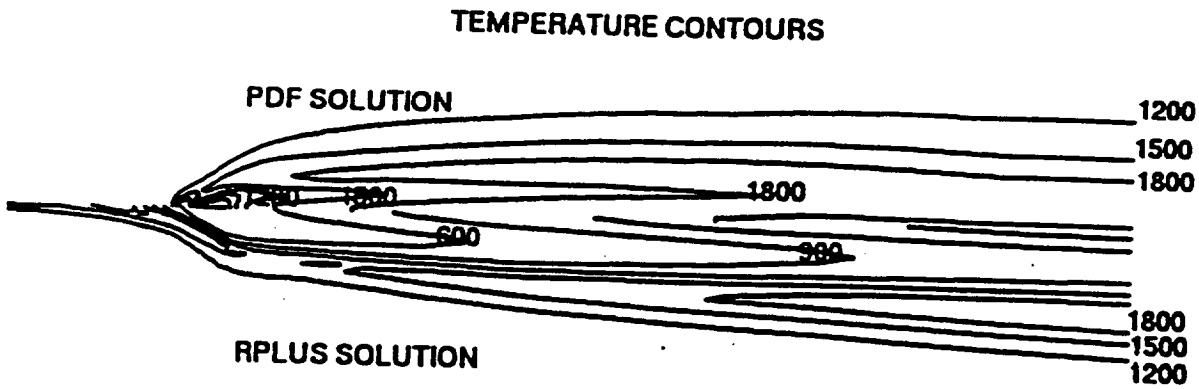

Fig. 4. Center plane temperature distribution for the 3D supersonic jet combustion problem.

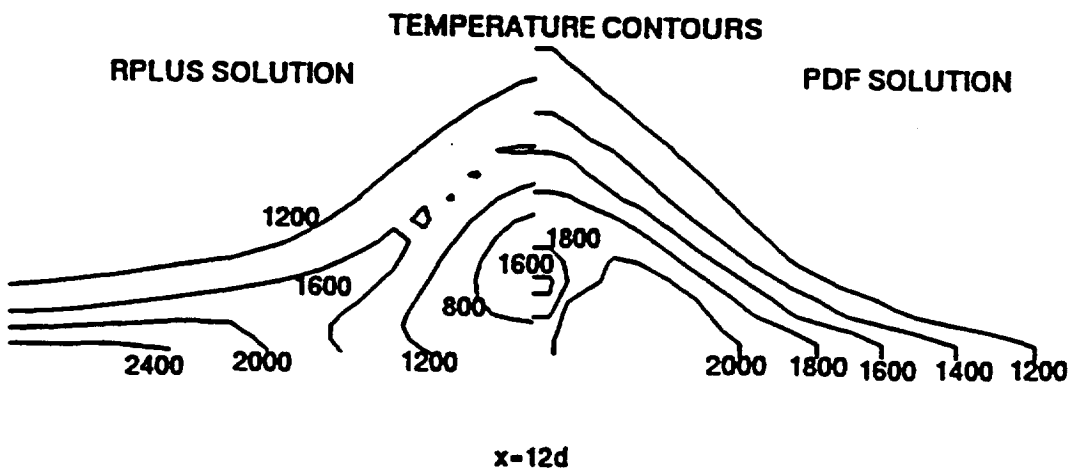

Fig. 5. Temperature distribution at x=12d for the 3D supersonic jet combustion problem.

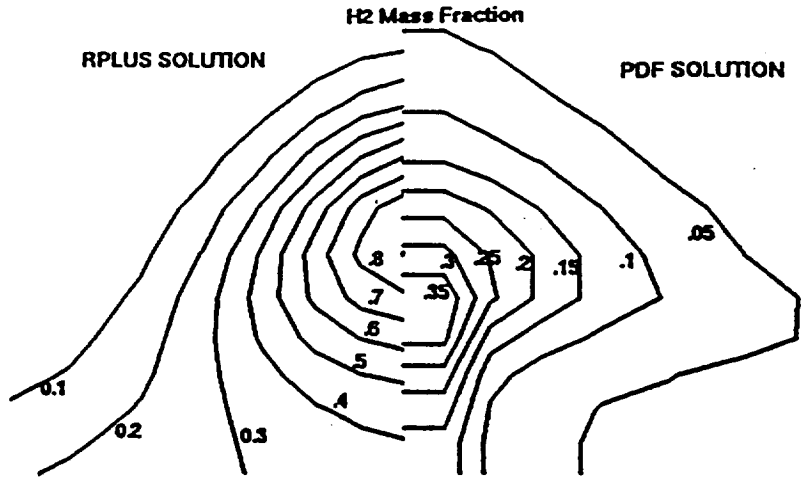

Fig. 6. Hydrogen distribution at x=12d for the 3D supersonic jet combustion problem.

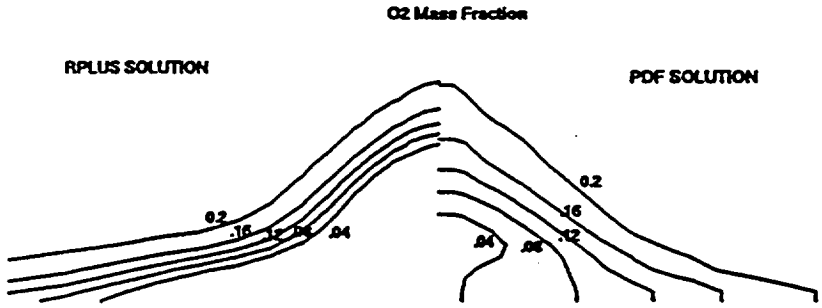

Fig. 7. Oxygen distribution at x=12d for the 3D supersonic jet combustion problem.

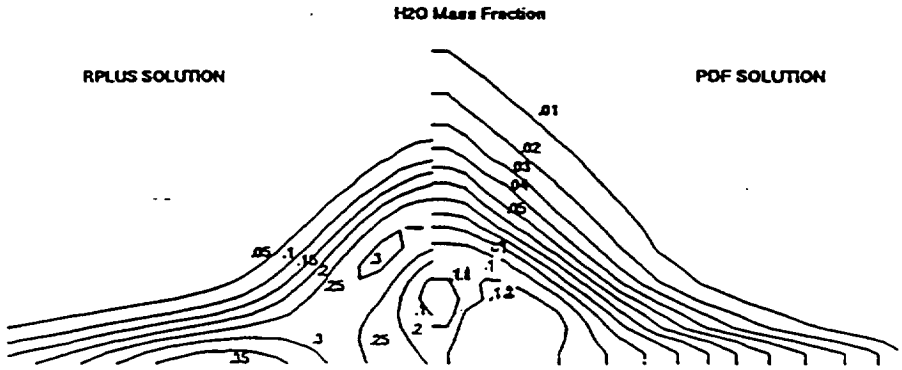

Fig. 8. Water vapor distribution at x=12d for the 3D supersonic jet combustion problem.

Turbulence Model Development for NPARC

J. Zhu, Z. Yang, and T. H. Shih

1. Motivation and Objective

The purpose of this research is to enhance the turbulence modeling capability of NPARC. The outcome of this research is a turbulence subprogram which is independent of NPARC but linked to NPARC in code execution. In the solution process, the turbulence subprogram interacts with the NPARC code, the mean field solver, to produce the solution. This turbulence subprogram contains a number of turbulence models suitable for aerospace and aero-propulsion system applications. These models are chosen from the state of the art of turbulence models developed by both CMOTT researchers and researchers from other groups of the turbulence modeling community. The turbulence subprogram with advanced turbulence models serves the following purposes: first, it will enhance the turbulence modeling capability of NPARC; second it will provide a vehicle for incorporating future turbulence models, and third it can be used to validate turbulence models against complex flows of industry interest.

NPARC is a general purpose computational fluid dynamics (CFD) code. It solves Navier-Stokes equations in a conservation form in a general coordinate system. It can handle complex geometries and different types of boundary conditions. The NPARC code is widely used in the aerospace and aero-propulsion community. Up to now, many flows of practical interest have been calculated using the NPARC code, ranging from an inlet flow in an air-breathing engine to the flows around a maneuvering airplane. A description of the code and its numerical scheme is given by Cooper and Sirbaugh[1]. Updates of code capabilities and a listing of bibliographies of using the NPARC code to calculate flows of practical interests can be found in the current version of the NPARC User Guide[2]. The NPARC code is actively supported by NASA Lewis Research Center via the NPARC Alliance, a partnership formed between NASA Lewis Research Center and Air Force Arnold Engineering Development Center. The NPARC users are represented by the NPARC Association currently headed by Boeing Company and McDonnell Douglas Company.

2. Work Accomplished

To enhance the turbulence modeling capabilities of NPARC, a turbulence module approach is adopted in the present project. In the following, the turbulence module for NPARC is briefly described. We will then list the turbulence models that are available in the current version of the turbulence module. NPARC calculations using the turbulence module for some propulsion flows will also be presented.

The work accomplished is done by J. Zhu, Z. Yang, T. H. Shih at Center for Modeling of Turbulence and Transition (CMOTT), and by N. Georgiadis at NASA Lewis Research Center. This project is coordinated by D. R. Reddy of NASA Lewis Research Center.

PAGE 72 INTENTIONALLY BLANK

PRECEDING PAGE BLANK NOT FILMED

2.1 Introduction to Turbulence Models in NPARC

Most of the flows in aerospace and aero-propulsion systems are turbulent because of the high Reynolds numbers of the flows. Thus, for a code with a well developed numerical scheme such as the NPARC code, its turbulence modeling capability is the pacing item for computational accuracy. Currently, NPARC contains a number of mixing length eddy viscosity models[3,4] and the Chien $k-\epsilon$ eddy viscosity model[5]. A mixing length eddy viscosity model has the advantage of being simple in implementation and fast in execution; however it is a 'one physics/one flow' model, i.e., the mode is tailered to a particular physics/flow, and its performance deteriorates drastically when used to calculate other flows. In comparison, a $k-\epsilon$ eddy viscosity model is much more general than mixing length eddy viscosity models and could be used for a much wider range of flows, for example, both free shear flows and wall-bounded flows. Among the existing low-Reynolds number $k-\epsilon$ eddy viscosity models, the Chien $k-\epsilon$ eddy viscosity model is perhaps the simplest and gives a reasonable performance for attached boundary layer flows. However, it has some well known deficiencies. For example, its performance is rather poor for flows with transition, separation and reattachment, because y^+ is used in modeling the near-wall effect. These deficiencies can be removed and the applicability of $k-\epsilon$ model can be substantially expanded. Recently, a CMOTT $k-\epsilon$ eddy viscosity model has been implemented into the NPARC code. This model does not contain the friction velocity, unlike the Chien $k-\epsilon$ model, and can thus be used for flows with separation and reattachment. The detail of the model form and the results of model performance will be presented in later subsections.

2.2 CMOTT Approach – Turbulence Subprogram for NPARC

In the effort of enhancing the turbulence modeling capabilities of NPARC, we implement different turbulence models in a stand-alone turbulence subprogram (also referred to as turbulence module) instead of implementing them in the NPARC code directly. We feel that this is a preferred approach in a situation that a gap exists between turbulence model developers and CFD users. The former mainly use simple flows to verify new modeling concepts and evaluate the resulting models, while the latter are usually reluctant to implement new turbulence models unless they see that such models have shown a good performance for a wide range of complex flows relevant to industry situations. In order to bridge this gap, we develop turbulence modules for industry's CFD codes. Since the NPARC code is a major industry code with a well established numerical scheme and a large user group in the aerospace and aero-propulsion community, we use the NPARC code as our reference CFD code to write the turbulence modules. With minor modifications, the turbulence module written for the NPARC code can be adopted for other industry CFD codes.

The turbulence module is written in a self-contained manner so that the user can use any turbulence model in the module without worrying about how it is implemented and solved. The inputs to the turbulence module are mean flow variables, boundary and geometric information which are provided by a mean flow solver. The outputs of the turbulence module are the Reynolds stresses and heat fluxes which are needed for the mean flow calculation. In the current formulation, the Reynolds

stresses and heat fluxes are expressed in terms of turbulent diffusivities and relevant turbulent source terms. The interaction between the mean flow solver and the turbulence module gives the final turbulent flow solution. With the aid of the turbulence module, we can take the advantage of the well-established and sophisticated CFD codes to test turbulence models for a variety of complex flows which are intractable with the simple research codes. The turbulence module, on the other hand, enhances the turbulence modeling capabilities of existing CFD codes and provides a vehicle to facilitate the technology transfer from the model development to model applications.

In the turbulence subprogram for NPARC, the governing transport equations for turbulence quantities (k and ϵ) are written in conservation form and a finite-volume procedure is used to solve these equations. Comparing with the NPARC code, the turbulence subprogram has the following features: (a) the cell-corner arrangement is used, i.e., the flow variables are stored at grid nodes rather than at the centers of control volumes; (b) contrary to the NPARC code and most other codes for compressible flows, the non-delta form of equations is used which leads to a simpler linearization and is more effective to ensure the positiveness of the turbulent kinetic energy and its dissipation rate (k and ϵ) than the delta form. To reduce numerical diffusion while maintaining necessary stability, the second-order accurate HLPA scheme[6] is used for the convective terms of the turbulent transport equations. This scheme is implemented such as to blend two schemes by a parameter λ, with limiting values λ=0 for the (first-order) upwind and λ=1 for the second-order and bounded solution scheme. The turbulence subprogram includes four most commonly used boundary conditions - the inflow condition, the outflow condition, the symmetry plane condition, and the condition on the solid wall. The turbulence subprogram also allows the user to introduce boundary conditions other than these four types. Care has been taken to make the turbulence module user-friendly. This is achieved by providing a few parameters that the user can define in model selection and problem specification. The resulting algebraic set of equations are solved iteratively via a under-relaxation procedure. The user can also control the relaxation parameters in the problem specific part of the subprogram. The turbulence module is written in a similar manner as the FAST2D code written by Zhu[7]. A detailed description of the turbulence module for the NPARC code is going to be presented in a paper by Zhu and Shih[8] in the upcoming 31st AIAA Joint Propulsion Conference.

2.3 Turbulence Models in the Subprogram

Currently, four turbulence models are available in the turbulence subprogram. They are the mixing length eddy viscosity model of Baldwin-Lomax[3], the low Reynolds number $k-\epsilon$ eddy viscosity model of Chien[5], the low Reynolds number $k-\epsilon$ eddy viscosity model of Shih and Lumley[9], and a new low Reynolds number realizable $k-\epsilon$ eddy viscosity model developed here at CMOTT.

Because of the increasing computer power available and the increasing demand for more accurate flow prediction, it is recommended that a $k-\epsilon$ eddy viscosity model is used for calculating flows of engineering interests. The Baldwin-Lomax

mixing length eddy viscosity model is included in the turbulence subprogram for two reasons. First, it is chosen as a representative of the mixing length models. Second, it can be used to generate the initial field for $k-\epsilon$ model calculations.

The Baldwin-Lomax mixing-length model, the Chien $k-\epsilon$ model, and the Shih-Lumley $k-\epsilon$ model have been published in archival journals. Here, only the newly developed low Reynolds number realizable $k-\epsilon$ eddy viscosity model is described. The model has the same model form as the Shih-Lumley low Reynolds number $k-\epsilon$ eddy viscosity model, i.e, it has the same form of transport equations for k and ϵ, it uses the same near-wall boundary conditions for k and ϵ as derived from the Kolmogorov behavior of the turbulence field near the wall, and it uses the same parameter $R_y = yk^{1/2}/\nu$ to construct the damping function f_μ. The boundary conditions based on Kolmogorov behaviors of near wall turbulence makes the computing robust. The parameter R_y is a better choice for modeling of near wall turbulence than y^+ since it does not involve the skin friction u_τ. The major improvement in the present realizable $k-\epsilon$ eddy viscosity model compared with the Shih-Lumley model is that a realizable formulation for C_μ is used. In an isotropic eddy viscosity model, the Reynolds stresses are related to the mean velocity field by

$$-\overline{u_i u_j} = \nu_T(U_{i,j} + U_{j,i} - \frac{2}{3}U_{k,k}\delta_{ij}) - \frac{2}{3}k\delta_{ij} \tag{1}$$

In the framework of $k-\epsilon$ two equation eddy viscosity model, the eddy viscosity ν_T is further expressed as

$$\nu_T = C_\mu f_\mu \frac{k^2}{\epsilon} \tag{2}$$

where the damping function f_μ is introduced to account for the effects of wall.

Traditionally, a constant value of $C_\mu = 0.09$ is used in equation (2). However, any two-equation eddy viscosity model with a constant C_μ is unrealizable in the sense that the turbulent component energy given by the model can become negative in certain flow situations. In addition, data from direct numerical simulations and from experiments suggest that C_μ vary with flow situations. For example, to match the data, different C_μ values should be used for homogeneous shear flows and for turbulent flows in a two dimensional channel. In this study, a variable C_μ formulation is used, in which C_μ depends on the solutions of the mean flow field and the turbulence field. The C_μ formulation was derived based on the realizability constrains, rapid distortion theory (RDT), and the invariants theory and takes the following form

$$C_\mu = \frac{1}{A_0 + A_s U^* \frac{k}{\epsilon}}. \tag{3}$$

In equation (3), k/ϵ represents the characteristic time scale associated with the turbulent motion. U^* is related to the characteristic time scale of the mean field

and it is given by

$$
\begin{aligned}
U^* &= \sqrt{S^*_{ij}S^*_{ij} + \overline{\Omega}^*_{ij}\overline{\Omega}^*_{ij}} \\
S^*_{ij} &= S_{ij} - \frac{1}{3}U_{k,k}\delta_{i,j} \\
\overline{\Omega}^*_{ij} &= \Omega^*_{ij} - 2\epsilon_{ijk}\omega_k
\end{aligned}
\tag{4}
$$

where S_{ij} is the mean strain tensor, Ω^*_{ij} is the mean rotation tensor in the inertia frame, and ω_k is the angular velocity of the rotating reference frame. The mean rotation tensors in the inertia frame and in the rotating frame are related by

$$
\Omega^*_{ij} = \Omega_{ij} - \epsilon_{ijk}\omega_k. \tag{5}
$$

In a rotating frame, the mean strain tensor S_{ij} and the mean rotation tensor Ω_{ij} are related to the mean velocity field by

$$
S_{ij} = \frac{1}{2}(U_{i,j} + U_{j,i}), \quad \Omega_{ij} = \frac{1}{2}(U_{i,j} - U_{j,i}). \tag{6}
$$

It is worth noting that the effect of frame rotation is included in the present model directly via its effect on U^*, and consequently on C_μ and ν_T.

The parameter A_s in equation (3) is a scalar function formed from the invariants of the mean velocity field. It has the following expression

$$
\begin{aligned}
A_s &= \sqrt{6}\cos\phi, \quad \phi = \frac{1}{3}arc\cos(\sqrt{6}W) \\
W &= \frac{S_{ij}S_{jk}S_{ki}}{S^3}, \quad S = \sqrt{S_{ij}S_{ij}}.
\end{aligned}
\tag{7}
$$

As shown in Reynolds[10], the choice of A_s guarantees the correct limiting behavior of the model in the rapid distortion limit.

The parameter A_0 in equation (3) is a model constant. In the present study, $A_0 = 4.0$ is chosen so that the present C_μ formulation gives a C_μ value of 0.09 for the equilibrium log layer regions of two-dimensional turbulent boundary layer flows. It was based on the experimental data for these flows that a constant value of $C_\mu = 0.09$ was first suggested.

Equations (3) — (7) give the C_μ formulation that we use in the present study. For such a C_μ formulation, the resulting Reynolds stresses are always realizable in that no physically un-admissible Reynolds stresses will be produced. In addition, the variations of C_μ with flow situations are in the right direction, i.e., the value of C_μ is smaller than 0.09 in regions where it should be. Thus, it can be expected that the current formulation of C_μ will improve the performance of $k-\epsilon$ eddy viscosity model considerably, particularly in regions where strain rate is large.

In a paper by Shih et al.[11], the above mentioned C_μ formulation was used in conjunction with a new (high-Reynolds number) $k-\epsilon$ eddy viscosity model, in which the dissipation rate equation was derived based on the asymptotic behavior of the fluctuating vorticity equation in the limit of large Reynolds numbers.

The paper shows that the C_μ formulation helps the model performances for rotating homogeneous shear flows, free shear flows, and wall boundary flows. For wall bounded flows, the near-wall boundary conditions were provided by the standard wall function formulation presented in Launder and Spalding[12].

2.4 Flows Calculations using NPARC and Turbulence Module

A series of flow calculations have been made using the NPARC code to solve the mean flow field and the turbulence module to solve the turbulence model equations. The turbulence module was first validated against the turbulent boundary layer flow over a flat plate with zero pressure gradient. Complex flows of aero-propulsion interest were then calculated. These include an ejector nozzle flow which provides a good test for flow mixing; a transonic diffuser flow which tests shock wave/turbulent boundary layer interactions; and a boat-tail nozzle flow which tests flow separation and jet-boundary layer interactions. In each case, the numerical convergence and the grid sensitivity are checked to make sure that the numerical solutions obtained are creditable. In the following, each flow case is briefly reported. These calculations are going to be presented in a paper at the upcoming 31st AIAA Joint Propulsion Conference by Yang et al.[13].

2.4.1 Flow over a flat plate

The purpose of calculating this flow is for code validation. The computational domain is shown in figure 1. The total grid points are 111 by 81 with 111 grid points in the x (streamwise) direction and 81 grid points in the y direction. In the x direction, 14 grid points are located before the leading edge of the flat plate. In the y direction, grid points are stretched so that the first off wall points have an average y^+ value of about 1. Since the NPARC code is for compressible flows, and computational results are going to be compared with an incompressible turbulent boundary layer, a freestream Mach number of 0.2 is used in the present calculation.

Although straightforward on the surface, the calculation of this flow is quite demanding in that the flow starts from a laminar-like flow, then undergoes a transition process, and then finally settles down to flow of the turbulent boundary layer type. It is very difficult to capture all three flow regions accurately. In the present computation, we are mainly interested in the solutions in the turbulent boundary layer region. Figure 2 shows the skin friction coefficient distribution as a function of Re_θ, the Reynolds number based on the momentum thickness of the boundary layer. Both the model predictions and the experimental results of Wieghardt and Willmann[14] are shown for comparison. It is seen that all models give similar results and all model predictions are close to the experimental data. Comparisons were also made between solutions of the NPARC code with built-in turbulence models and solutions of the NPARC code with the turbulence module. These solutions are found to be the same, thus the code with the turbulence module is validated.

2.4.2 Flow in an ejector nozzle

Ejector nozzle flows have important applications in propulsion systems because ejector nozzle is a candidate device to reduce the jet noise from the engine. The

noise reduction is particularly relevant to the High Speed Research (HSR) Program and the High Speed Civil Transport (HSCT) Program in NASA. A decade or two ago, ejector nozzle was also studied for its applications in the vertical land/taking off aircraft.

The geometry for an ejector nozzle is shown in figure 3. The performance of the ejector nozzle is measured by its mixing properties. To see the mixing effect, computed velocity and temperature profiles at a few stations along the streamwise direction are shown in figure 4 and figure 5, respectively, along with the experimental data of Gilbert and Hill[15]. It is seen that different $k - \epsilon$ eddy viscosity models give similar results and that results from $k - \epsilon$ eddy viscosity models are much better than those from the mixing length eddy viscosity models. The same conclusion was also reached by Georgiadis and Yoder[16] who calculated this flow using the NPARC code with its built-in turbulence models.

2.4.3 Flow in transonic diffuser

Transonic diffuser flow is another flow of interest in propulsion systems. In the present calculation, the experiment by Salmon, Bogar, and Sajben[17] is chosen as the test case. Depending on the pressure at the nozzle exit, there can be three different kinds of flow patterns. They are the no-shock case, the weak-shock case, and the strong-shock case. All these three cases were calculated in the present study, however, only the results for the strong-shock case, which is also the most difficult case, are shown here.

Figure 6 shows the diffuser geometry, together with grid information. The pressure distribution along the upper wall of the diffuser is shown in figure 7. Both the experimental results and the results from different model predictions are shown. For this flow, the critical parameters that are of interest to the design engineers are the location of the shock wave and the pressure recovery after the shock wave. Among the model predictions, the new realizable $k - \epsilon$ eddy viscosity model gives the best performance in these critical parameters. Figure 8 shows the velocity profile at $X = 2.88$, a station located after the shock wave where the experimental data are available. The realizable $k - \epsilon$ eddy viscosity model gives a much better prediction for both the overall feature of the field and the size of the separation. Since the controlling mechanism for this flow is the shock wave/turbulent boundary layer interaction, we can conclude that the new realizable $k - \epsilon$ eddy viscosity model captures this mechanism much better than the $k - \epsilon$ eddy viscosity model with constant C_μ, such as the Chien $k - \epsilon$ eddy viscosity model. The Chien $k - \epsilon$ model is itself much better than the Baldwin-Lomax mixing length eddy viscosity model for this flow.

2.4.4 Flow around a boat-tail nozzle

Boat-tail nozzle is a device commonly found in propulsion systems. A particular interest of the present study is on the effect of the jet plume on the turbulent boundary layer formed on the nozzle afterbody. Depending on the flow situations, the boundary layer can be either separated or attached. Boat-tail nozzle flow also provides a good test case for the two dimensional version of the NPARC code in

that it tests the code's capability for axisymmetric flows.

The experimental studies of Mason and Putnam[18], Abeyounis and Putnam[19] are chosen to validate the model calculation. In these studies, the freestream Mach number is 0.8. The stagnation pressure in the nozzle is such that the jet exits the nozzle at the local sonic speed, i.e. at Mach number of one. The nozzle geometry and the computational domain is shown in figure 9. Figure 10 shows the pressure distribution on the nozzle afterbody from both the computation and the experiment. It is seen that both the Chien $k-\epsilon$ model and the new realizable eddy viscosity model give similar results, and they are all fairly close to the experimental data. The $k-\epsilon$ eddy viscosity models give improved predictions compared with the mixing length eddy viscosity model.

3. Future Plans

Turbulence model development for NPARC is a long term activity. What was reported above represents the first part of this project. Many other activities need to be carried out in this project. For example, the numerical capability of the turbulence module needs to be enhanced; more advanced turbulence models need to be incorporated into the turbulence subprogram; and NPARC calculations with the turbulence modules need to be carried out for a large range of flows relevant to propulsion systems. To this end, a research team has been formed. In addition to the CMOTT members for this project (J. Zhu, Z. Yang, and T.H. Shih), this research team also includes N. Georgiadis and D.R. Reddy of NASA Lewis Research Center, and J.R. Sirbaugh at NYMA Inc. The activities of this research team has been incorporated into the NPARC Development Plan of the NPARC Alliance. The following are some of the planned highlights of these activities.

3.1 Turbulence Module for 3D Flows

Currently, the turbulence module is written for 2D flows (both planar flows and axisymmetric flows.) Two dimensional flows provide a basis for code and model validation. However, a code for 2D flows is only the first step in the coding process since almost all practical flows in aerospace and aero-propulsion systems are three dimensional. Thus, the next step is to extend the turbulence module to three dimensional flows and to test the turbulence module and models accordingly. It is expected that a 3D version of the turbulence module will be available by Summer 1995.

3.2 Tensorial and Galilean Invariant Eddy Viscosity Model

So far, all the $k-\epsilon$ eddy viscosity models in the turbulence module depend on geometry information in their near wall treatment, e.g. the distance from wall appears in the damping function. Models with geometry information are undesirable for flows with very complex geometries because in those situations, the definition of wall distance can be ambiguous. In addition, models without geometry information can be easily incorporated into CFD codes using unstructured grids while models with geometry information can not. To propose such a tensorial invariant model, it is necessary to use parameters other than R_y or y^+ to calibrate the near wall effect.

In the paper by Jones and Launder[20], in which the first low-Reynolds number $k-\epsilon$ eddy viscosity model was proposed, R_t, the turbulence Reynolds number, was used. In a more recent paper by Yang and Shih[21], a new parameter, $R = k/(S\nu)$, was introduced to model the near wall effects. Both R_t and R are field variables and are candidates to construct tensorial invariant models for near wall turbulence. These two parameters will be tested in the turbulence module for the NPARC code for complex flow calculations.

3.3 Wall Function Features for NPARC

An alternative to the low-Reynolds number turbulence model approach, in which the integration is carried down to the wall, is to use the wall functions which provide boundary conditions for the solutions at the equilibrium log layer of a turbulent boundary layer instead of the wall. The wall function approach has the appeal that it reduces the near-wall grid resolution requirements considerably, and consequently reduces the numerical stiffness as well. However, the traditional wall functions were developed based on the turbulent boundary layer flow over a flat plate at zero pressure gradient. It does not contain the pressure gradient effect and it can not be used for flows with separation, a common feature for flows in propulsion systems. Better wall functions have been developed by Yang and Shih[22] and Shih et al.[23] These new wall functions take into account the effect of the pressure gradient. In addition, the paper by Shih et al.[23] also addresses the issue of how to implement wall functions to calculate flows with separation and reattachment. These new wall functions are going to be incorporated into the turbulence module for the NPARC code. We expect that the wall function feature would be available by the end of 1995.

3.3 Anisotropic Algebraic Reynolds Stress Model for NPARC

All the turbulence models mentioned above are isotropic eddy viscosity models which assume a linear relationship between the Reynolds stresses and the mean strain rate. This assumption is not valid for complex flows. Anisotropic Reynolds stress models overcome this deficiency and will give a better performance than the current isotropic eddy viscosity models for flows where anisotropy is important, for example, the stagnation point flow and flows with massive separation. Recently, one such anisotropic algebraic Reynolds stresses model was developed by Shih et al.[24] and has shown improved predictions for a large range of complex flows including the confined jet flow and the swirling jet flow. This anisotropic algebraic Reynolds stress model is going to be implemented into the turbulence module for the NPARC code, and the resulting turbulence module will be used together with the NPARC code to calculated a large range of practical flows. To implement this model, the NPARC code for the mean flow solver has to be modified because in addition to the eddy viscosity term, the anisotropic Reynolds stresses model also brings other source-like terms into the mean momentum equations. The planned milestone for this work is the end of FY96.

4. References

[1] Cooper, G.K. and Sirbaugh, J.R., *PARC code: theory and usage*, AEDC-TR-89-15, Arnold Engineering Development Center, 1989.

[2] NPARC Alliance Technical Team, *A User's Guide to NPARC*, Version 2.0, 1994.

[3] Baldwin, B. S. and and Lomax, H., "Thin layer approximation and algebraic model for separated turbulent flows," AIAA Paper 78-256 (1978).

[4] Thomas, P. D., *Numerical method for predicting flow characteristics and performance of nonaxisymmetric nozzles, Theory*, NASA CR-3147, 1979.

[5] Chien, K.Y., "Predictions of channel and boundary-layer flows with a low Reynolds number turbulence model," AIAA J. **20** pp.33-38, (1982).

[6] Zhu, J., "On the higher-order bounded discretization schemes for finite-volume computations of incompressible flows," Comp. Meths. Appl. Mech. Eng. **98**, pp.345-360 (1992).

[7] Zhu, J., *FAST-2D: A computer program for numerical simulation of two-dimensional incompressible flows with complex boundaries*, Rep. No. 690, Institute for Hydromechanics, University of Karlsruhe, 1991.

[8] Zhu, J. and Shih, T.H., "A turbulence module for the NPARC code," to be presented at the AIAA Joint Propulsion Conference, San Diego, July (1995).

[9] Shih, T.-H., and Lumley, J.L., "Kolmogorov behavior of near-wall turbulence and its application in turbulence modeling," Comp. Fluid Dyn. **1**, pp.43-56 (1993).

[10] Reynolds, W.C., *Fundamentals of turbulence for turbulence modeling and simulation*, Lecture Notes for Von Karman Institute, AGARD Report No. 755, 1987.

[11] Shih, T.-H., Liou, W.W., Shabbir, A., Yang, Z. and Zhu, J., "A new k-ϵ eddy viscosity model for high Reynolds number turbulent flows - Model development and validation," J. of Computers and Fluids, **24**, no. 3, 1995.

[12] Launder, B.E. and Spalding, D.B., "The numerical computation of turbulent flow," Computer Methods in Applied Mechanics and Engineering **3**, 269 (1974).

[13] Yang, Z., Georgiadis, N., Zhu, J. and Shih, T.H., "Calculations of inlet/nozzle flows using a new k-ϵ model," to be presented at the AIAA Joint Propulsion Conference, San Diego, July (1995).

[14] Wieghardt, K. and Willmann, W., "On the turbulent friction layer for rising pressure," NACA TM-1314 (1951).

[15] Gilbert, G. B. and Hill, P. G., "Analysis and testing of two-dimensional slot nozzle ejectors with variable area mixing sections," NASA CR-2251, 1973.

[16] Georgiadis, N. J. and Yoder, D. A., "Use of Navier-Stokes methods for calculation of high speed nozzle flow fields," AIAA Paper 94-3212, June 1994.

[17] Salmon, J. T., Bogar, T. J., and Sajben, M., "Laser Doppler velocimeter measurements in unsteady, separated transonic diffuser flows," AIAA J. **21**, 1690 (1983).

[18] Mason, M.L., and Putnam, L.E., "Pitot pressure measurements in flow fields behind circular-arc nozzles with exhaust jets at subsonic free-stream Mach numbers," NASA TM-80169, December 1979.

[19] Abeyounis, W.K., and Putnam, L.E., "Investigation of the flow field surrounding circular-arc boattail nozzles at subsonic speeds," NASA TP-1633, May 1980.

[20] Jones, W.P., and Launder, B.E., "The calculation of low-Reynolds number phenomena with a two-equation model of turbulence," Intl. J. of Heat and Mass Transfer **16**, 1119 (1973).

[21] Yang, Z. and Shih, T.H., "A Galilean and tensorial invariant $k-\epsilon$ model for near wall turbulence," AIAA Paper 93-3105 (1993).

[22] Yang, Z. and Shih, T.H., "On the wall functions for two equation turbulence models," presented in 42nd APS/DFD meeting, Albuquerque, New Mexico, 1993.

[23] Shih, T.-H., Yang, Z., Zhu, J., and Shabbir, A., "Surface flows in a turbulent boundary layer", In preparation.

[24] Shih, T.-H., Zhu, J. and Lumley, J.L., "A new Reynolds stress algebraic equation model," NASA TM 106644 (1994), also to appear in *Computer Methods in Applied Mechanics and Engineering.*

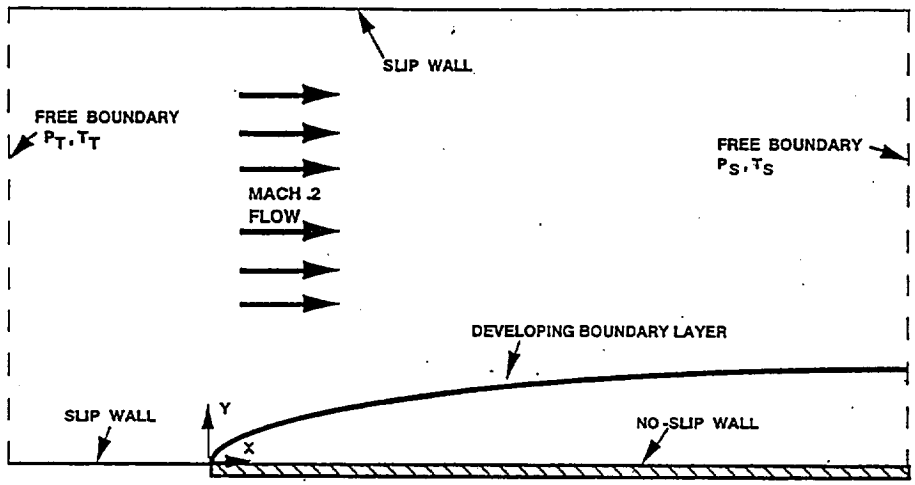

Figure 1: Configuration for turbulent boundary layer flow over a flat plate

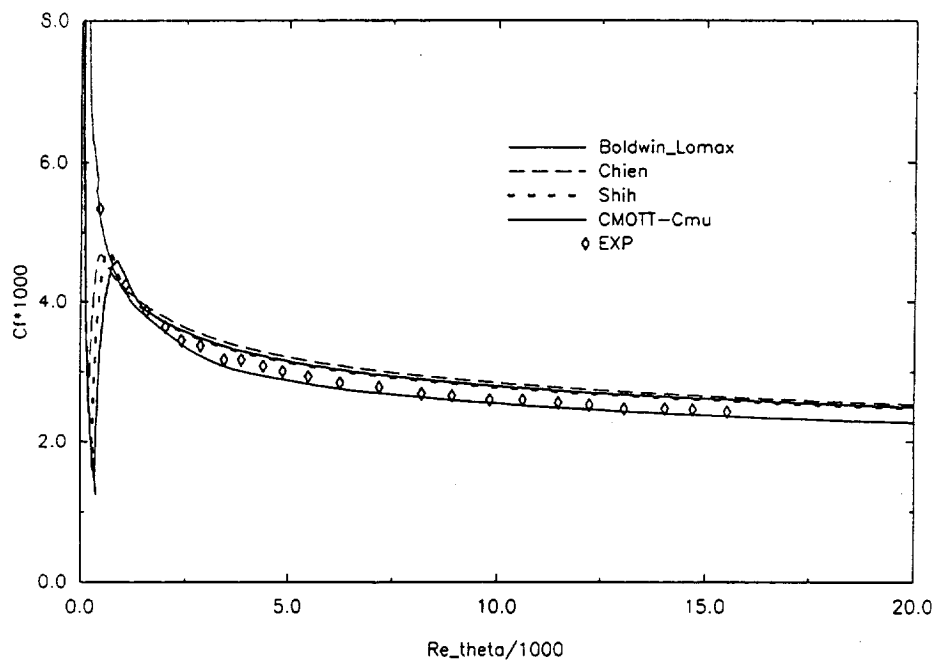

Figure 2: Skin friction distribution for the turbulent boundary layer flow

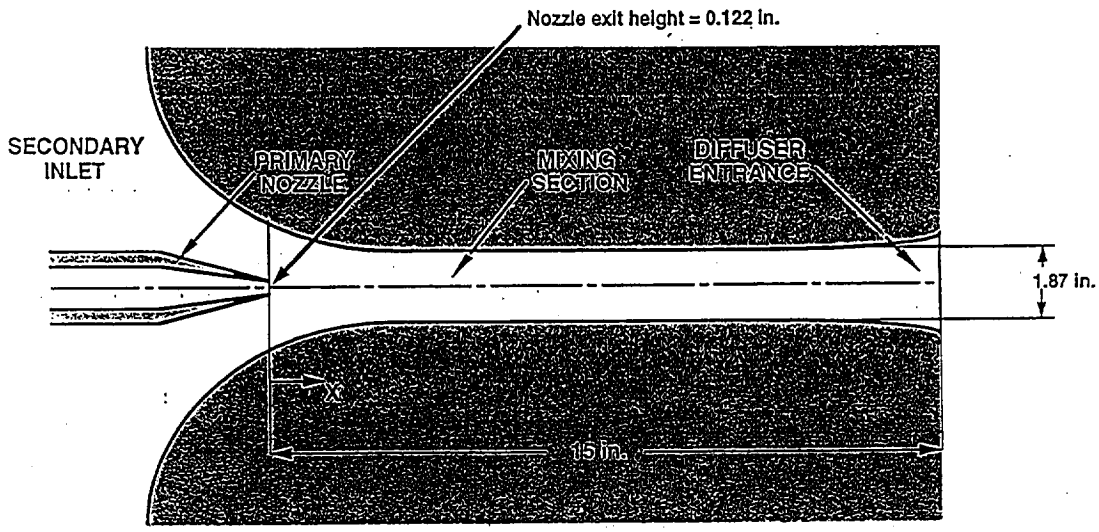

Figure 3: Configuration for an ejector nozzle flow

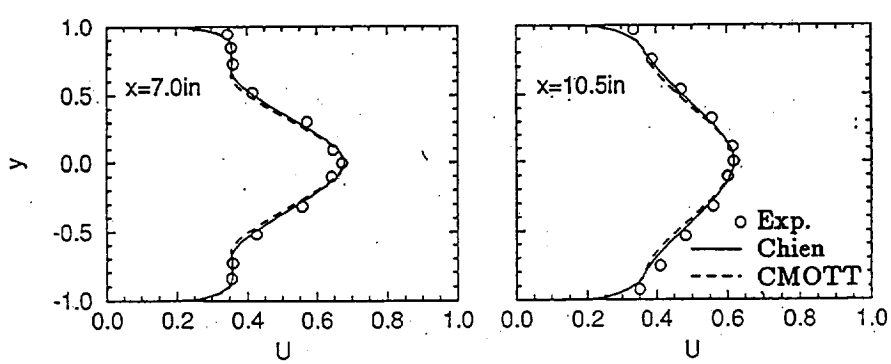

Figure 4: Velocity distributions in the ejector nozzle flow

ORIGINAL PAGE IS
OF POOR QUALITY

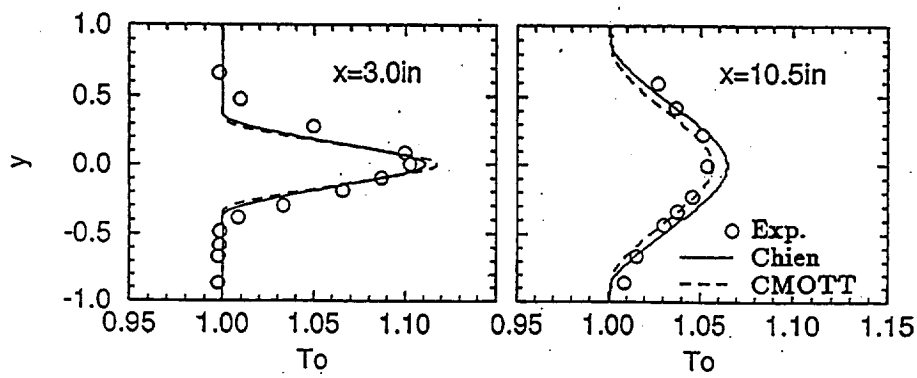

Figure 5: Temperature distributions in the ejector nozzle flow

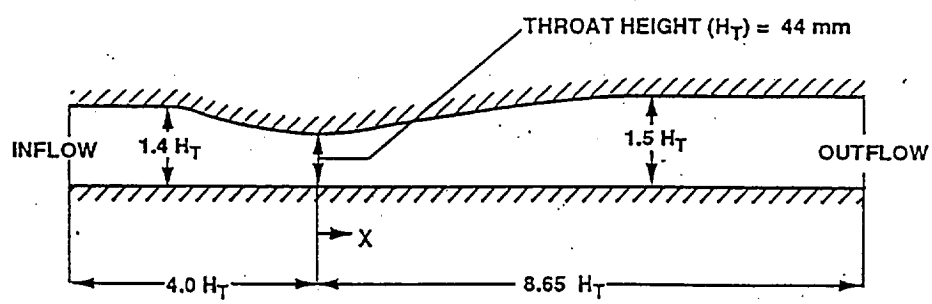

Figure 6: Configuration for an transonic diffuser flow

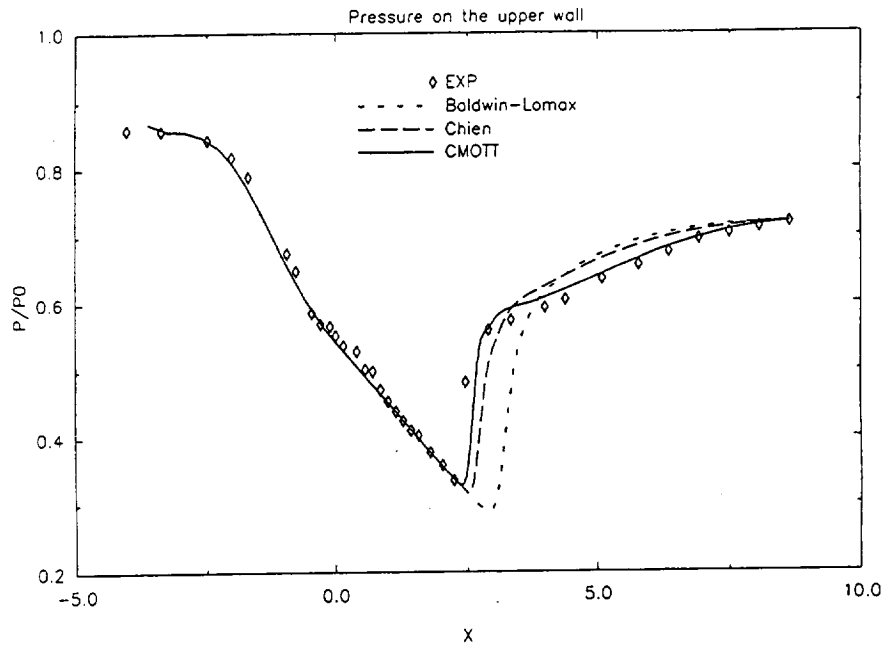

Figure 7: Pressure distribution on the upper wall of the diffuser

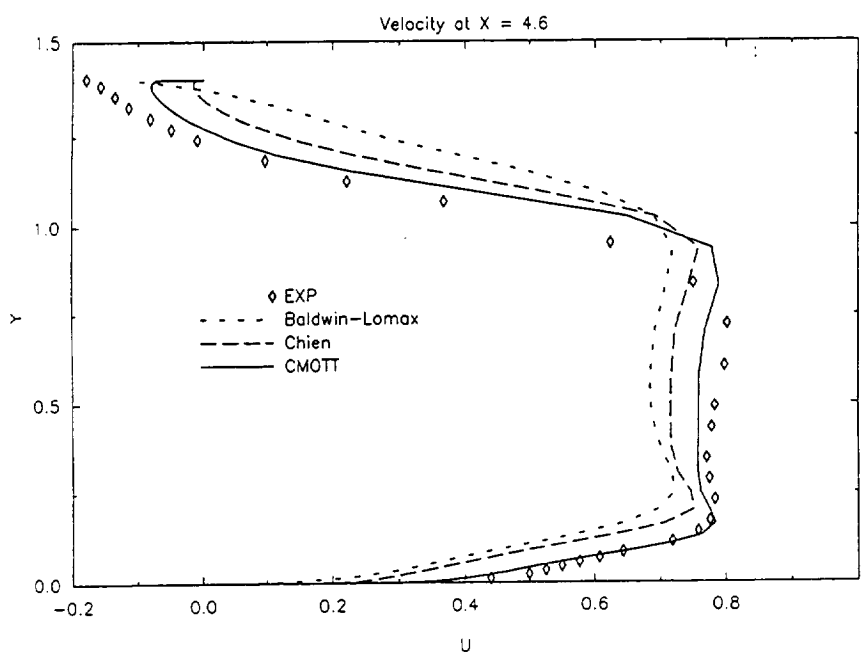

Figure 8: Velocity profiles after the shock-wave

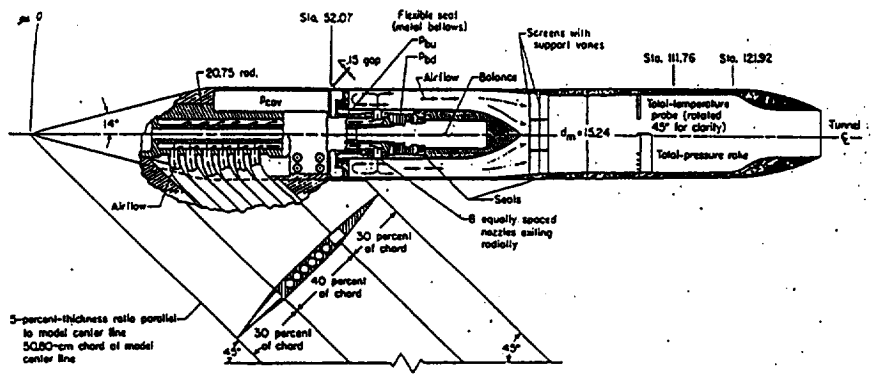

Figure 9: Configuration for a boat-tail nozzle flow

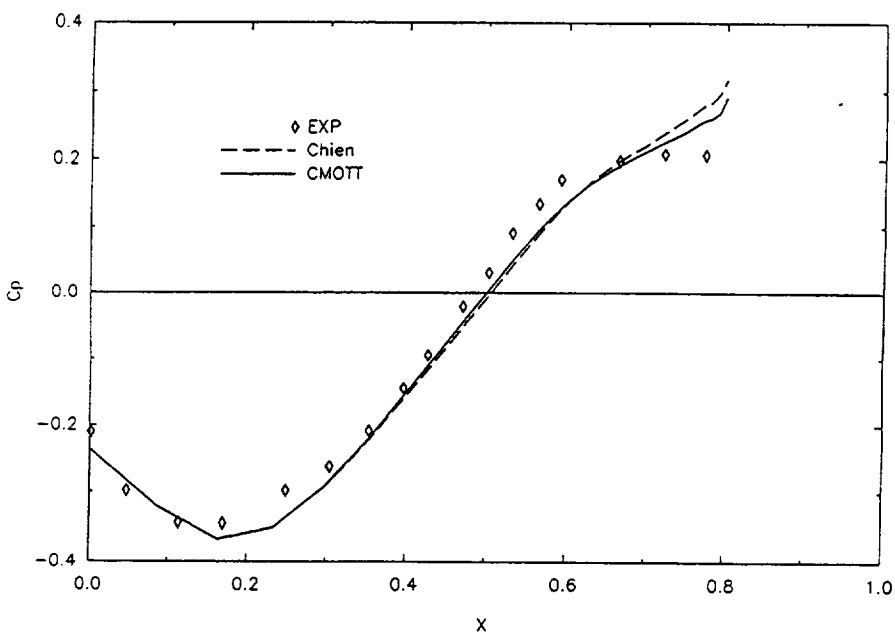

Figure 10: Pressure distribution on the after-body of the boat-tail nozzle

Calculations of Turbulent Reacting Flows in Can Combustors

A. T. Norris and W. W. Liou

1. Motivation and Objective

A newly developed probability density function (PDF) code is applied in the numerical simulation of swirling can combustor flows.

Due to enviromental concern over NO_x emissions, the design of future gas turbine combustors, operating at high pressures and temperatures, requires a detailed knowledge of the combustion processes in the different operating conditions of an engine. Therefore, robust and accurate computational modeling of the comubstor flow fields are necessary in the design of efficient, low emission combustors.

In modeling turbulent reactive flows, PDF methods have an advantage over the more traditional moment closure schemes. PDF methods treat the chemical reaction source term in an exact manner, while moment closure schemes model the mean reaction rate. For example, the commonly used laminar chemistry approximation is based on the assumption that the effects of turbulence on the chemistry are negligible. This, or similar assumptions fail for flows with high turbulence levels and finite rate chemistry.

2. Hybrid PDF Method

The hybrid PDF scheme used is a combination of moment closure and PDF methods. The continuity and momentum equations are solved by a moment closure method while the transport equation for the joint PDF of composition is used to solve the scalar fields. This combination has the advantage in that the PDF part of the code can be added to an existing moment closure method with a minimal amount of coding. Thus existing combustion codes can be extended to include the PDF model of turbulent chemical reactions without the need for extensive rewriting.

3. Experiment

The flow chosen to test the new code, is the axisymmetric can combustor (ASCC) tested by UC Irvine.[1] This combustor is cylindrical, with an 80 mm ID and is 320 mm long. A sketch of the combustor is shown in Fig. 1. The ASCC is operated at 1 atmosphere pressure. The fuel is gaseous propane, which is injected through an annular cone nozzle with an inner radius of 5.4 mm and an average injection velocity of 12.4 m/s. Air swirling is achieved by 12 curved blades. The flow rate of the center swriling air was kept the same as the outer dilution air.

4. Numerical Solutions

The mean velocity field is obtained from the solutions of Navier–Stokes equations using the FAST-2D code. The code uses a finite volumn scheme with cell–centered

nodes. The pressure –velocity coupling is handled with the SIMPLEC algorithm. The standard high–Reynolds number $k - \epsilon$ models were used to provide the turbulence mixing characteristics.

The scalar PDF code is similar to that developed by Hsu et al [2] but with a several important numerical changes. These changes primarily involve the treatment of the convection and molecular mixing. Details of these changes will be discussed in a future paper.

5. Initial Conditions

The first flow measurement was reported at 0.5 cm downstream of the nozzle exit plane. This was found unsatisfactory for use as initial conditions for a numerical solution of the flow field. Therefore, the numerical initial velocity profiles for the streamwise, radial, and azimuthal directions were determined by the air and fuel mass flow rates, the angle of the swirl vanes, and the gaseus propane injection angle at the nozzle exit. The initial turbulent kinetic energy was set at 1% of the mean flow energy. The turbulent dissipation rate was then determined by assuming an equavilent laminar viscosity.

Species initial conditions are simply pure fuel and air. To ignite the flame, we set the initial species and temperature in the combustor to correspond to a fully burnt fuel-air mixture at the experimental equivalence ratio.

6. Thermochemistry

Calculations were performed using the equilibrium chemistry assumption. In this it is assumed that the chemical time scales are much smaller than the turbulent time scales. In the future, a full mechanism, simplified by the Intrinsic Low-Dimensional Manifold (ILDM) method of Pope and Maas [3], will be used.

7. Results

The calculated temperature and axial velocity profiles at four different streamwise locations in the combustor are compared with the measurement in Figs. 2 and 3, respectively. For comparison, the results obtained by a moment closure model for the same combustor are also included. Fig. 2 shows the comparison of the axial mean velocity profiles. At x=1 cm, the present calculation correctly predicts the magnitude and the radial location of the peak velocity, which roughly corresponds the edge of the air swirler. The reciculation zone indicated by the measurement near the inner edge of the swirler is not predicted well by either the present calculation based on PDF method or the moment closure chemistry model. Therefore, it is possible that this may be due to the $k - \epsilon$ turbulence model, which is known to underpredict flow recirculation in highly swirling flows. At the next three axial stations, the PDF calculation does a better job capturing the correct local characteristics of the flow than the momentum closure procedure.

Fig. 3 show the radial temperature distributions at the same four axial locations as in Fig. 2. The PDF method has returned better prediction for the peak termperature and profiles in the region near the nozzle exit, x=1 and 4 cm than

the momentum closure chemistry model. The slightly higher predicted temperature may be due to either the insufficient turbulent mixing in the recirculation zone returned by the $k - \epsilon$ model or the equilibrium chemistry. The PDF method also correctly predicted the centerline temperature. At farther downstream the PDF model also show better temperature profile distribution. This can also be observed from the relatively uniform temperature coutours in this region, Fig. 4. Note that the experimenal flow shows higher turbulent mixing, resulting in more uniform temperature near the center region of the combustor. Again, this broad temperature plateau region may be due to the deficiency of the turbulence models or the equilibrium chemistry. The preliminary results of finite rate chemistry calculations shows a lower peak temperature at x=1 cm.

8. References

[1] R. Charles, "Detailed Data Set: Velocity and temperature measurements in the axisymmetric can combustor (ASCC) for a parametric variation in inlet conditions" UCI-ARTR-87-6, University of California, Irvine 1988.

[2] A. T. Hsu, M. S. Raju and A. T. Norris, "Application of a PDF method to compressible turbulent reacting flows" AIAA 94-0781, Reno NV 1994.

[3] S.B.Pope and U.Maas, "Simplifying chemical Kinetics: Trajectory-generated low-dimensional manifolds" FDA-93-11, Cornell University, Ithaca NY 1993.

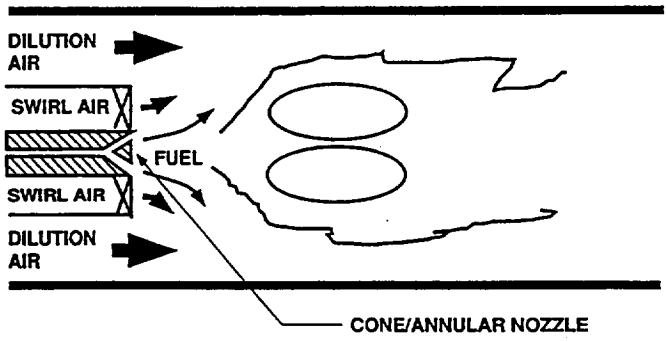

Figure 1. A sketch of the UC Irvine axisymmetric can combustor

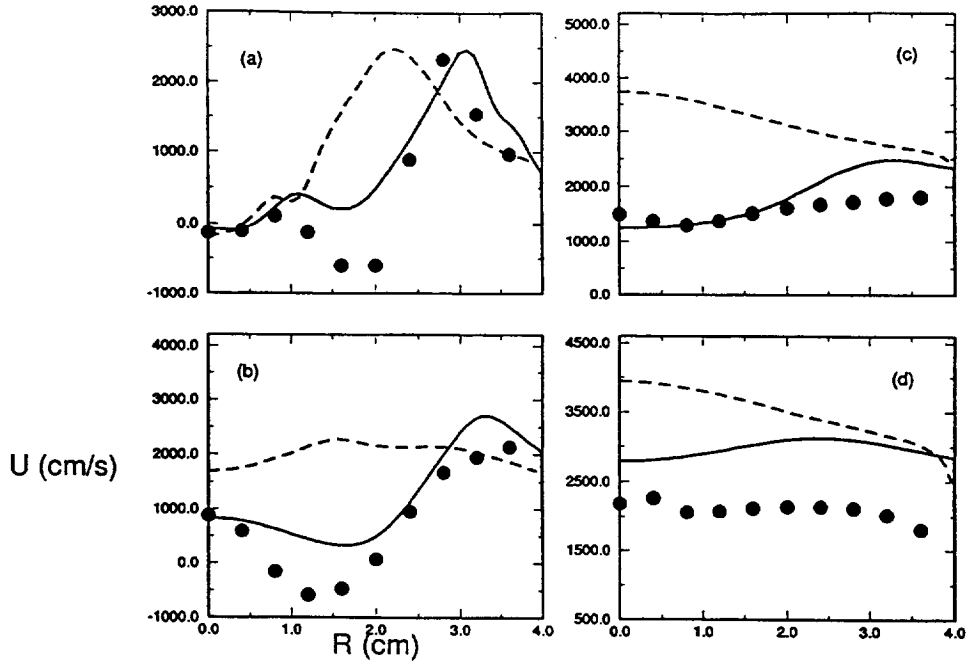

Figure 2. Radial distribution of the mean streamwise velocity. •, measurement[1]; – – –, Micklow *et. al*[4]; ——, present.

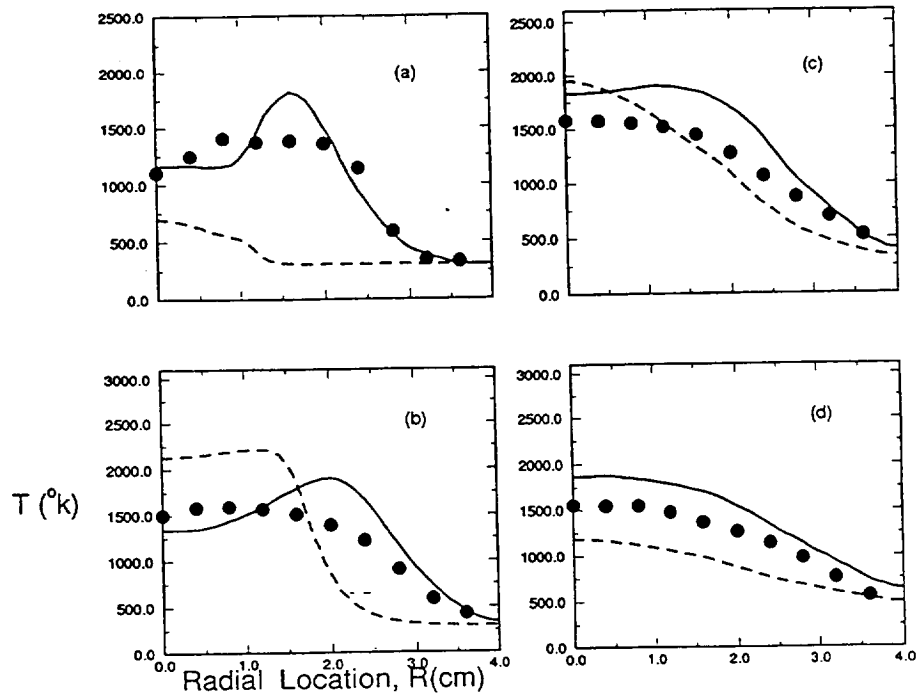

Figure 3. Comparison of Radial distribution of temperature. •, measurement[1]; – – –, Micklow *et. al*[4]; ——, present.

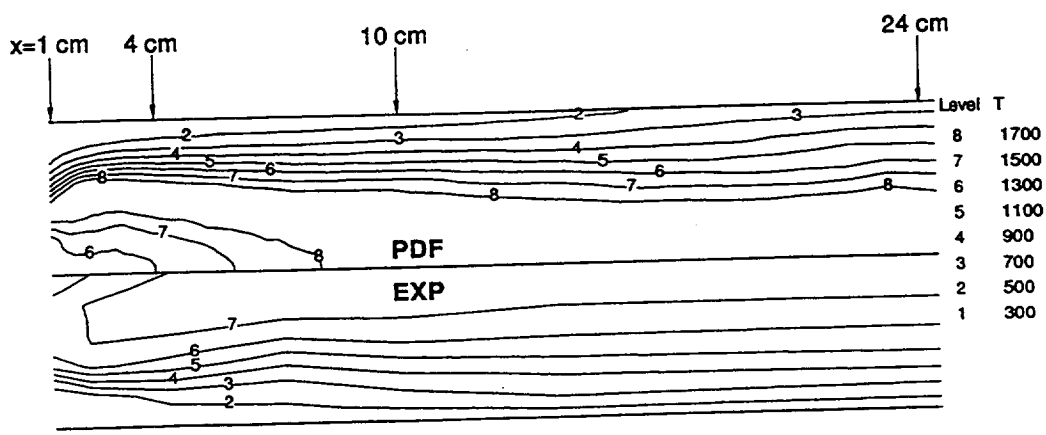

Figure 4. Temperature contours

Assessment of Turbulence Models in Turbomachinery Flows

1. Motivation and Objectives

Turbomachinery flows pose a major challenge for CFD since they are three-dimensional and time dependent. NASA Lewis Research Center is playing a lead role in developing CFD tools which can be used by industry in the analysis of their designs.

Recently, a blind test case for a rotor compressor (ROTOR 37) was organized by the ASME/International Gas Turbine Conference held at the Hague (A. Strazisar, J. Wood, and K. Suder[1]). The objective was to judge the predictive capabilities of turbomachinery CFD tools. A total of 12 groups submitted their predictions for this case, which were then compared with the detailed experimental data. The results, which are given in the above reference, showed a wide scatter relative to the experimental data. There were several reasons for this, one of them being the inadequacies of the turbulence models.

Since different codes using the same turbulence models produced different results in the ROTOR 37 blind test case, it is obvious that there is a need to assess the performance of different turbulence models from the same numerical platform. If different turbulence models are implemented in a single CFD code, then the differences in the results can be attributed only to the differences in the models. In this way the impact of different models on the prediction of turbomachinery flows can be assessed in a systematic manner. In order to answer this question, CMOTT has started a joint project with the turbomachinery group at the Lewis Research Academy. Since the Average Passage Equation code, VSTAGE, predicted the ROTOR 37 blind test case reasonably well[2], it was selected as the numerical platform to carry out this task.

The approach taken is to implement several turbulence models, of varying sophistication, in the VSTAGE code in the form of a subroutine. To begin with the standard $k-\epsilon$ model of Launder and Spaulding[3] will be implemented. This will be followed by implementing an improvement to this model which has been developed by CMOTT. This improvement has already shown to give better results over the standard $k-\epsilon$ model for a some benchmark flows. Eventually a complete CMOTT two equation model (Shih, et. al.[4]) will be implemented.

All of the above models will be used with the wall functions. The standard wall functions approach in CFD calculations assumes the existence of the law of the wall, even though this is true for a flat plate boundary layer only. This approach is popular because it requires a mesh size that is computationally affordable and because it, apparently, provides good engineering accuracy. At a later time, and based on the results obtained using the above models, there may be a need to assess

PRECEDING PAGE BLANK NOT FILMED

the performance of the different wall functions on the prediction of turbomachinery flows. It should be pointed out that all of the turbulence model assessment will be done against the ROTOR 37 data.

In the course of this project we may find some deficiencies in the turbulence models. It is also the objective of this effort to identify and remedy these.

This project will make the following two important contributions. First an assessment of the hierarchy of turbulence models (including those that CMOTT has developed) in the context of turbomachinery flows. This information will be extremely useful to the turbomachinery community. Second the models which perform the best against the test cases can be incorporated in the Average Passage Equation codes for both the single stage and the multistage turbomachinery. This will lead to an improved turbomachinery CFD tool.

2. Work in Progress

We have finished implementing the standard two equation $k - \epsilon$ model and its CMOTT improvement in the VSTAGE code. The preliminary results for the ROTOR 37 test case look promising. We are currently conducting a grid sensitivity study. The results of this work will be presented in an upcoming report. This work is being carried out by A. Shabbir, J. Zhu, M. Celestina, J.J. Adamczyk, and T.-H. Shih.

3. References

[1] Strazisar, A., Wood, J., and Suder, K. ASME/International Gas Turbine Conference, The Hague, Netherlands, 1994.

[2] Celestina, M. ASME/International Gas Turbine Conference, The Hague, Netherlands, 1994.

[3] Launder, B.E., and Spaulding, D.B., "The numerical computation of turbulent flows", Comp. Meth. Appl. Mech. Engg., 3, 269-289, 1974.

[4] Shih, T.-H., W.W. Liou, A. Shabbir, Z. Yang and J. Zhu. "A new high Reynolds number $k - \epsilon$ model", Computers Fluids, 24, 3,227-238, 1995.

Appendix A

Industry-Wide Workshop on Computational Turbulence Modeling

CMOTT organized an Industry-wide Workshop on Computational Turbulence Modeling on October 6-7, 1994. The purpose of the workshop was to initiate the transfer of technology developed at Lewis Research Center (LeRC) to industry and to discuss the current status and the future needs of turbulence models in industrial CFD. The workshop organizing committee and the titles of presentations are listed below. Details of the presentations can be found in the NASA CP 10165.

Workshop Organizing Committee

Industries

C. Prakash, General Electric
M. Sindir, Rocketdyne
S. Syed, Pratt & Whitney

Universities

J.Y. Chen, University of California, Berkeley
J.L. Lumley, Cornell University

National Aeronautics and Space Administration

L.A. Povinelli, Chairman
R. Mankbadi, Lewis Research Center
D.R. Reddy, Lewis Research Center
P. Richardson, Headquarters
R.J. Shaw, Lewis Research Center

Institute for Computational Mechanics in Propulsion

T. Keith, Ohio Aerospace Institute
A. Shabbir, Center for Modeling of Turbulence and Transition
T.-H. Shih, Center for Modeling of Turbulence and Transition

Workshop Presentations

TURBULENCE PROGRAM FOR PROPULSION SYSTEMS
Tsan-Hsing Shih, Institute for Computational Mechanics in Propulsion and Center for Modeling of Turbulence and Transition, NASA Lewis Research Center

TURBULENCE MODEL DEVELOPMENT AND APPLICATION AT LOCKHEED FORT WORTH COMPANY
Brian R. Smith, CFD Group, Lockheed Fort Worth Company

A SUMMARY OF COMPUTATIONAL EXPERIENCE AT GE AIRCRAFT ENGINES FOR COMPLEX TURBULENT FLOWS IN GAS TURBINES
R. Zerkle and C. Prakash, GE Aircraft Engines

THE APPLICABILITY OF TURBULENCE MODELS TO AERODYNAMIC AND PROPULSION FLOWFIELDS AT McDONNELL DOUGLAS AEROSPACE
Linda D. Kral, John A. Ladd, and Mori Mani, McDonnell Douglas Aerospace

EXPERIENCE WITH k-ε TURBULENCE MODELS FOR HEAT TRANSFER COMPUTATIONS IN ROTATING
Prabhat Tekriwal, GE Corporate Research and Development

TURBULENCE MODELS FOR GAS TURBINE COMBUSTORS
Andreja Brankovic, CFD Group, Pratt & Whitney

COMBUSTION SYSTEM CFD MODELING AT GE AIRCRAFT ENGINES
D. Burrus and H. Mongia, GE Aircraft Engines, and A. Tolpadi, S. Correa, and M. Braaten, GE Corporate Research and Development

RECENT PROGRESS IN THE JOINT VELOCITY-SCALAR PDF METHOD
M.S. Anand, Allison Engine Company

OVERVIEW OF TURBULENCE MODEL DEVELOPMENT AND APPLICATIONS AT ROCKETDYNE
A.H. Hadid, E.D. Lynch, and M.M. Sindir, Rocketdyne Division, Rockwell International

RECENT ADVANCES IN PDF MODELING OF TURBULENT REACTING FLOWS
A.D. Leonard and F. Dai, CFD Research Corporation

EXPERIENCE WITH TURBULENCE INTERACTION AND TURBULENCE-CHEMISTRY MODELS AT FLUENT INC.
D. Choudhury, S.E. Kim, D.P. Tselepidakis, and M. Missaghi, Fluent Inc.

EXPERIENCES WITH TWO-EQUATION TURBULENCE MODELS
Ashok K. Singhal, Yong G. Lai, and Ram K. Avva, CFD Research Corporation

PROGRESS IN SIMULATING INDUSTRIAL FLOWS USING TWO-EQUATION MODELS: CAN MORE BE ACHIEVED WITH FURTHER RESEARCH?
Vahé Haroutunian, Fluid Dynamics International, Inc

C-2.

TURBULENCE MODELING NEEDS OF COMMERCIAL CFD CODES: COMPLEX FLOWS IN THE AEROSPACE AND AUTOMOTIVE INDUSTRIES
Bizhan A. Befrui, adapco

TURBULENCE REQUIREMENTS OF A COMMERCIAL CFD CODE
J.P. Van Doormaal, C.M. Mueller, and M.J. Raw, Advanced Scientific Computing Ltd.

SECOND-ORDER CLOSURES FOR COMPRESSIBLE TURBULENCE
J.L. Lumley, S. Savarese, and C.C. Volte, Mechanical and Aerospace Engineering Department, Cornell University

MODELING OF TURBULENT CHEMICAL REACTION
J.-Y. Chen, Department of Mechanical Engineering, University of California, Berkeley

INTRODUCTION TO TURBULENCE SUBPROGRAM
T.-H. Shih and J. Zhu, Institute for Computational Mechanics in Propulsion and Center for Modeling of Turbulence and Transition, Lewis Research Center

DESCRIPTION OF TURBULENCE SUB-PROGRAM
J. Zhu, Institute for Computational Mechanics in Propulsion, NASA Lewis Research Center

OVERVIEW OF PROBABILITY DENSITY FUNCTION (PDF) MODELING AT LeRC
D.R. Reddy, Internal Fluid Mechanics Division, NASA Lewis Research Center

PDF METHODS FOR TURBULENT REACTIVE FLOWS
Andrew T. Hsu, NYMA, Inc., NASA Lewis Research Center

A COMPOSITION JOINT PDF METHOD FOR THE MODELING OF SPRAY FLAMES
M.S. Raju, Nyma, Inc., NASA Lewis Research Center

IMPROVEMENTS AND NEW FEATURES IN THE PDF MODULE
A.T. Norris, Institute for Computational Mechanics in Propulsion

Appendix B

Organization - 1995

Position Chart

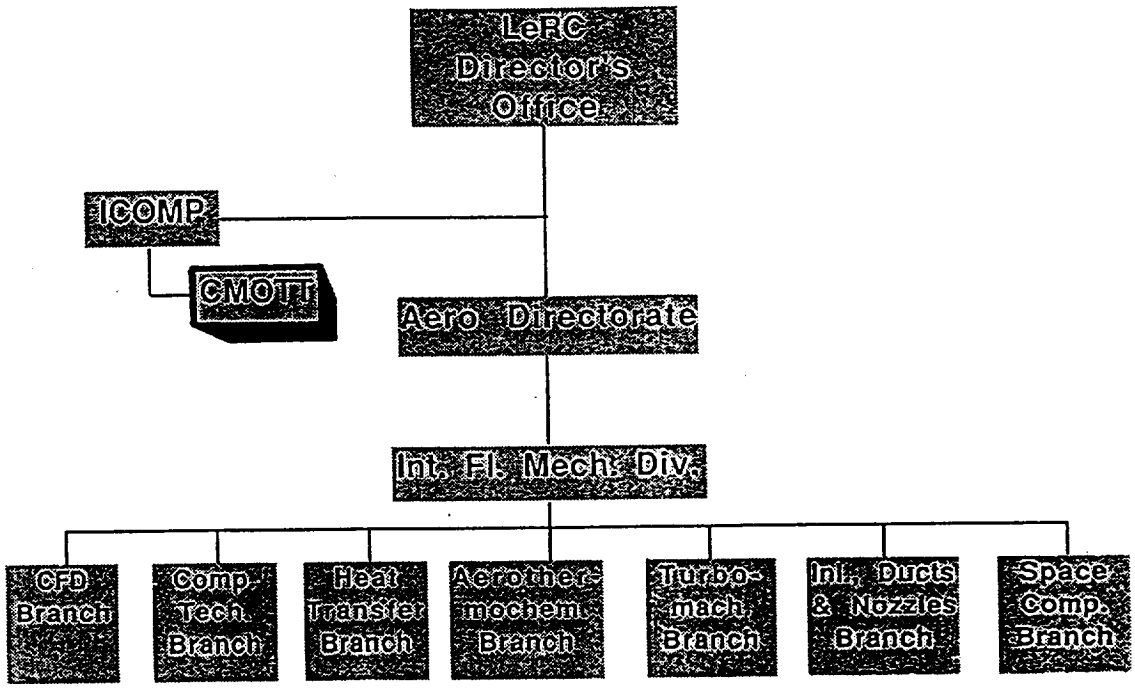

PRECEDING PAGE BLANK NOT FILMED

ICOMP Director	Dr. Louis A. Povinelli Deputy Chief Internal Fluid Mechanics Division NASA Lewis Research Center
CMOTT Technical Leader	Dr. Tsan-Hsing Shih Senior Research Associate ICOMP, NASA Lewis Research Center
Advisors	Dr. Marvin E. Goldstein Chief Scientist NASA Lewis Research Center Professor John L. Lumley Sibley School of Mechanical and Aerospace Engineering Cornell University
	Professor Eli Reshotko Department of Mechanical and Aerospace Engineering Case Western Reserve University

Listing of current Members

Names/Term	Affiliation	Research Areas
Liou, William W. 11/1990 - present	ICOMP	Compressible Flow Modeling, Weakly Nonlinear Wave Models
Norris, Andrew 4/1993 - present	ICOMP	PDF Turbulence Modeling, DNS
Shabbir, Aamir 5/1990 - present	ICOMP	Buoyancy Effects on Turbulence, Turbulence Modeling
Shih, Tsan-Hsing 5/1990 - present	ICOMP	Turbulence Modeling
Yang, Zhigang 7/1990 - present	ICOMP	Modeling of Bypass Transition
Zhu, Jiang 4/1992 - present	ICOMP	Application of Turbulence Models in Complex Flows

Appendix C
List of Member's Publications

Barton, J. M., Rubinstein, R. and Kirtley, K. R. "Nonlinear Reynolds stress model for turbulent shear flows, " AIAA Paper No. 91-0609, (Jan. 1991).

Barton, J. M. and Rubinstein, R., "Nonlinerar algebraic Reynolds stress model for anisotropic turbulent flows, " 11th U. S. National Congress of Applied Mechanics, Tucson, AZ (May 1990).

Barton, J. M. and Rubinstein, R., "Renormalization group theory and turbulence modeling, " 2nd International Workshop on Chaos and Turbulence, Tsukuba, Japan (Jan. 1992).

Barton, J. M. and Rubinstein, R., "Renormalization group analysis of turbulence- driven secondary flows, " 11th Australian Fluid Mechanics Conference, Hobart, Australia (Dec. 1992).

Brown, S., Leibovich, S., and Yang, Z., "On the linear instability of the Hall-Stewartson vortex," Theo. and Comp. Fluid Dynamics, Vol 2, no. 1, (1990).

Duncan, B. S., Liou, W. W. and Shih, T.-H., "A multiple-scale turbulence model for incompressible flow," AIAA 93-0086 (1993).

Duncan, B.S., Lumley, J.L., Shih, T.H. and To, W.M., "A new model for the turbulent dissipation" International Conference of Fluid Mechanics and Theoretical Physics, Bejing, China (1992).

Durbin, P.A. and Yang, Z., "A transport equation for eddy viscosity," *Proc. of the 1992 Summer Program*, CTR, Stanford, 1992.

Georgiadis, N.J., Chitsomboon, T. and Zhu, J., "Modification of the two-equation turbulence model in NPARC to a Chien low Reynolds number k-ϵ formulation," NASA TM 106710 (1994).

Hsu, A.T., Raju, M.S., and Norris, A.T., Application of a PDF method to compressible turbulent reacting flows. In AIAA 32nd Aerospace Sciences Meeting and Exhibit, Reno, Nevada, pages AIAA–94–0781, 1994.

Hsu, A.T. and Liou, M., "Computational analysis of underexpanded jets in the hypersonic regime," Journal of Propulsion and Power, **7**, No. 2, (1991).

Hsu, A.T., "Progress in the development of PDF turbulence models for combustion," 10th NASP Symposium, April 23-16, 1991, Monterey, California.

Hsu, A.T., "A study of hydrogen diffusion flames using PDF turbulence model," AIAA 91-1780, AIAA 22nd Fluid Dynamics Conference, June 24-26, 1991, Honolulu, Hawaii.

PRECEDING PAGE BLANK NOT FILMED

Hsu, A.T. and Chen, J.Y., "A continuous mixing Model for PDF simulations and its applications to combusting shear flows," 8th International Symposium on Turbulence Shear Flows, Sept. 9-11, 1991, Munich, Germany.

Hsu, A.T., Raju, M.S., and Norris, A.T., Application of a PDF method to compressible turbulent reacting flows. In AIAA 32nd Aerospace Sciences Meeting and Exhibit, Reno, Nevada, pages AIAA–94–0781, 1994. Huang, P.G. and Liou, W.W., "Numerical calculations of shock–wave/boundary–layer flow interactions," NASA TM 106694 (1994).

Lang, N.J. and Shih, T.-H., "A critical comparison of two-equation turbulence models," NASA TM 105237, (1991).

Liou, M. S. and Steffen, Jr., C. J., "A new flux splitting scheme," NASA TM 104404 (1991).

Liou, W. W. and Shih, T.-H., "Transonic flow predictions with new two–equation turbulence models," AIAA 95–1805.

Liou, W. W. and Shih, T.-H., "Compressible turbulent boundary layer predictions using a multiple-scale model," NASA TM (in preparation) (1995).

Liou, W. W., Shih, T.-H., and Duncan, B.D., "A multiple–scale model for compressible turbulent flows," Phys. Fluids, **7** (3), 658–666 (1995).

Liou, W. W., "Linear instability of curved free shear layer," Phys. Fluids, **6** (2), 541–549 (1994).

Liou, W. W. and Shih, T.-H., "On the basic equations for sencond-order modeling of compressible turbulence," NASA TM 105277 (1991).

Liou, W. W. and Morris, P. J., "Weakly nonlinear models for turbulentmixing in a plane mixing layer," Phy. Fluids, **4**, 2788-2808 (1992).

Liou, W. W. and Morris, P. J., "The eigenvalue specturm of the Rayleigh equation for a plane shear layer," International Journal of Numerical Methods in Fluids, **15**, 1407-1415 (1992).

Liou, W. W., "A new energy transfer model for turbulent free shear flow," NASA TM 105854 (1992).

Mansour, N N. and Shih, T.-H. and Reynolds, W. C., "The effects of rotation on initially anisotropic homogeneous flows," Physics of fluid A, **3**, 10, 2421-2425 (1991).

Michelassi, V. and Shih, T.-H., "Low Reynolds number two-equation modeling of turbulent flows," NASA TM 104368, (1991).

Michelassi, V. and Shih, T.-H., "Elliptic flow computation by low Reynolds number two-equation turbulence models ," NASA TM 105376, (1991).

Moin, P., Shih, T.-H., Driver, D. and Mansour, N., "Direct numerical simulation of a three-dimensional turbulent boundary layer," Physics of Fluids A **2**, 10, 1846-1853 (1990).

Norris, A.T. and Pope, S.B., Modeling of extinction in turbulent diffusion flames by the velocity-dissipation-composition PDF method. Combustion and Flame., **100**(1/2):211–220, 1994.

Norris, A.T. and Hsu, A.,T., Comparison of PDF and moment closure methods in the modeling of turbulent reacting flows. In 30th AIAA/ASME/SAE/ASEE Joint Propulsion Conference, Indianapolis, Indiana, pages AIAA–94–3356, 1994.

Norris, A.T., "The application of PDF methods to piloted diffusion flames," Ph.D. Thesis, Cornell University, 1993.

Rubinstein, R. and Barton, J. M., "Renormalization group analysis of the Reynolds stress transport equations, nonlinear Reynolds stress models and the renormalization group," Phys. Fluids A **4**, 1759 1766 (1992).

Rubinstein, R. and Barton, J. M., "Nonlinear Reynolds stress models and the renormalization group," Phys. Fluids A **2**, 1472 (1990).

Rubinstein, R. and Barton, J. M., "Renormalization group analysis of anisotropic diffusion in turbulent shear flow," Phys. Fluids A **3**, 415 (1991).

Rubinstein, R. and Barton, J. M., "Renormalization group analysis of the Reynolds stress transport equation," Phys. of Fluids A **4**, 1579 (1992).

Shabbir, A., and George, W.K. "Experiments on round turbulent buoyant plume", J. Fluid Mech, 1994, 275, 1-32.

Shabbir, A., Beuther, P.D. and George, W.K. "X-Wire response in turbulent flows of high intensity turbulence and low mean velocities", 1995, Accepted to Experimental Fluid & Thermal Science.

Shabbir, A., "Experimental balances for the second moments for a buoyant plume and their implication on turbulence modeling," Eighth Symposium on Turbulent Shear Flows, 27-1-1 to 27-1-6 (1991).

Shabbir, A. and Shih, T.-H., "Critical comparison of second order turbulence models in homogeneous flows," Presented at the AIAA Annual meeting in Reno, Jan. 1992.

Shabbir, A. and Taulbee, D.B., Evaluation of Turbulence Models for Predicting Buoyant Flows. J. Heat Transfer, 1990, Vol 112, No 4, pp 945-951.

Shabbir, A. and Taullbee, D.B., Evaluation of the Coefficients of the Reynolds Stress Models Using Experiments on Homogeneous Turbulence. A. Shabbir and D.B. Taulbee. Forum on Turbulent Flows. ASME (1987), FED, 51, pp 67-72.

Shih, T.-H., Zhu, J. and Lumley, J.L., "A new Reynolds stress algebraic equation model,"NASA TM 106644 (1994).

Shih, T.-H., Zhu, J. and Lumley, J.L., "Modeling of wall-bounded complex flows and free shear flows," NASA TM 106513 (1994).

Shih, T.H., Liou, W.W., Shabbir, A., Yang, Z., and Zhu, J., "A new $k-\epsilon$ eddy viscosity model for high Reynolds number turbulent flows," J. Computers and Fluids, **24**, (1995).

Shih, T.-H. and Shabbir, A., "Methods of ensuring realizability for non-realizable second order closures," NASA TM 106681 (1994).

Shih, T.-H., Shabbir, A. and Lumley, J.L., "Realizability in second moment turbulence closures revisted,", NASA TM 106469 (1994).

Shih, T.-H., Liou, W.W., Shabbir, A., Yang, Z., and Zhu, J., "A vorticity dynamics based model for the turbulent dissipation," NASA TM 106177 (1993).

Shih, T.-H. and Lumley, J.L., "Remarks on turbulent constitutive relations," NASA TM 106116 (1993).

Shih, T.-H. and Lumley, J.L., "Kolmogorov behavior of near-wall turbulence and its application in turbulence modeling," NASA TM 105663 (1992)

Shih, T.-H., Chen, J.-Y. and Lumley, J. L., "Second order modeling of free turbulent shear flows," AIAA Journal, **30**, 6, 1553-1560 (1992).

Shih, T.-H. and Lumley, J.L., "A critical comparison of second order closures with direct numerical simulation of homogeneous turbulence," NASA TM 105351 (1991).

Shih, T.-H. and Hsu, A.-T., "An improved $k-\epsilon$ model for near-wall turbulence," AIAA paper, 91-0611 (1991).

Shih, T.-H. Shih, Shabbir, A. and Lumley, J.L., "Advances in modeling the pressure correlation terms in the second moment equations," *The Lumley Symposium: Resent Developments in Turbulence*, November, 12-13, 1990, ICASE, NASA Langley Research Center, Edited by Gatski, T.B., Sarkar, S., Speziale, C.G.

Shih, T.-H., "An improved $k-\epsilon$ model for near-wall turbulence and comparison with direct numerical simulation," NASA TM 103221 (1990).

Shih, T.-H. and Mansour, N. N., "Modeling of near-wall turbulence," *Engineering Turbulence Modeling and Experiments*, September 24-28, 1990, Dubrovnik, Yugoslavia, Editors: W.Rodi, E.N. Ganic.

Shih, T.-H. and Reynolds, W. C., "A spectrum model for weakly anisotropic turbulence," Physics of Fluids A, **2**, 8, (1990).

Steffen, Jr., C. J., "A critical comparison of several low Reynolds number k-epsilon turbulence models for flow over a backward-facing step," NASA TM 106173 (1993).

Steffen, Jr., C. J., "An investigation of DTNS2D for use as an incompressible turbulence modelling test-bed," NASA TM 105593 (1992).

Steffen, Jr., C. J. and Beard, L. M., "Incompressible Navier Stokes solutions using the pseudo compressibility technique," *Proceeding of the 23rd Annual Pittsburgh Conference on Modeling and Simulation*, in print (1992).

Van der Vegt, Jaap, "ENO-Osher schems for Euler equations," AIAA Paper 93-0335 (1993)

Van der Vegt, J., "Assessment of flux splitting for viscous compressible flows," AIAA Paper 91-0243 (1991).

Van der Vegt, Jaap, "Overview of the Osher approximate Riemann solver for three-dimensional flows," NASA TM, in print (1992).

Yang, Z. and Leibovich, S., "On the lindar marginal stability of the trailing line vortex," Submitted for publication.

Yang, Z. and Leibovich, S, "Nonlinear dynamics near the stability margin in rotating pipe flow," J. Fluid Mech. **233**, 329-347, (1991).

Yang, Z. and Leibovich, S., "Unstable viscous wall modes in rotating pipe flow," AIAA Paper 91-1801, (1991). Also submitted to Physics Fluids A for publication.

Yang, Z. and Shih, T.H., "A $k-\epsilon$ modeling of near wall turbulence," Proc. of 4th Intl. Sym. on CFD, Davis, CA, 1305-1310, (1991). Also available as NASA TM 105238.

Yang, Z. and Shih, T.H., "A $k-\epsilon$ calculation of transitional boundary layers," *Instability, Transition, and Turbulence*, M.Y. Hussaini, A. Kumar and C.L. Steett, ed. Springer-Verlag, 1992.

Yang, Z. and Leibovich, S., "On the lindar marginal stability of the trailing line vortex," Presented at the 18th International Congress of Theoretical and Applied Mechanics, September 1992, Haifa, Israel. Submitted for publication.

Yang, Z. and Shih, T.H. "A new time scale based $k-\epsilon$ model for near wall turbulence," AIAA J. **31**, 1191 (1993).

Yang, Z. and Shih, T.H., "A $k-\epsilon$ model for turbulent and transitional boundary layers," *Proc. Near Wall Turbulent Flows,* B.E. Launder, C. Speziale and R.M.C. So, ed. Elsevier, 1993.

Yang, Z. and Shih, T.H., "A Galilean and tnesorial invariant $k-\epsilon$ model for near wall turbulence," AIAA Paper 93-3105 (1993).

Yang, Z. and Shih, T.H., "Flow inhomogeneity and the dissipation rate equation." Accepted for presentation at the 5th European Turbulence Conference, July 1994, Siena, Italy. In preparation for publication.

Yang, Z., Georgiadis, N., Zhu, J., and Shih, T. H., "Calculations of inlet/nozzle flows using a new k-ϵ model," to be presented at the AIAA Joint Propulsion Conference, San Diego, July (1995).

Zhu, J. and Shih, T.H., "Calculations of turbulent separated flows," NASA TM 106154 (1993). also in CFD Journal 3, pp.343-354 (1994).

Zhu, J. and Shih, T.H., "A numerical study of confined turbulent jets," NASA TM 106197 (1993), also in J. Fluids Eng. 116, pp.702-706 (1994).

Zhu, J. and Shih, T.H., "Computation of confined coflow jets with three turbulence models," AIAA Paper 93-3120, also in Int. J. for Num. Methods in Fluids 19, pp.939-956 (1994).

Zhu, G., Lai, M.-C and Shih, T.-H., "Second-order closure modeling of turbulent buoyant wall plumes," NASA TM (in print) (1992).

Zhu, J., "FAST-2D: A computer program for numerical simulation of two dimensional incompressible flows with complex boundaries," Rept. No.690, Institute for Hydromechanics, University of Karlsruhe (1991).

REPORT DOCUMENTATION PAGE

Form Approved
OMB No. 0704-0188

Public reporting burden for this collection of information is estimated to average 1 hour per response, including the time for reviewing instructions, searching existing data sources, gathering and maintaining the data needed, and completing and reviewing the collection of information. Send comments regarding this burden estimate or any other aspect of this collection of information, including suggestions for reducing this burden, to Washington Headquarters Services, Directorate for Information Operations and Reports, 1215 Jefferson Davis Highway, Suite 1204, Arlington, VA 22202-4302, and to the Office of Management and Budget, Paperwork Reduction Project (0704-0188), Washington, DC 20503.

1. AGENCY USE ONLY (*Leave blank*)

2. REPORT DATE
October 1995

3. REPORT TYPE AND DATES COVERED
Contractor Report

4. TITLE AND SUBTITLE
Center for Modeling of Turbulence and Transition: Research Briefs—1995

5. FUNDING NUMBERS
WU-505-90-5K
NCC3-370

6. AUTHOR(S)
Center for Modeling of Turbulence and Transition

7. PERFORMING ORGANIZATION NAME(S) AND ADDRESS(ES)
Institute for Computational Mechanics in Propulsion
22800 Cedar Point Road
Cleveland, Ohio 44142

8. PERFORMING ORGANIZATION REPORT NUMBER
E-9932

9. SPONSORING/MONITORING AGENCY NAME(S) AND ADDRESS(ES)
National Aeronautics and Space Administration
Lewis Research Center
Cleveland, Ohio 44135-3191

10. SPONSORING/MONITORING AGENCY REPORT NUMBER
NASA CR-198408
ICOMP-95-17
CMOTT-95-3

11. SUPPLEMENTARY NOTES
ICOMP Program Director, Louis A. Povinelli, organization code 2600, (216) 433-5818.

12a. DISTRIBUTION/AVAILABILITY STATEMENT
Unclassified - Unlimited
Subject Category 34
This publication is available from the NASA Center for Aerospace Information, (301) 621-0390.

12b. DISTRIBUTION CODE

13. ABSTRACT ***(Maximum 200 words)***

This research brief contains the progress reports of the research staff of the Center for Modeling of Turbulence and Transition (CMOTT) from July 1993 to July 1995. It also constitutes a progress report to the Institute of Computational Mechanics in Propulsion located at the Ohio Aerospace Institute and the Lewis Research Center. CMOTT has been in existence for about four years. In the first three years, its main activities were to develop and validate turbulence and combustion models for propulsion systems, in an effort to remove the deficiencies of existing models. Three workshops on computational turbulence modeling were held at LeRC (1991, 1993, 1994). At present, CMOTT is integrating the CMOTT developed/improved models into CFD tools which can be used by the propulsion systems community. This activity has resulted in an increased collaboration with the Lewis CFD researchers.

14. SUBJECT TERMS
Turbulence modeling

15. NUMBER OF PAGES
114

16. PRICE CODE
A06

17. SECURITY CLASSIFICATION OF REPORT
Unclassified

18. SECURITY CLASSIFICATION OF THIS PAGE
Unclassified

19. SECURITY CLASSIFICATION OF ABSTRACT
Unclassified

20. LIMITATION OF ABSTRACT